

5-2010

## DAMAGE-INDUCED INFLAMMATION AND NOCICEPTIVE HYPERSENSITIVITY IN DROSOPHILA LARVAE

Daniel T. Babcock

Follow this and additional works at: [https://digitalcommons.library.tmc.edu/utgsbs\\_dissertations](https://digitalcommons.library.tmc.edu/utgsbs_dissertations)



Part of the [Genetics Commons](#), and the [Molecular and Cellular Neuroscience Commons](#)

---

### Recommended Citation

Babcock, Daniel T., "DAMAGE-INDUCED INFLAMMATION AND NOCICEPTIVE HYPERSENSITIVITY IN DROSOPHILA LARVAE" (2010). *The University of Texas MD Anderson Cancer Center UTHealth Graduate School of Biomedical Sciences Dissertations and Theses (Open Access)*. 6.  
[https://digitalcommons.library.tmc.edu/utgsbs\\_dissertations/6](https://digitalcommons.library.tmc.edu/utgsbs_dissertations/6)

This Dissertation (PhD) is brought to you for free and open access by the The University of Texas MD Anderson Cancer Center UTHealth Graduate School of Biomedical Sciences at DigitalCommons@TMC. It has been accepted for inclusion in The University of Texas MD Anderson Cancer Center UTHealth Graduate School of Biomedical Sciences Dissertations and Theses (Open Access) by an authorized administrator of DigitalCommons@TMC. For more information, please contact [digitalcommons@library.tmc.edu](mailto:digitalcommons@library.tmc.edu).

**DAMAGE-INDUCED INFLAMMATION AND NOCICEPTIVE  
HYPERSENSITIVITY IN *DROSOPHILA* LARVAE**

A  
DISSERTATION

Presented to the Faculty of  
The University of Texas  
Health Science Center at Houston  
and  
The University of Texas  
M.D. Anderson Cancer Center  
Graduate School of Biomedical Sciences

in Partial Fulfillment  
  
of the Requirements  
  
for the Degree of  
  
DOCTOR OF PHILOSOPHY

by  
  
**Daniel Talbot Babcock, B.A.**

Houston, Texas

May, 2010

## **Acknowledgments**

I would like to thank my advisor, Dr. Michael Galko, for his continuous support and encouragement, for creating an amazing work environment, and for exuding enthusiasm for science that is contagious.

I would also like to thank my fellow lab members, both past and present, for helpful comments and discussions, Committee members for offering their time and advice, and neighbors and colleagues for generously sharing reagents.

Special thanks go to Christian Landry for helping to design and construct our heat probe, Jodie Polan and Hank Adams for microscope and equipment training, Shana Palla for help with our statistical analysis, Yan Wang for providing Transmission Electron Microscopy data, and Felona Gunawan for her work on a number of experiments, and most notably her role in carrying out our screen for thermal allodynia. I also thank the Department of Biochemistry and Molecular Biology, the George and Mary Josephine Hamman Foundation, and the American Heart Association for funding.

Most of all, I would like to thank my family for their unwavering love and support.

# **DAMAGE-INDUCED INFLAMMATION AND NOCICEPTIVE HYPERSENSITIVITY IN *DROSOPHILA* LARVAE**

Publication No. \_\_\_\_\_

**Daniel Talbot Babcock, B.A.**

Supervisory Professor: Michael J. Galko, Ph.D.

Mounting an effective response to tissue damage requires a concerted effort, with significant roles for the immune and nervous systems. Immune-responsive blood cells fight infection and clear debris from damaged tissues, and specialized pain receptors become hypersensitive to promote behavior that protects the damaged area. To uncover the mechanisms underlying these processes, we developed a genetically tractable model of damage-induced inflammation and pain hypersensitivity using *Drosophila* larvae.

To study wound-induced inflammation, we generated transgenic larvae with fluorescent epidermal cells and blood cells to monitor the circulatory dynamics of blood cells and the mechanism by which they accumulate at epidermal wounds. We found that blood cells attach to wound sites directly from circulation, a mechanism once thought to work exclusively in species with a closed circulatory system.

To study damage-induced pain hypersensitivity, we developed a “sunburn assay” and found that larvae have a lowered pain threshold (allodynia) and an exaggerated response to noxious stimuli (hyperalgesia) following UV damage. We screened for genes required for the development of allodynia in pain receptors (nociceptors), and discovered a number of novel mediators that have well conserved mammalian homologs.

Together, these results help us to understand how cells in the immune and nervous systems detect and respond to tissue damage, and provide a platform for further genetic dissection of these processes.



## Table of Contents

Acceptance Page .....	i
Title Page .....	ii
Acknowledgments .....	iii
Abstract .....	iv
Table of Contents .....	v
List of Illustrations .....	vii
List of Tables .....	ix
Abbreviations .....	x
Chapter 1: Background and Significance.....	1
Chapter 2: Wound-Induced inflammation in <i>Drosophila</i> larvae .....	6
Introduction .....	7
Results .....	9
Discussion .....	22
Chapter 3: Damage-Induced nociceptive hypersensitivity in <i>Drosophila</i> larvae .....	27
Introduction .....	28
Results .....	31
Discussion .....	48
Chapter 4: Genetic screen for UV-Induced thermal allodynia .....	57
Introduction .....	58
Results .....	59
Discussion .....	77
Chapter 5: Conclusions and future directions .....	80

Chapter 6: Materials and methods .....	89
Bibliography .....	99
Vita .....	122

## List of Illustrations

Figure 2.1 – Construction of a live reporter for wound-induced inflammation .....	10
Figure 2.2 – Circulatory dynamics of hemocytes in third-instar larvae .....	11
Figure 2.3 – Pinch-wounding causes epidermal damage .....	13
Figure 2.4 – Accumulation of hemocytes at wound sites .....	14
Figure 2.5 – Larval wound-induced inflammation is independent of cell migration ...	16
Figure 2.6 – Hemocytes attach to wound sites directly from circulation .....	17
Figure 2.7 – Peristalsis facilitates wound-induced inflammation .....	19
Figure 2.8 – Live scoring of hemocytes accumulation at wound sites .....	20
Figure 2.9 – Hemocytes engulf epidermal debris at wound sites .....	21
Figure 2.10 – Hemocytes are not required for wound closure .....	23
Figure 2.11 – Developmental shift in wound-induced inflammation .....	24
Figure 3.1 – Using <i>Drosophila</i> larvae to study nociception .....	30
Figure 3.2 – Baseline threshold for thermal nociception .....	32
Figure 3.3 – Description of larval sunburn assay .....	34
Figure 3.4 – UV irradiation causes morphological damage to the epidermis .....	35
Figure 3.5 – Larval nociceptors remain intact following UV damage .....	36
Figure 3.6 – UV damage is localized to the dorsal surface .....	37
Figure 3.7 – UV irradiation causes thermal allodynia .....	39
Figure 3.8 – UV irradiation causes thermal hyperalgesia .....	41
Figure 3.9 – Time-course of events following UV damage .....	42
Figure 3.10 – Epidermal knockdown of Dronc blocks UV-induced cell death .....	44



## **List of Tables**

Table 3.1 – Differences between thermal allodynia and hyperalgesia .....	54
Table 4.1 – Genes regulating thermal allodynia in nociceptors .....	62

## **Abbreviations**

ANOVA – Analysis of Variance

DMSO - Dimethylsulfoxide

DN – Dominant-Negative

DRG – Dorsal Root Ganglia

ERK – Extracellular signal-Related Kinase

GFP – Green Fluorescent Protein

GPCR – G-Protein-Coupled Receptor

Hh - Hedgehog

IR – Inverted Repeat

JNK – Jun N-Terminal Kinase

NF- $\kappa$ B – Nuclear Factor-kappa B

NIG – National Institute of Genetics

NMJ – Neuromuscular Junction

PBS – Phosphate Buffered Saline

PKC – Protein Kinase C

SEM – Scanning Electron Microscopy

S.E.M. – Standard Error of the Mean

TEM – Transmission Electron Microscopy

TeTxLC – Tetanus Toxin Light-Chain

TGF $\beta$  – Transforming Growth Factor Beta

TNF – Tumor Necrosis Factor

TRP – Transient Receptor Potential

TRPVI – Transient Receptor Potential Vanilloid 1

UAS – Upstream Activation Sequence

UV – Ultraviolet

VDRC – Vienna Drosophila RNAi Center

YFP – Yellow Fluorescent Protein

## **Chapter 1: Background and Significance**



### Orchestrating an efficient tissue repair response

The ability of multi-cellular organisms to repair damaged tissue is critical for survival. The major goal of the tissue repair response is to re-establish both the integrity and function of the damaged tissue. Numerous cell types are involved in mounting an effective repair response, with significant inputs from the immune and nervous systems.

In vertebrates, the immune system initiates a robust inflammatory response following tissue damage, whereby several populations of blood cells make their way to the site of damage. These immune-responsive blood cells carry out a number of functions, including platelets that aid in the formation of clots to prevent blood loss, neutrophils that prevent infection by killing microbes, and macrophages that engulf cellular debris (1). In addition, these cells also interact with the nervous system by initiating changes in pain sensitivity.

The detection of painful stimuli (nociception) is mediated by specialized sensory neurons called nociceptors. While these cells normally respond only to stimuli of sufficient magnitude, tissue damage and inflammation can induce hypersensitivity, characterized by a lowering of the nociceptive threshold (allodynia) and an exaggerated response to noxious stimuli (hyperalgesia) (2, 3). This enhanced nociceptive sensitivity fosters protective behavior, thus preventing additional injury to the damaged tissue and allowing the repair response to proceed unhindered.

### Sounding the alarm on tissue damage

Changes to nociceptive sensitivity are often mediated by factors released from damaged and dying cells as well as immune-responsive blood cells. Damaged cells, for

example, can release protons, purines such as ATP and adenosine, and peptides like bradykinin into the extracellular space. These factors can in turn target corresponding membrane receptors on neighboring nociceptors, such as acid-sensing ion channels, purinergic receptors, and BK<sub>2</sub> receptors, respectively. Immune cells such as macrophages, neutrophils, and mast cells also release a number modulatory factors. These include cytokines such as Tumor Necrosis Factor-alpha (TNF $\alpha$ ) and Interleukin-1-beta (IL-1 $\beta$ ), prostaglandins, histamine, and neurotrophins such as Nerve Growth Factor (NGF) (4-6). Some of these factors sensitize nociceptors directly by targeting ion channels or G-Protein-Coupled Receptors (GPCRs), while others initiate an inflammatory cascade that serves to further propagate the inflammatory response by inducing other immune cells to release modulators (3, 7).

#### Damage-induced changes within nociceptors

Inflammatory mediators produce several changes that alter the behavior of nociceptors. Targeting ion channels such as ASICs and purinergic P2X receptors depolarize the nociceptor directly, while activation of metabotropic receptors can cause long-term alterations in sensitivity (2). The latter may induce changes through activation of various kinase signaling pathways, including protein kinase A (PKA), protein kinase C (PKC), phosphatidylinositol 3-kinase (PI3K), as well as the mitogen-activated protein kinases (MAPKs) p38, Extracellular signal-Regulated Kinase (ERK), and c-Jun N-terminal kinase (JNK) (8). Activation of these pathways often leads to changes in the expression level and/or gating properties of ion channels and receptors.

One of the most extensively studied channels related to nociception is the capsaicin receptor, Transient Receptor Potential Vanilloid-1 (TRPV1) (9). This channel is regulated by several kinases. For example, activation of p38 MAPK in nociceptors increases the expression levels of TRPV1 (10). PKC induces hypersensitivity by increasing the probability of channel gating both in response to lower temperatures as well as lower concentrations of capsaicin (11, 12), while PKA prevents desensitization of the channel (13). Together, these types of signaling mechanisms help to enhance nociceptive sensitivity following tissue damage.

#### Addressing the need for invertebrate models

Although vertebrate models of inflammation and nociceptive hypersensitivity have succeeded in identifying a number of factors regulating these processes, the complexity of the interactions between the immune and nervous systems as well as the functional redundancy of several of the inflammatory mediators illustrate the importance of simpler invertebrate models of tissue repair.

*Drosophila melanogaster* has long served as a genetically tractable model organism to study human disease. *Drosophila* have a well-established inflammatory response to tissue damage (14-17), mediated by blood cells (hemocytes) that perform many of the same functions as mammalian blood cells (18). They have also proven to be useful for modeling nociception, as the identification of the *painless* gene (19), a TRP channel that is functionally similar to TRPV1 in vertebrates, illustrates conservation of nociceptive signaling mechanisms. We hypothesize that signaling mechanisms underlying damage-induced inflammation and changes in nociceptive hypersensitivity

are also conserved, and we believe that *Drosophila* will serve as a useful model to test this hypothesis.

## **Chapter 2: Wound-Induced inflammation in *Drosophila* larvae**

## **Introduction**

Healing damaged tissue requires a concerted effort between a variety of cell types. One of the major steps in the wound healing process is the inflammatory response, characterized in part by the recruitment of blood cells to the site of injury. Specific types of blood cells perform a wide range of tasks, including limiting blood loss by clot formation, fighting infection from invading pathogens, and clearing cellular debris from the damaged area (1).

The ability of the immune system to detect and respond to tissue damage is considered to be an ancient survival response (20). How these blood cells detect tissue damage and subsequently arrive at sites of injury is of great importance to understanding the role of the immune system during tissue repair. In vertebrates, two separate mechanisms allow for this accumulation of blood cells. First, circulating white blood cells flow out of damaged blood vessels and attach directly to the damaged tissue. Second, blood cells still circulating in nearby blood vessels slow down and stick to the vascular walls, and then proceed to diapedese through or between the endothelial cells and migrate to the site of injury (1, 21). This second mechanism is thought to involve the release of diffusible signals, such as hydrogen peroxide (22) from damaged tissue to activate a local immune response. However, much less is known about the molecular mechanisms underlying the attachment of blood cells directly from circulation.

*Drosophila* are also capable of mounting an effective immune response to both tissue damage (16, 17, 23, 24) and infection from microorganisms (15, 25). The major cellular components of the *Drosophila* immune system are blood cells (hemocytes) that perform many of the same functions as mammalian macrophages (26). The three major

types of hemocytes in *Drosophila* are plasmatocytes, which predominantly function as phagocytes (27), crystal cells that are required for melanization and clotting of the blood (hemolymph) (16), and lamellocytes which are produced only in response to infection (26, 28). During embryonic development, hemocytes are derived from the head mesoderm (29) and subsequently disperse throughout the open body cavity through migration (30). These embryonic hemocytes also migrate in response to tissue damage, though through distinct chemoattractant signals (23).

Hemocytes in *Drosophila* larvae accumulate at sites of damage resulting from epidermal wounds (16) and tumors created in imaginal discs (24). How these hemocytes arrive at sites of injury, however, remains unclear. Here we show that the flow of hemolymph, required for the distribution of nutrients and removal of waste (31), also produces a circulation of hemocytes within the open body cavity and the heart-like dorsal vessel. The accumulation of hemocytes at epidermal wounds is due to direct capture from circulation. Upon binding to damaged tissue, these hemocytes alter their morphology and phagocytose cellular debris. As the epidermal wound closes, these cells disperse back into circulation (32). Our results demonstrate that the mechanism of adhesive capture is present in an organism with an open circulatory system, suggesting that this is an ancient conserved mechanism for detecting and responding to tissue damage. This also opens the door to use *Drosophila* genetics to uncover the cellular and molecular mechanisms underlying this detection and adherence of hemocytes to sites of injury.

## **Results**

### **Creating a live reporter to study hemocyte dynamics in wounded and unwounded larvae:**

To visualize hemocyte dynamics within third instar larvae, we created a fly strain bearing fluorescent transgenes to label both epidermal cell membranes and hemocytes. Epidermal cell membranes are labeled by a *neuroglian* protein-trap Green Fluorescent Protein (GFP) insertion (33), and hemocytes are labeled by a UAS-Yellow Fluorescent Protein (YFP) (34) driven by the peroxidase promoter (*pxn-Gal4*) (17) (Figure 2.1 A). These fluorescent proteins allow live visualization of both cell types simultaneously in a live animal under a wide-pass GFP filter (Figure 2.1 B).

Using this reporter, we mounted third instar larvae and filmed them in real time to monitor the hemocyte movement patterns. When viewing the dorsal side of the larvae (Figure 2.2 A and B), we found two distinct populations of hemocytes: sessile cells that were firmly adherent to the epidermis (red dots in Figure 2.2 B), as well as cells that were flowing from anterior to posterior within the open body cavity (green arrows in Figure 2.2 B). When viewing the larvae from the ventral side, we saw the same types of hemocytes (Figure 2.2 C). To return to the anterior portion of the body cavity, these hemocytes were pumped very rapidly through the heart-like dorsal vessel (Figure 2.2 D). Cells transported through the dorsal vessel travelled much faster than those flowing through the rest of the body cavity. Whereas cells moving through the dorsal vessel travelled at a rate of approximately 3.2 mm/second, cells flowing toward the posterior moved at about 83  $\mu\text{m}/\text{second}$ . These movements allow a robust circulation of hemocytes within the body cavity. Although the hemocytes began to pool at the posterior over time (Figure 2.2 E and F), likely due to a bottleneck at the entry to the



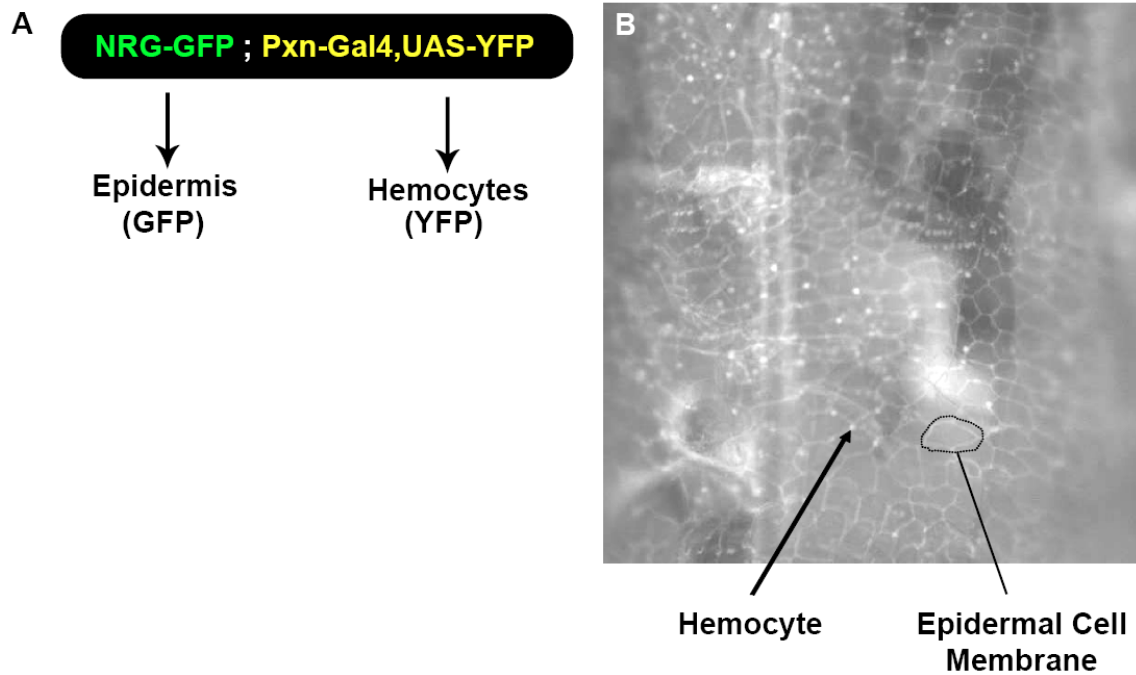


**Figure 2.1 Construction of a live reporter for wound-induced inflammation**

(A) Genotype and (B) live image of reporter larvae used to view wound-induced inflammation. Epidermal cell membranes are labeled green (circled in B) via a Neuroglian-GFP fusion protein. Hemocytes are labeled yellow (arrow in B) by YFP driven by the *Pxn-Gal4* driver.

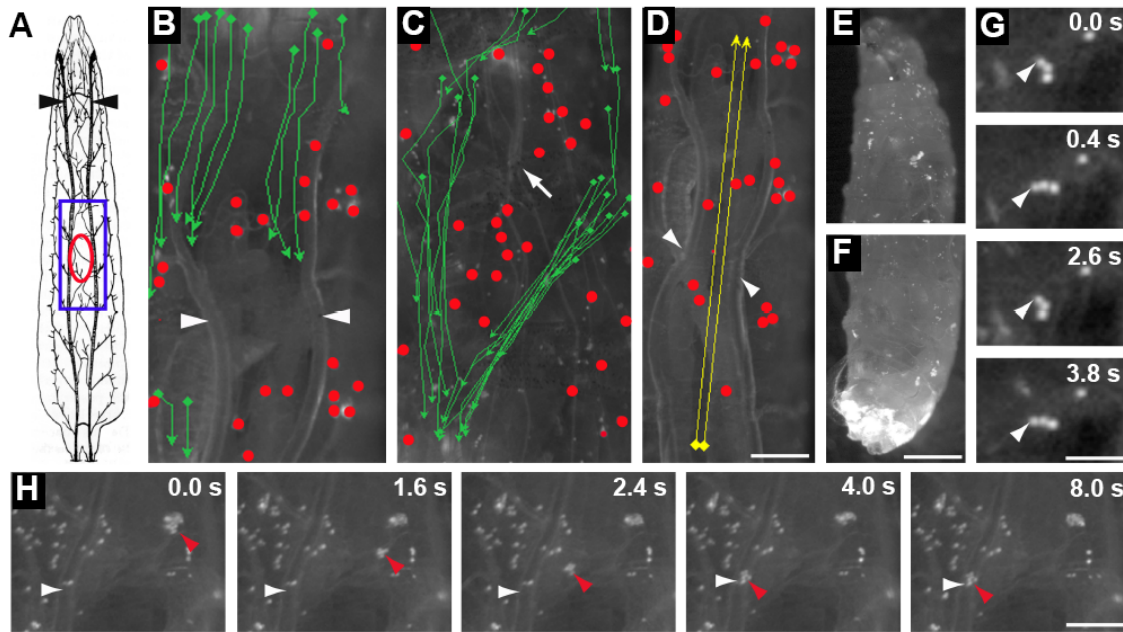


**Figure 2.2 Circulatory dynamics of hemocytes in third-instar larvae**

(A) Illustration of a third-instar larva, displaying the dorsal trunks of the tracheal system (arrowheads), field of view of live movies (blue box), and size of wounds (red oval). (B-D) Motion paths of circulating hemocytes viewed from the dorsal (B) or ventral (C) side in the open body cavity (green arrows in B & C) and dorsal vessel (yellow arrows in D) and sessile hemocytes (red dots). (E-F) Pooling of hemocytes at the posterior end of larvae. (G) A clump of hemocytes adheres to and pivots along the epidermis. (H) A clump of hemocytes (red arrowhead) detaches from the epidermis and adheres to other internal tissues (white arrowhead). Scale bar (D) 100  $\mu\text{m}$  for B-D, (F) 100  $\mu\text{m}$  for E-F, (G) 50  $\mu\text{m}$ , (H) 100  $\mu\text{m}$ . Originally published in (32), and modified with permission.

dorsal vessel, we continued to see this circulation all throughout larval development.

Most of the sessile hemocytes remained firmly adherent during our observations, although we did notice a clump of cells that swiveled among a single attachment point to the epidermis (Figure 2.2 G). We also observed a clump of hemocytes that detached from the epidermis into circulation briefly, then reattached to a separate internal structure (Figure 2.2 H). These observations suggest that there is a small amount of interchange between these two populations of hemocytes, although they remain separate for the most part. A more recent study also suggested an important distinction exists between the circulating and sessile cells, demonstrating that only the sessile hemocytes are a source of lamellocyte production in response to infection (35).

#### Accumulation and turnover of hemocytes at wound sites:

As mentioned previously, *Drosophila* larvae have a very robust inflammatory response following tissue damage. In our model of tissue damage, the epidermal monolayer is damaged using a pair of blunted dissecting forceps, creating a gap in the epidermal sheet called a “pinch-wound” (Figure 2.3 and 2.4 A and B). In this assay, the wound gap is characterized by exposed bare cuticle along with epidermal debris, while the barrier cuticle itself remains intact (Figure 2.3 and 2.4 E-H). Because the barrier is never compromised, these wounds are essentially sterile with no risk of infection. This allows us to differentiate between the immune responses directly related to wound closure and those involved in fighting infection. Immediately after wounding, a clear gap appeared in the epidermal sheet that was almost completely devoid of hemocytes (Figure 2.4 B). Over the next several hours, however, these wound gaps began to fill

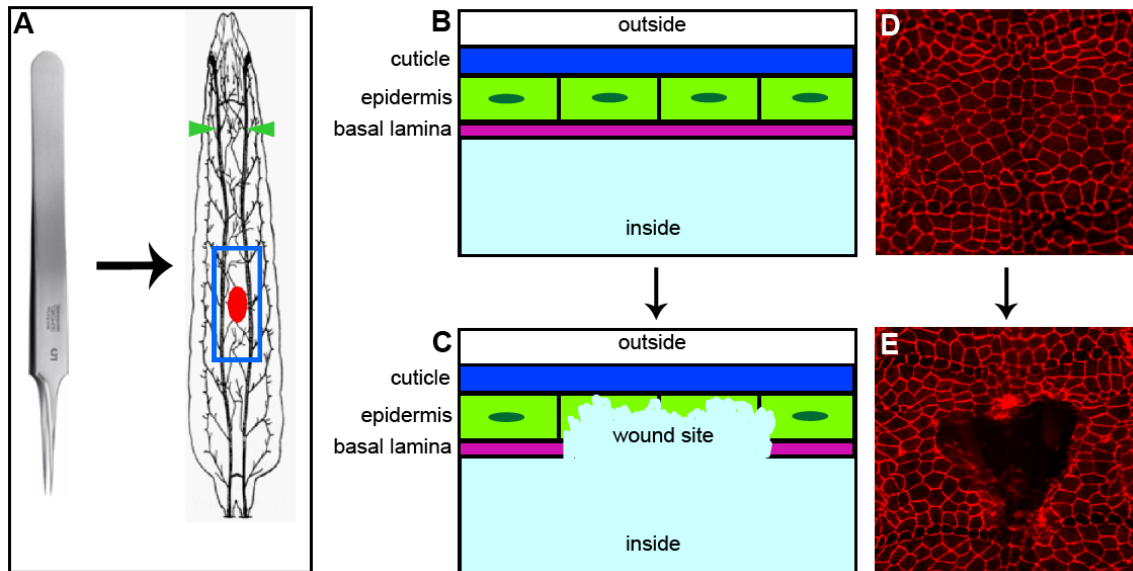


**Figure 2.3 Pinch-wounding causes epidermal damage**

(A) Diagram of pinch-wounding assay using dissecting forceps. Approximate area of wound is red. (B-C) Cartoon of a cross-section showing the unwounded (B) and wounded (C) epidermis, with an outlying barrier cuticle and an underlying basal lamina (not to scale). Pinch wounding damages the epidermis and basal lamina, leaving cellular debris in the wound site. (D-E) Epidermal whole-mounts showing the unwounded (D) and wounded (E) epidermis. Panels D & E originally published in (32), and reproduced with permission.

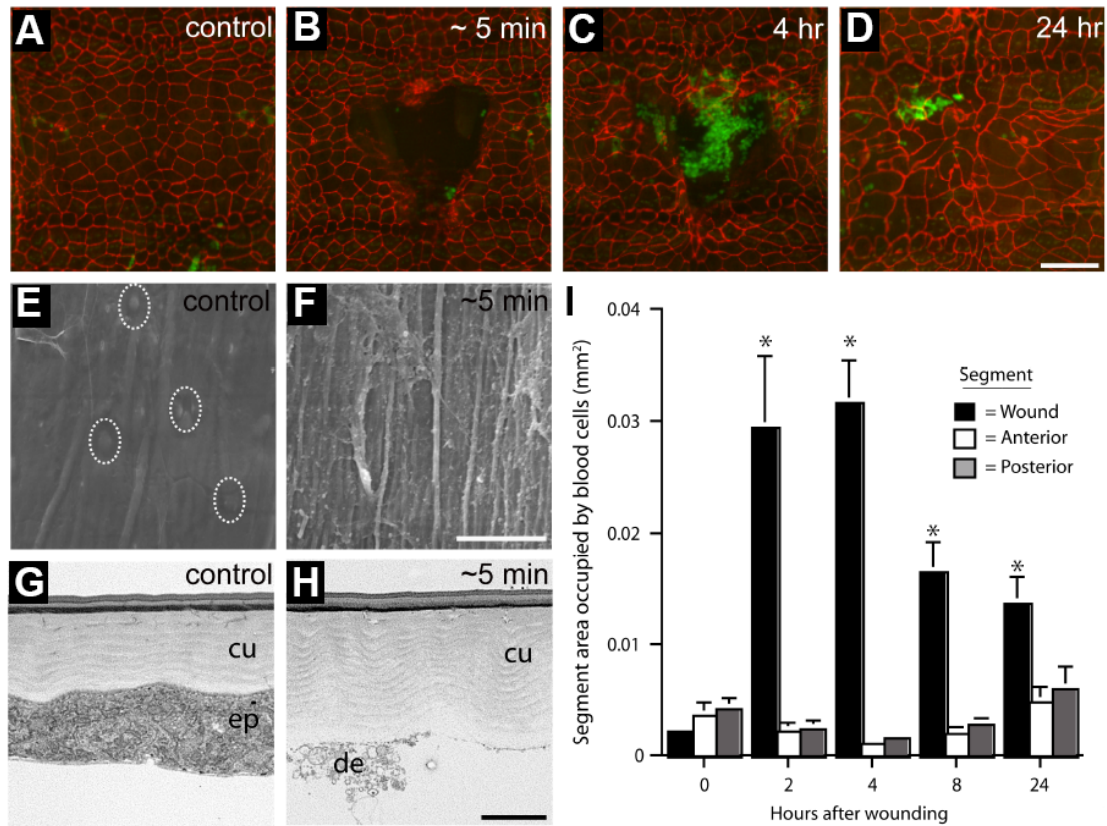


**Figure 2.4 Accumulation of hemocytes at wound sites**

(A-D) Epidermal whole-mounts showing hemocyte accumulation after pinch-wounding. Epidermal cell membranes stained with anti-Fasciclin-III (red) and hemocytes with anti-GFP (green). (E-F) SEM showing unwounded epidermal cells (E) with nuclei encircled, and exposed cuticle after wounding (F). (G-H) TEM showing unwounded (G) and wounded (H) epidermis (ep), cuticle (cu), and epidermal debris (de). (I) Quantitation of the number of hemocytes present in wounded body segments (black) and segments anterior (white) and posterior (gray) to the wound up to 24 h post wounding. \*,  $p < 0.001$  using ANOVA for each time-point. Scale bar in (D) 100  $\mu\text{m}$  for A-D, (F) 33  $\mu\text{m}$  for E-F, (H) 2  $\mu\text{m}$  for G-H. Error bars represent Standard Error of the Mean (S.E.M). Originally published in (32), and reproduced with permission.

with hundreds or even thousands of hemocytes (Figure 2.4 C and I). As these wounds fully closed within 24 hours, the hemocytes dispersed (Figure 2.4 D and I). To uncover the mechanism by which these hemocytes arrive at the wound site, we used our live reporter and time-lapse video microscopy to visualize hemocyte behavior in wounded larvae.

Circulating hemocytes arrive at wound sites via adhesive capture:

The accumulation of hemocytes to sites of tissue damage is well studied in *Drosophila* embryos. Previous studies demonstrated that embryonic hemocytes detect tissue damage and migrate to the area by crawling along specific chemoattractant gradients (36). The crawling behavior displayed in embryonic hemocytes depends on the family of Rho GTPases, as interfering with *rac*, *rho*, or *cdc42* prevented the inflammation response to wounding (17). Our data, however, suggest that a separate mechanism of accumulation is in place in the larval stage. We found no such effects when interfering with Rho GTPases in our larval wounding assay. Expressing dominant-negative forms of any of these genes within hemocytes had no effect on accumulation at wound sites (Figure 2.5). Also, cell migration alone could not account for the large number of hemocytes that rapidly accumulate at wound sites, since only a small number of cells occupied the area surrounding the wound initially (Figure 2.4 I). Finally, our time-lapse movies showed that the sessile cells located directly next to the wound border failed to migrate into the wound site over the course of several hours (Figure 2.6 B'). Taken together, this suggests that a separate mechanism is responsible for hemocyte accumulation at larval wound sites.

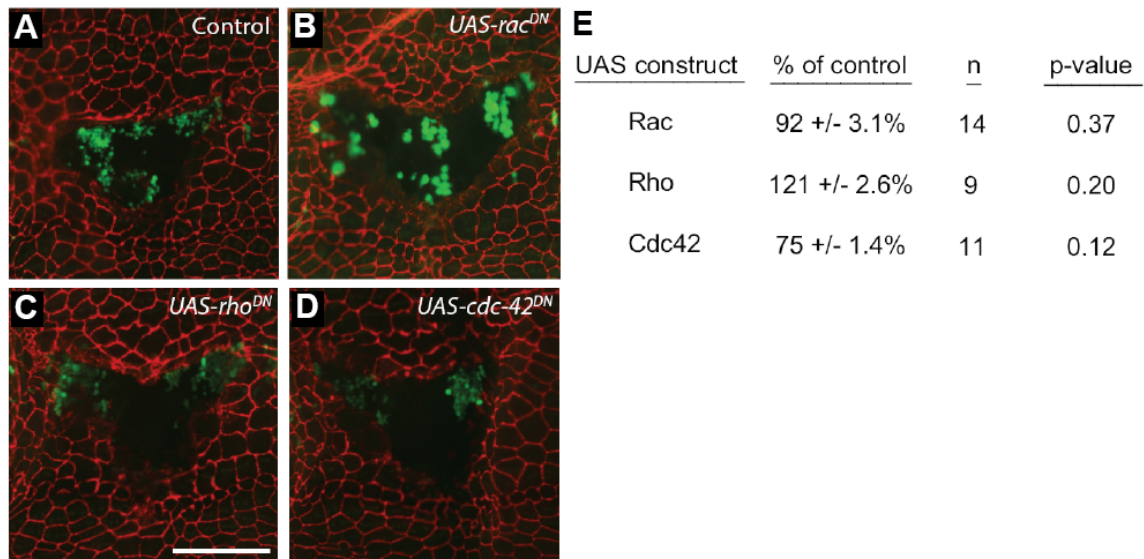


### Figure 2.5 Larval wound-induced inflammation is independent of cell migration

(A-D) Images of wound-induced inflammation in control larvae (A) or in cases where GTPase function is inhibited (B-D) in hemocytes. Epidermal cell membranes are stained with anti-Fasciclin-III (red) and hemocytes (green) with anti-GFP. (E) Quantitation of hemocyte accumulation at wound sites in each case as a percentage of controls (ANOVA). Scale bar (C) 100  $\mu$ m for A-D. Originally published in (32), and reproduced with permission.



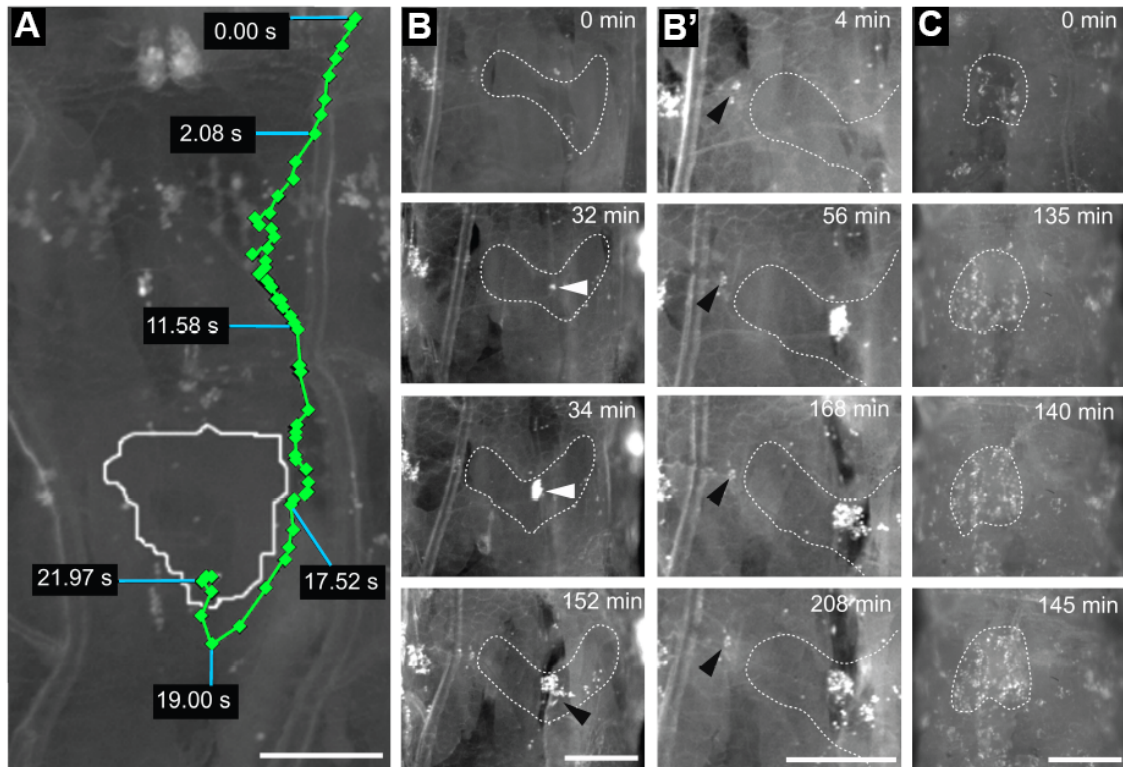


**Figure 2.6 Hemocytes attach to wound sites directly from circulation**

(A) Circulating hemocyte attaches directly to a wound site (outlined in white) from circulation. Green line denotes motion path of the hemocytes before capture, with its position marked (diamonds) across a span of 22 s. (B) Still frames from a time-lapse movie showing a clump of hemocytes (white arrowhead) attaching to the wound site (outlined in white) from circulation. The clump is not present 32 minutes after the wound, but is completely in the wound site in the next frame (34 minutes). (B') Still from the same movie showing that sessile hemocytes next to the wound (black arrowhead) do not respond to the nearby wound. (C) Stills from a time-lapse movie showing a massive "sheet" of hemocytes that rapidly fill the wound site (white) over a 10-minute period. Scale bars are 100  $\mu$ m. Originally published in (32), and modified with permission.



To uncover this mechanism, we mounted larvae from our live reporter stock immediately after wounding, visualizing the accumulation of hemocytes at wound sites using real-time and time-lapse video microscopy. Real-time movies demonstrated that free-flowing hemocytes attached directly to wound sites shortly after wounding (Figure 2.6 A). Time-lapse movies demonstrated that accumulation via these attachment events continued over the next several hours. The hemocytes appeared able to attach to wound sites individually (Figure 2.6 A), as aggregated clumps (Figure 2.6 B), or as a wave or “sheet” that rapidly filled the wound site (Figure 2.6 C).

We also found that larval movement, known to contribute to hemolymph flow in the larvae (31), facilitates wound-induced inflammation. Interfering with the peristaltic motion and crawling behavior of larvae severely reduced hemocyte accumulation at wounds (Figure 2.7 and 2.8). These results clearly demonstrate that hemocytes attach to larval wound sites directly from circulation.

#### Wound-responsive hemocytes change morphology and become phagocytically active:

To uncover the functional role of wound-adherent hemocytes, we analyzed the morphology of these cells compared to those not attached to wounds. Whereas the majority of hemocytes in unwounded larvae are characterized by a spherical shape (Figure 2.9 A), we found that wound-adherent cells appear flattened with several processes extended in all directions (Figure 2.9 B). This morphology is very similar to that of cultured cells adhering to the bottom of a dish. The cytoplasmic extensions engulf epidermal debris left at wound sites (Figure 2.9 C-C’'), and they also allow these hemocytes to stick to one another (Figure 2.9 D-D’’).

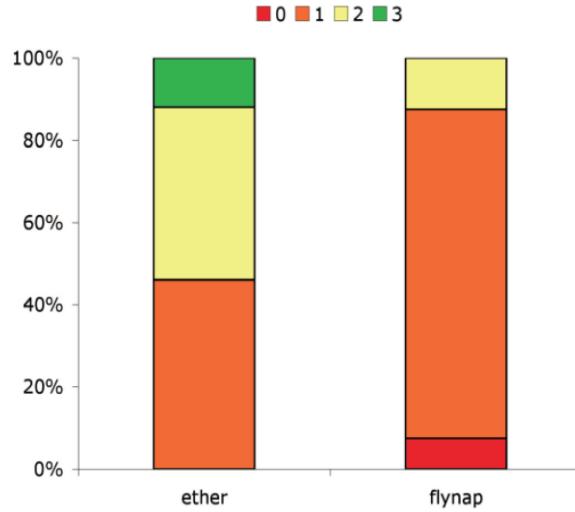


**Figure 2.7 Peristalsis facilitates wound-induced inflammation**

Measurement of wound-induced inflammation using a semi-quantitative scale (see Figure 1.8). *w, NRG-GFP ; pxn-Gal4, UAS-YFP* larvae were anesthetized using ether or immobilized using Flynap, which blocked peristaltic motion. Measurements were taken 4 h after wounding. Originally published in (32), and reproduced with permission.

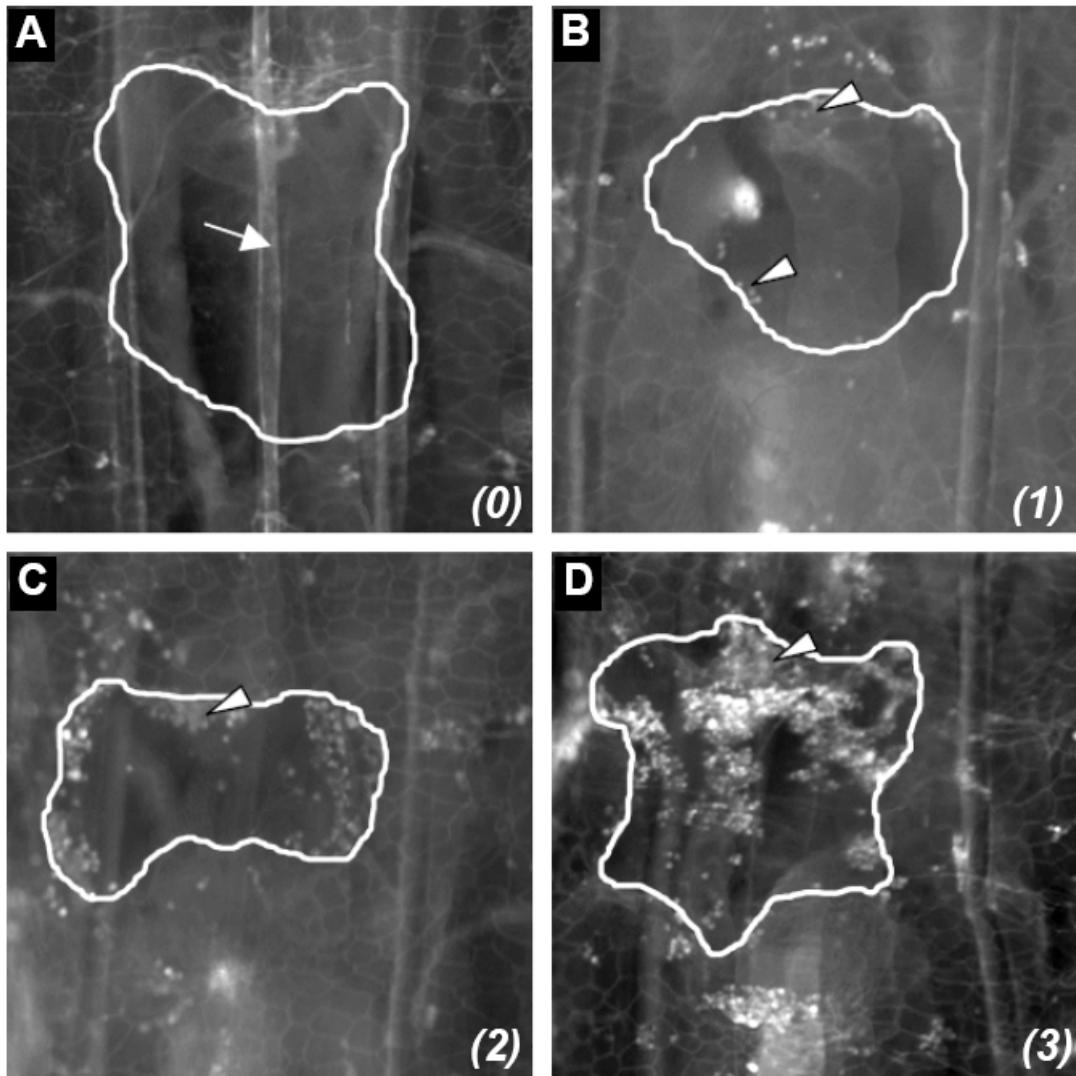


**Figure 2.8 Live scoring of hemocyte accumulation at wound sites**

Semi-quantitative scale for live measurement of hemocyte accumulation at epidermal wounds. Scores were ranked as: 0 = no accumulation (A), 1 = minor accumulation (B), 2 = moderate accumulation throughout the wound gap (C), and 3 = dense accumulation throughout the wound gap (D). Originally published in (32), and modified with permission.

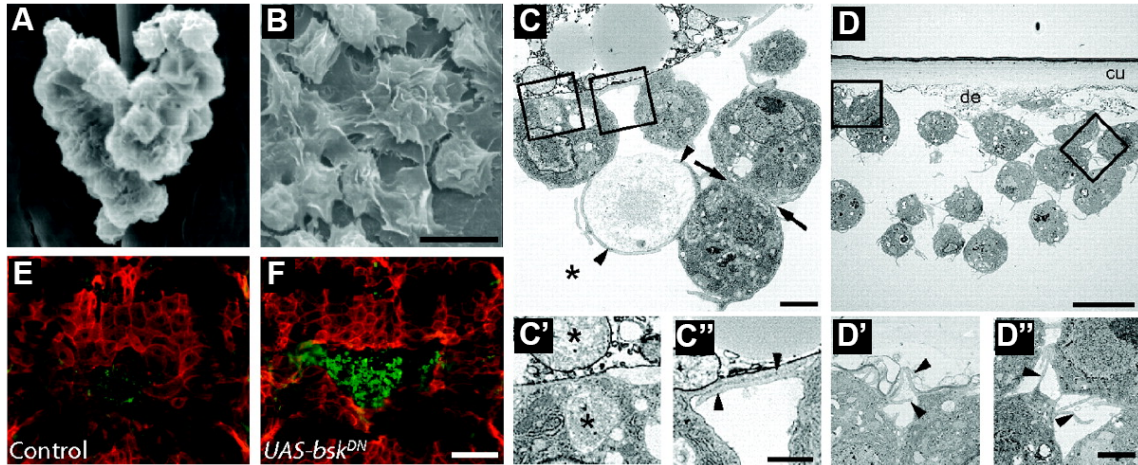


**Figure 2.9 Hemocytes engulf epidermal debris at wound sites**

(A-D) SEM (A-B) and TEM (C-D) of tissue-bound hemocytes. (A) Cluster of hemocytes bound to the epidermis in an unwounded larva. (B) Cells adherent to a wound site develop a flattened morphology 4 h after wounding. (C) 2 h after wounding, hemocytes extend phagocytic processes (arrowheads) to engulf cellular debris (asterisk). (C') Close-up of left box in C, showing cell debris at a wound site (upper asterisk) and within hemocytes (lower asterisk). (C'') Close-up of right box in C. Overlapping extensions of neighboring hemocytes (arrowheads). (D) 4 h after wounding, showing processes from hemocytes attached to cellular debris (arrowheads in D') and other hemocytes (arrowheads in D''). (E) 24 h after wounding, wound area is closed in control larvae, with epidermal cells (red) filling the wound gap and a lack of hemocytes (green). (F) Larvae expressing *UAS-bsk<sup>DN</sup>* in the epidermis have wounds that remain open, and hemocytes remain 24 h after wounding. Scale bar (B) 10  $\mu$ m for A-B, (C) 10  $\mu$ m, (C'') 2  $\mu$ m for C' and C'', (D) 2  $\mu$ m, (D'') 1  $\mu$ m for D' and D'', (F) 100  $\mu$ m for E-F. Originally published in (32), and modified with permission.

Despite the large amount of cellular debris present at wound sites, the clearance of this debris by hemocytes had no effect on the efficiency of wound closure. When hemocytes were ablated by expression of the pro-apoptotic gene *hid*, wounds closed at the same rate as those in control larvae (Figure 2.10).

#### Wound closure is required for hemocyte dispersal

As the larval epidermal wounds closed, the wound-adherent hemocytes dispersed (Figure 2.4 D and I). Although mammalian blood cells often undergo apoptosis after wound closure, we saw no evidence of this happening, as we saw no staining with an antibody specific to cleaved caspase-3 (data not shown). Rather, we hypothesized that the hemocytes are removed by physical displacement as epidermal cells migrate to close the wound gap. To test this, we expressed a dominant-negative form of *basket* (*bsk<sup>DN</sup>*), the Jun N-terminal Kinase (JNK) in *Drosophila*. Expression of *bsk<sup>DN</sup>* prevented cell migration in epidermal cells, prohibiting wound closure (16). In chronically open wounds, hemocytes remained in place long after they dispersed in control larvae (Figure 2.9 E and F). This suggests that the closure of the wound itself physically displaces wound-adherent hemocytes, presumably back into circulation.

#### Discussion

Our results demonstrate that immune-responsive hemocytes circulate within the open body cavity of third-instar *Drosophila* larvae, and accumulate at wound sites by direct capture from circulation. This mechanism is distinct from the cell migration that regulates wound-induced inflammation in the embryo, suggesting that there is a switch at some point during development (37) (Figure 2.11). The reason for this change could

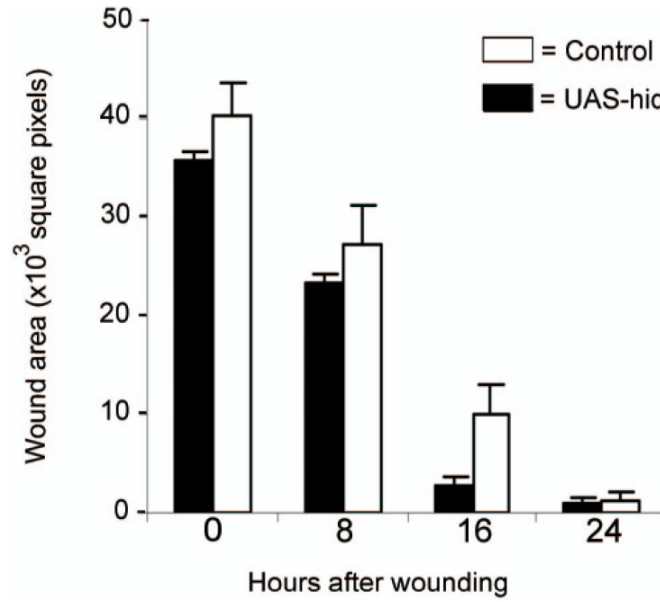


**Figure 2.10 Hemocytes are not required for wound closure**

Measurement of wound size over time in control larvae (*Pxn-Gal4,UAS-GFP* x *W<sup>1118</sup>*) or in larvae lacking hemocytes (*Pxn-Gal4,UAS-GFP* x *UAS-hid*).  $p > 0.05$  for all time-points (Student's t test). Error bars represent S.E.M. Originally published in (32), and reproduced with permission.

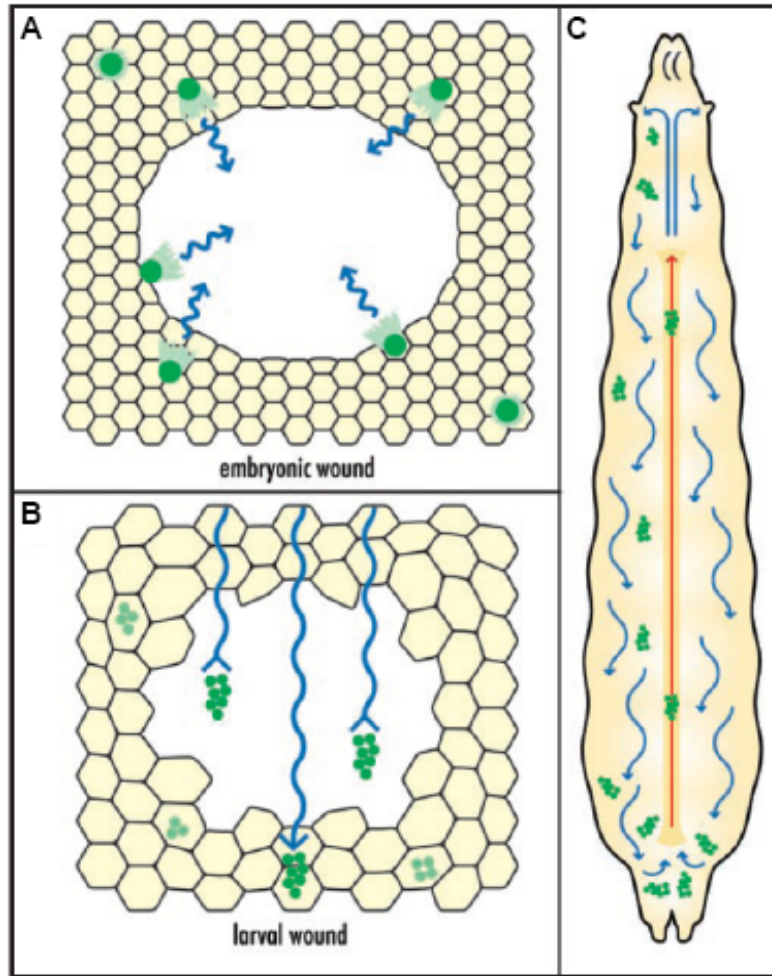


**Figure 2.11 Developmental shift in wound-induced inflammation**

Illustrations showing wound-induced inflammation regulated by cell migration in embryos (A) and regulated by direct capture from circulation in larvae (B). (C)

Illustration of circulatory dynamics of hemocytes in third-instar larvae. Hemocytes flow from anterior to posterior within the main body cavity (blue arrows) and travel back to the anterior through the heart-like dorsal vessel (red arrow). Originally published in (37), and reproduced with permission.

simply be a matter of body size. By the end of larval development, the body size is several times larger than that of the embryo, and thus the amount of tissue to protect is much greater. At this point, responding to nearby chemical signals by crawling to sites of injury may no longer be an efficient way to deal with tissue damage. Having the hemocytes circulate within the body cavity allows the same number of cells to “patrol” a much greater area and therefore mount an effective immune response much more rapidly. Future studies should be able to determine precisely when this change in hemocytes occurs.

Another area to explore is the nature of the attachment mechanism. Whether the circulating hemocytes attach passively or if it involves a more active process is currently unclear. Perhaps the hemocytes already have the capacity to bind to damaged tissue before wounding, and the cells that pass alongside the wound simply stick to it. If this is true, then there must be something inherent about the wound site that allows the hemocytes to bind. Recent studies suggest that immune cells are capable of detecting hydrophobic molecules that are normally sequestered on the inside of neighboring cells (38, 39). When the barrier of the damaged cells is compromised, these hydrophobic molecules become exposed to the extracellular space. Some researchers suggest that this serves as a damage signal to the immune system, and the damaged tissue is targeted in the same manner as “non-self” tissue, such as an invading pathogen (20). Our results support the idea that the damaged tissue itself is regarded as a specific target, as most of the hemocytes accumulating at pinch wounds were bound to the epidermal debris within the wound site as opposed to the areas of bare cuticle (see Figure 2.9 C-C’’).



Whether the hemocytes need to be activated to attach to this debris is also not yet determined. Studies involving other insects demonstrated the involvement of granular cells in the encapsulation of pathogens by other types of hemocytes (40), along with identification of a spreading peptide needed to induce an immune response to invading pathogens (36, 41). It is possible that a signal from damaged tissue also induces the adherent behavior we see after pinch wounding. The observation that circulating hemocytes respond to epidermal damage while sessile hemocytes respond specifically to invading pathogens (35) suggests that there are likely several signaling mechanisms involved in the immune response. Future studies could aim to identify what signals, if any, are sent from damaged tissue in this model. A more promising approach, however, would be to identify what receptors in the hemocytes allow them to attach to damaged tissue, since this is something that should be present regardless of whether it is always expressed or only selectively after wounding.

The results here demonstrate the conservation of a mechanism of attachment of circulating blood cells to damaged tissue, meaning that this ancient mechanism predates the establishment of a closed circulatory system. More importantly, this will allow the vast number of genetic tools available in *Drosophila* research to complement current models already in place to identify the cellular and molecular mechanisms involved in the immune response to tissue damage.

**Chapter 3: Damage-Induced nociceptive hypersensitivity in**  
*Drosophila* larvae

## **Introduction**

The nervous system plays an important role in the response to tissue damage and subsequent repair mechanisms, including alterations in pain sensation. The ability to detect and respond to painful or noxious stimuli (nociception) is an important defense mechanism against real or potential danger in the environment. A population of sensory neurons called nociceptors mediates nociception (2, 42, 43). These cells only respond to high-intensity stimuli under normal conditions, but may become hypersensitive resulting from either inflammation or tissue damage. One form of hypersensitivity is allodynia, when a normally innocuous stimulus elicits a pain response due to a lowered pain threshold. Another common form of hypersensitivity is hyperalgesia, which is an exaggerated response to a normally noxious stimulus (3). This hypersensitivity serves a useful function in response to tissue damage, as it promotes behavior aimed to protect the damaged area during the repair process.

Normally the hypersensitivity caused by tissue damage subsides after the healing process is complete, although in many cases chronic pain hypersensitivity develops. This chronic pain lasts long after the healing of the damaged tissue through unknown mechanisms, and represents a major healthcare burden (44, 45). Mammalian models have identified a number of mediators of nociceptive hypersensitivity (5, 8), but the signaling mechanisms within nociceptors underlying this sensitivity remain unclear.

Nociceptive behavior is also evident in a number of invertebrate models including *Aplysia* (46-48), *C. elegans* (49), *Manduca sexta* (50) and leeches (51), revealing a high level of conservation of nociceptive signaling mechanisms across animal phyla (52-54). The similarities shown for basic nociceptive signaling suggest

that a genetically tractable invertebrate model of nociceptive hypersensitivity would likely serve as a useful tool to identify the cellular and molecular mechanisms regulating the sensitivity of nociceptors.

*Drosophila* has long served as a model system to study the genetic basis of behavior (55), including the recent development of an assay to survey for nociception. When stimulated with a noxious thermal or mechanical stimulus, the larva will display a robust “corkscrew” withdrawal response that is distinct from normal crawling behavior (19) (Figure 3.1 A). Researchers used this behavioral paradigm to screen for genes necessary for nociception and identified *painless*, which encodes a temperature-sensitive ion channel belonging to the Transient Receptor Potential (TRP) family of ion channels (19), which are also involved in nociceptive signaling in vertebrates (9, 56, 57). Further studies showed that the nociceptive withdrawal response is mediated by a subset of sensory neurons in the peripheral nervous system termed Class IV dendritic arborization (da) neurons (43). These sensory neurons are located in the dorsal, lateral, and ventral clusters of sensory neurons in each abdominal segment (58), and extend dendritic arbors along the nearby epidermis (Figure 3.1 B). These studies demonstrated the usefulness of *Drosophila* in the study of nociception, and we speculated that the same behavioral paradigm would serve as a useful model of damage-induced nociceptive hypersensitivity.

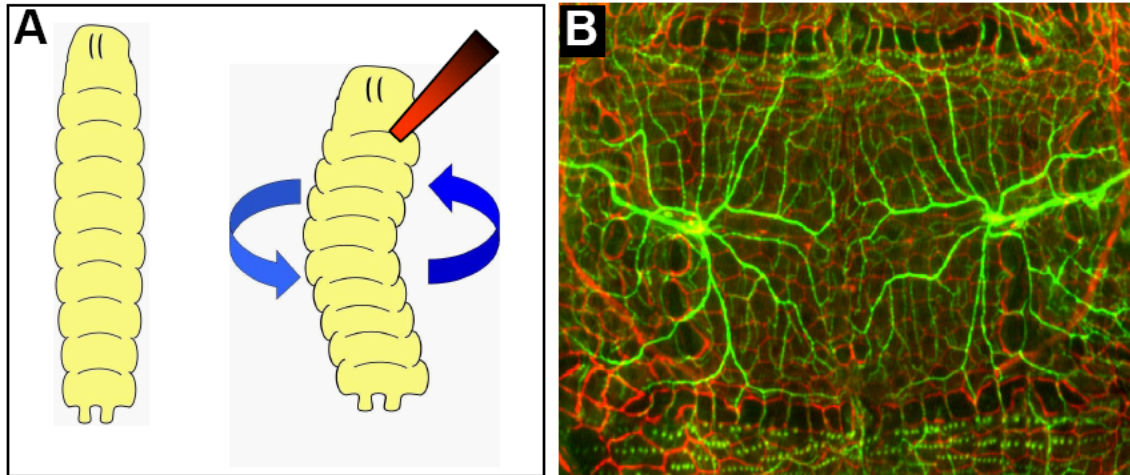


**Figure 3.1 Using *Drosophila* larvae to study nociception**

**(A)** Illustration of the larval withdrawal behavior. In response to a noxious stimulus such as a heat probe, larvae rapidly roll laterally in a corkscrew-like fashion. The withdrawal response is defined as at least one complete 360° roll in response to the stimulus. **(B)** Epidermal whole-mount of a *ppk-eGFP* larva, showing the epidermal cell membranes in red (anti-Fasciclin III) and underlying nociceptors in green (anti-GFP).

Panel B originally published in (65), and modified with permission.

## **Results**

### **Analysis of baseline nociception in third-instar larvae**

To establish the baseline threshold for thermal nociception, we stimulated third-instar *w<sup>1118</sup>* larvae with a wide range of temperatures using a custom-build heat probe (Figure 3.2 A and B). Larvae were presented with a stimulus for up to 20 s, and the withdrawal behavior was recorded in one of the following categories: “fast withdrawal” (response  $\leq$  5 s), “slow withdrawal” (5 s < response < 20 s), and “no withdrawal” (no response by 20 s). Stimulation at temperatures up to 38 °C produced no withdrawal response. A small percentage of larvae began to withdraw at 39 °C, with a greater proportion responding at progressively higher temperatures (Figure 3.2 C). All larvae withdrew from a 45 °C stimulus before the cutoff, although the majority displayed a slow response. At 48 °C and higher all larvae responded rapidly, withdrawing almost immediately from the stimulus. This demonstrates that the thermal nociception threshold is near 39-40 °C.

### **UV damage induces morphological damage to the epidermis**

To initiate widespread epidermal damage, we exposed larvae to a brief dose of ultraviolet (UV) radiation. UV radiation damages DNA by causing the production of thymine dimers, leading to cell death if the DNA repair mechanisms are overwhelmed (59, 60). Acute exposure to UV radiation also induces sunburn that is accompanied by nociceptive hypersensitivity in mammals (61, 62). Much of the DNA damage pathway initiated by acute UV damage is shared in *Drosophila* (63, 64), although its effect on nociception has not been tested.

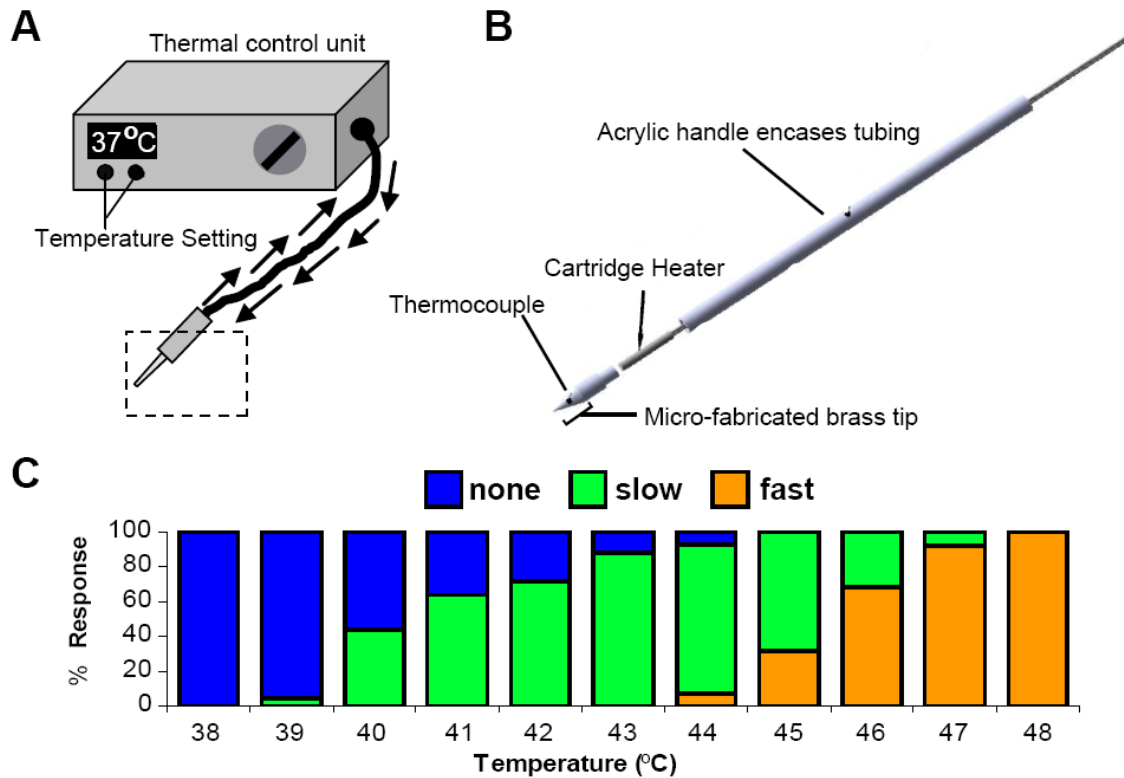


**Figure 3.2 Baseline threshold for thermal nociception**

(A) Diagram of a custom-built heat probe used to deliver noxious thermal stimuli.

Temperature set by a thermal control unit, which is connected to the probe itself. (B)

Diagram of heat probe components (inset box in panel A). The probe is encased in an acrylic handle. Stimuli are delivered along a micro-fabricated brass tip, with a cartridge heater and thermocouple directly behind it to send feedback to the control unit. (C)

Measurement of withdrawal behavior across a wide range of temperatures. Larvae were stimulated at each temperature for up to 20 s, and the behavior was categorized as “no withdrawal” (blue), “slow withdrawal” (green, response between 5 and 20 s), or “fast withdrawal” (orange, response  $\leq 5$  s).  $n = 50$  for each temperature. Originally published in (65), and reproduced with permission.

We determined the appropriate dose of UV radiation for our “sunburn assay” (65) by placing larvae in an ultraviolet crosslinker (Figure 3.3 A) and measuring viability to adulthood after exposure to increased doses. We used a crosslinker to allow simultaneous treatment of a large number of samples at a calibrated and easily replicated dose. We found that larvae could tolerate a dose of 20 mJ/cm<sup>2</sup> without affecting viability (Figure 3.3 B), while survival began to drop off at higher levels. This became the standard dose and was used for all subsequent experiments.

To assess the morphological damage caused by exposure to UV radiation, we dissected larvae at a range of time-points following UV treatment. The larval epidermis is a continuous monolayer composed of cells that are roughly equal in shape and size (Figure 3.4 A). There were no morphological changes shortly after UV treatment (Figure 3.4 E), but by 24 h there was a disruption of epidermal cell membrane integrity along the dorsal midline (Figure 3.4 I). This damage is largely healed by 48 h, with the remaining epidermal cells redistributing over the area (Figure 3.4 M). The damage appeared limited to the epidermis, however, as the nearby nociceptors remained fully intact during this process (Figure 3.4 B,F,J,N and Figure 3.5). We also find activation of *misshapen*, a component of the JNK signaling cascade and a reporter for cellular stress (16), as early as 4 h post UV and continuing through 48 h (Figure 3.4 C,G,K,O). Staining with an antibody for cleaved Caspase-3 demonstrated that the damaged epidermal cells were undergoing apoptosis (Figure 3.4 D,H,L,P). This damage extended the full length of the larvae along the anterior-posterior axis, but was limited to the dorsal side of the larvae that was exposed to the UV light (Figure 3.6).



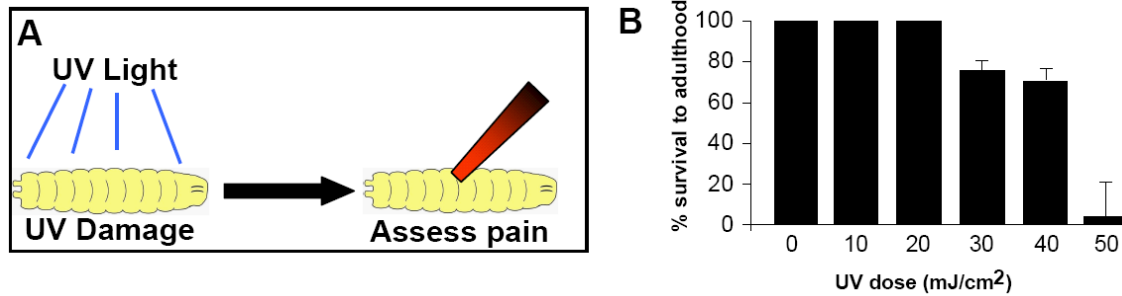


**Figure 3.3 Description of larval sunburn assay**

(A) Illustration of the “sunburn assay”, consisting of tissue damage induced by exposure to UV light and subsequent test for nociception using the heat probe. (B) Measurement of survivorship to varying doses of UV radiation. Here, survivorship is defined as the percentage of irradiated third-instar larvae that continued on to metamorphosis and eclosed as viable adults.  $n = 3$  sets of 50 larvae for each UV dose. Error bars represent S.E.M. Panel B was originally published in (65), and reproduced with permission.

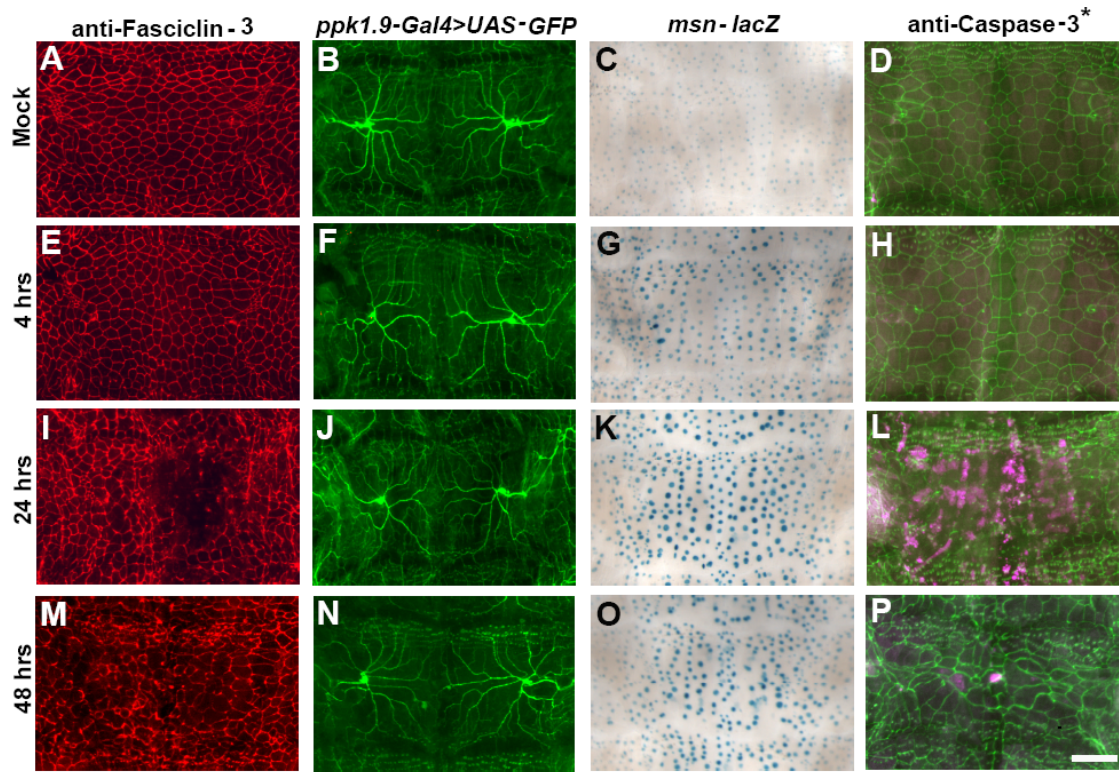


**Figure 3.4 UV irradiation causes morphological damage to the epidermis**

(A-P) Epidermal whole-mounts showing the morphology of epidermal cells and nociceptors following mock treatment (A-D) or UV treatment at 4 h (E-H), 24 h (I-L), and 48 h (M-P). (A,E,I, and M) *ppk1.9-Gal4,UAS-GFP* larvae are stained with anti-Fasciclin III (red) to label epidermal cell membranes. (B,F,J, and N) the same larvae are stained with anti-GFP (green) to label nociceptors in the same conditions. (C,G,K, and O) *msn-lacZ* larvae stained with X-gal to measure *msn* activity as a readout of JNK signaling. (D,H,L, and P) *w<sup>1118</sup>* larvae are stained with anti-Fasciclin III (green) to label epidermal cell membranes, and with anti-cleaved caspase-3 (purple) to identify apoptotic cells. Scale bar (P) 100  $\mu$ m. Originally published in (65), and reproduced with permission.

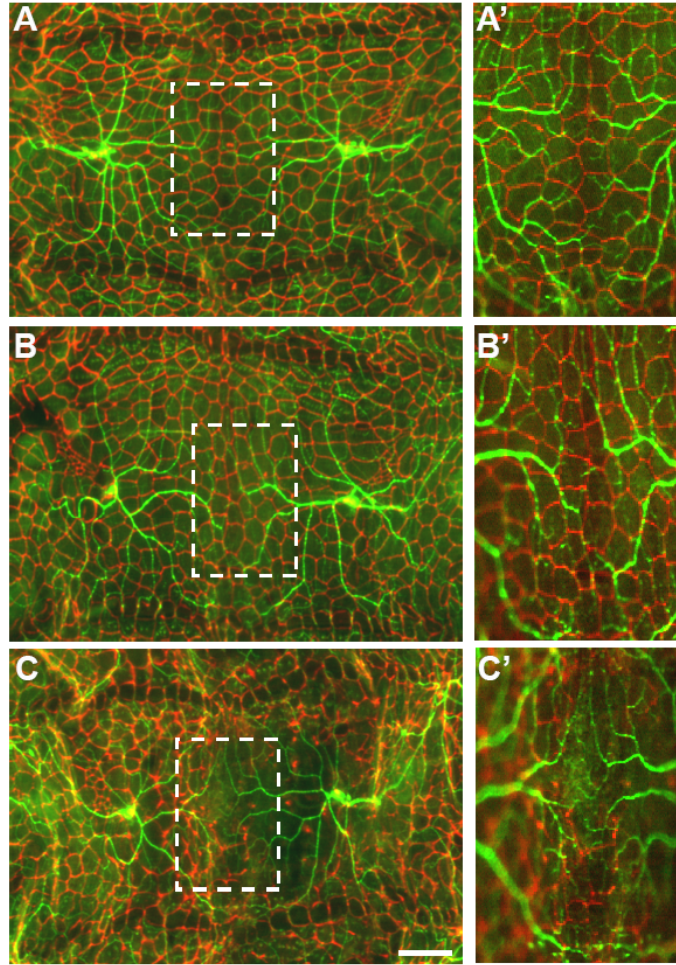


**Figure 3.5 Larval nociceptors remain intact following UV damage**

(A-C) Merged panels from Figure 2.4 illustrating epidermal cell (anti-Fasciclin III, red) and nociceptor (anti-GFP, green) morphology in mock treatment (A) or 4 h (B) and 24 h (C) after UV treatment. (A'-C') insets from panels A-C, showing that nociceptor morphology remains normal even in areas along the damaged epidermis. Scale bar (C) is 100  $\mu$ m. Originally published in (65), and reproduced with permission.

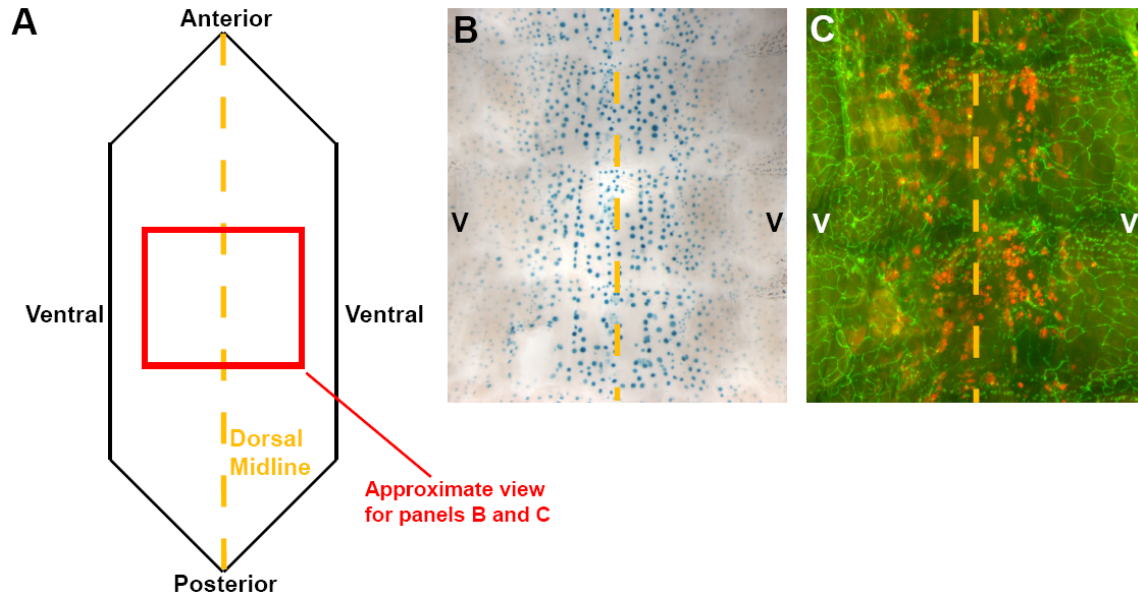


### Figure 3.6 UV damage is localized to the dorsal surface

(A) Diagram of dissected epidermal whole-mount layout, with the dorsal midline (orange line) in the center and the ventral surface (v) along the sides. Red box is the approximate field of view for subsequent images. (B-C) *msn-lacZ* larvae (B) stained with X-gal and *w<sup>1118</sup>* larvae (C) stained with anti-Fasciclin III (green) and anti-cleaved caspase-3 (red) 24 h after UV treatment. Both *msn-lacZ* activity and cleaved caspase-3 staining are localized to the dorsal surface that is exposed to UV radiation. Originally published in (65), and reproduced with permission.

### UV damage causes nociceptive hypersensitivity

To determine whether the UV damage lowers the threshold for thermal nociception, we irradiated groups of larvae and measured their response to a normally subthreshold temperature of 38 °C (see Figure 3.2 C) at various times following UV exposure. Whereas “mock-treated” control larvae, which were not exposed to UV, did not withdraw from this stimulus, some larvae began to respond as early as 4 h after UV (Figure 3.7A). The magnitude of the response was even greater for the 8 h and 16 h groups, and a peak response was reached at 24 h post UV. At this time nearly 70% of the larvae withdrew from the stimulus, half of which responded rapidly. Most of this hypersensitivity is gone by 48 h, coinciding with the healing of the damaged epidermis (Figure 3.4 N and P). It should be noted, however, that by 48 h after UV the larvae are approaching the end of larval development. At this point, the larvae do not crawl as rigorously, and the increased thickness of the cuticle could impede the detection of thermal stimuli. Thus, we cannot exclude these possibilities for the decrease in behavioral response at 48 h. Overall, these results demonstrate that there is a significant behavioral shift ( $p < .001$ ) in response to a normally subthreshold thermal stimulus, indicative of thermal allodynia.

Since the allodynia was most prevalent 24 h after UV exposure, we examined how far the thermal threshold decreased under this condition by measuring withdrawal behavior at progressively lower temperatures. The majority of mock-treated control larvae responded at temperatures as low as 42 °C, with the response decreasing at 40 °C and completely absent by 38 °C. Some of the larvae in UV treated groups, however, responded to temperatures as low as 30 °C (Figure 3.7 B), suggesting that the threshold

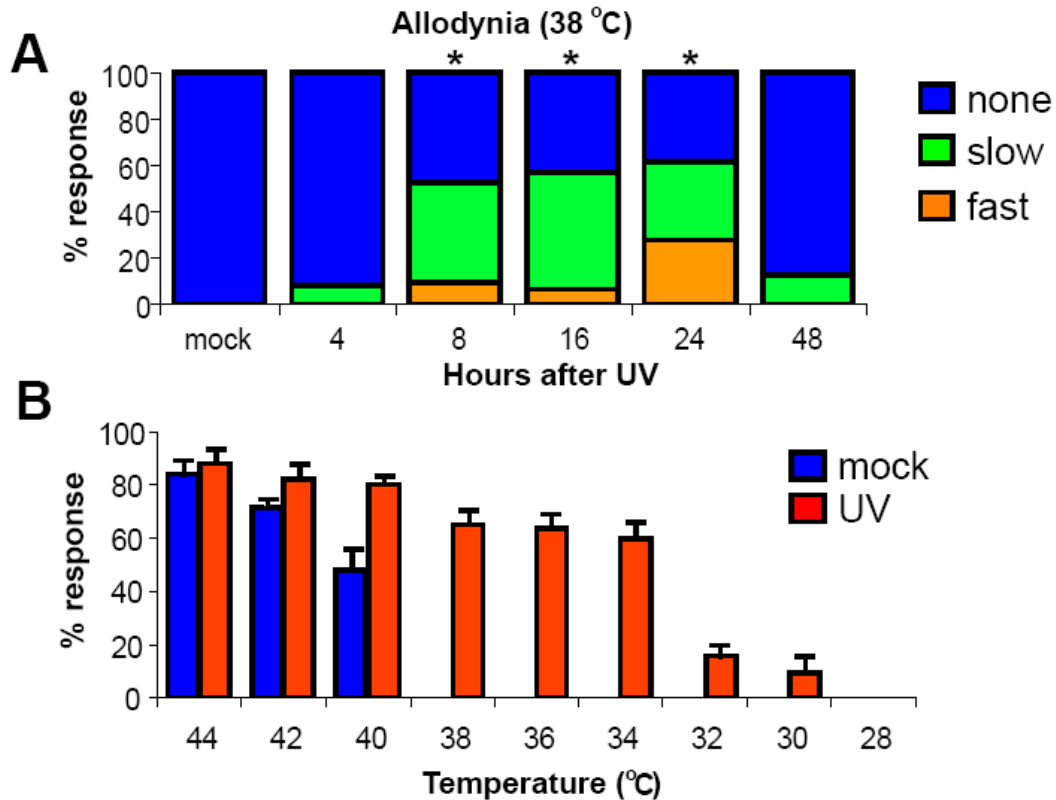


**Figure 3.7 UV irradiation causes thermal allodynia**

(A) Measurement of withdrawal responses to a normally subthreshold stimulus of 38 °C in mock-treated larvae and at various time-points following UV treatment. Responses were marked as “no response” (blue), “slow response” (green) or “fast response” (orange). \*,  $p < 0.001$  vs mock using Fisher’s Exact test, with Bonferroni correction for multiple comparisons. 3 sets of  $n = 30$  for each condition (B) Comparison of withdrawal responses to decreasing temperatures between mock-treated (blue) and UV-treated (red)  $w^{1118}$  larvae 24 h after treatment.  $n = 50$  for each condition. Error bars represent S.E.M. Originally published in (65), and reproduced with permission.

for thermal nociception drops by nearly 10 °C following UV damage. These results also demonstrate that the hypersensitivity is primarily due to the temperature of the probe as opposed to the physical force of the probe itself, as the response decreases along with the temperature and disappears completely by 28 °C.

We also examined if the larvae developed thermal hyperalgesia following UV damage. To test this, we measured the response of larvae to a normally noxious stimulus of 45 °C (see Figure 3.2 C) after irradiation. Mock-treated larvae always responded to a stimulus of this magnitude, although only 20% of the responses were fast. By 8 h following UV, nearly 100% of the responses were fast (Figure 3.8 A), and the average withdrawal latency decreased from  $7.8 \pm 0.6$  s for mock-treated larvae to  $3.2 \pm 0.2$  s 8 hours following UV treatment (Figure 3.8 B). By 16 h, this hyperalgesic response was abolished, with withdrawal responses returning to their baseline level. Interestingly, the peak response for thermal hyperalgesia was much earlier than that for thermal allodynia (Figure 3.9), suggesting that these two forms of hypersensitivity may be regulated by distinct mechanisms.

#### Caspase activity in epidermal cells is required for allodynia

Mammalian models of nociceptive hypersensitivity have demonstrated that damaged and dying cells release a number of factors that can influence nearby nociceptors. Several of these factors are thought to directly activate nociceptors, while others induce circulating leukocytes to release additional inflammatory molecules (66). To see whether similar processes underlie the nociceptive hypersensitivity in our model, we tested for the development of UV-induced thermal allodynia and hyperalgesia while blocking epidermal cell death. Using the GAL4/UAS system (67), we used an epidermal

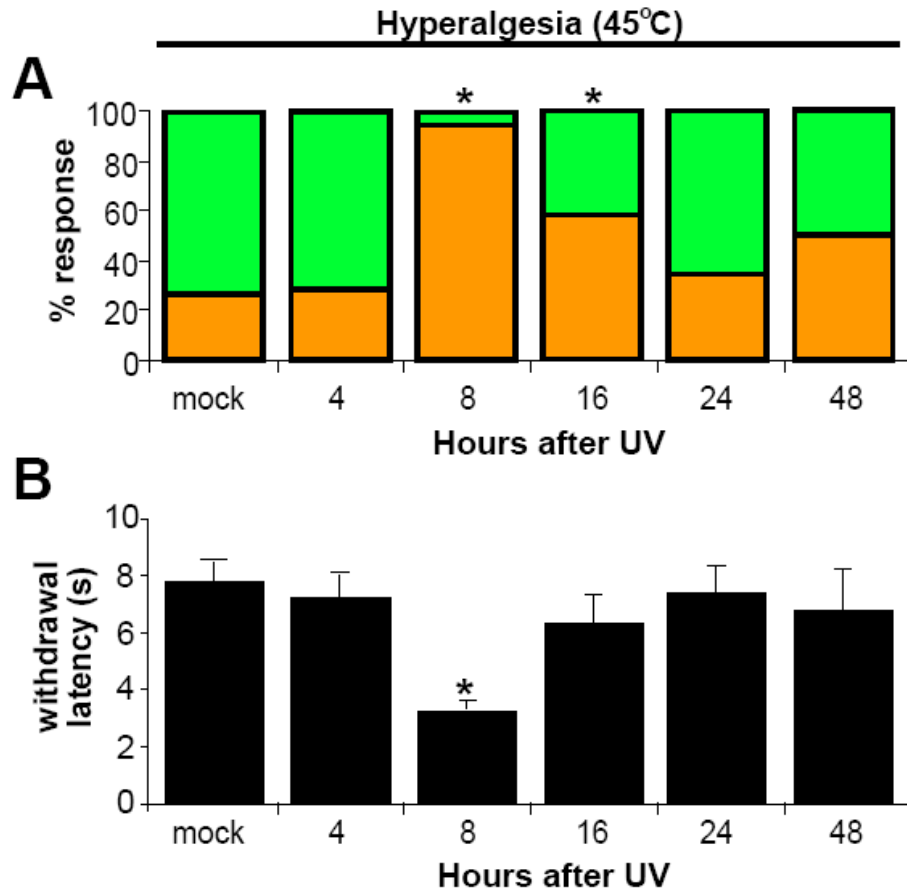


**Figure 3.8 UV irradiation causes thermal hyperalgesia**

(A) Measurement of withdrawal responses to a normally noxious stimulus of 45 °C in mock-treated *w<sup>1118</sup>* larvae and at various time-points following UV treatment.

Responses were marked as “no response” (blue), “slow response” (green) or “fast response” (orange). \*,  $p < 0.001$  using Fisher’s Exact test, with Bonferroni correction for multiple comparisons. 3 sets of  $n = 30$  for each condition. (B) Data from panel A displayed as the average withdrawal latency for each condition. \*,  $p < 0.001$  using ANOVA. Error bars represent S.E.M. Originally published in (65), and reproduced with permission.



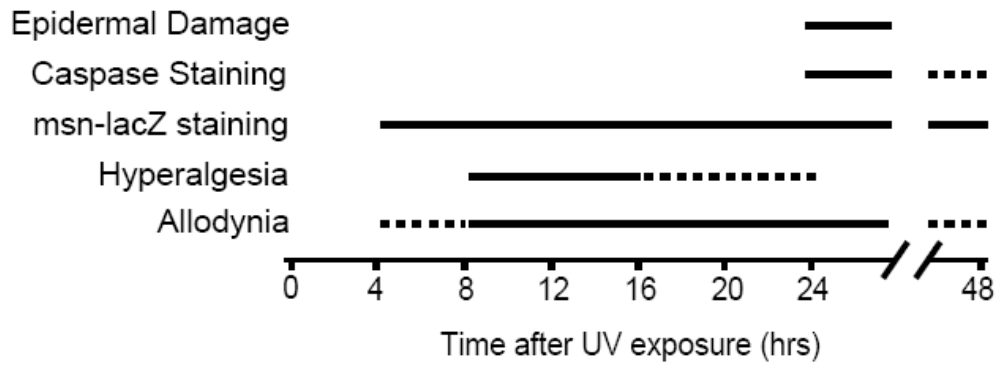


**Figure 3.9 Time-course of events following UV damage**

Timing of morphological and behavioral changes following UV damage. Overt morphological changes such as epidermal damage and caspase staining do not appear until 24 h post UV. Both thermal allodynia and hyperalgesia are evident before this morphological damage, with the onset appearing much closer to the initial readout of the stress-response reporter *msn-lacZ*, between 4 and 8 h post UV. Solid lines represent when the events are most notable, while dashed lines indicate an occasional or mild response. Originally published in (78), and reproduced with permission.

specific Gal4 driver (*A58-Gal4*) (16) to drive expression of an RNA-interference transgene targeting the apical caspase *Dronc* (68). Knockdown of *Dronc* within the epidermis prevented the morphological damage and activation of cleaved Caspase-3 24 hours following UV irradiation (Figure 3.10). Thus, knocking down *Dronc* is an effective method of preventing UV-induced cell death in the epidermis. Epidermal cell death is also required for the development of thermal allodynia, as the hypersensitive response to a 38 °C stimulus 24 hours after UV is almost completely absent (Figure 3.11 A). However, epidermal cell death seems to play no role in the development of thermal hyperalgesia, as the withdrawal latency to a 45 °C stimulus 8 h after UV treatment is just as fast as in control larvae (Figure 3.11 B).

We also tested the role of immune-responsive hemocytes in nociceptive hypersensitivity. We previously demonstrated that the majority of hemocytes can be ablated by expression of the pro-apoptotic gene *hid* (69) using a hemocytes-specific Gal4 driver (*pxn-Gal4*) (17). We found that eliminating the hemocytes had no effect on the development of either thermal allodynia or hyperalgesia (Figure 3.11 C-D). These results demonstrate that signaling from damaged epidermal cells, but not hemocytes, plays an important role in our model of nociceptive hypersensitivity.

### Cytokine signaling mediates allodynia

To understand the molecular mechanisms responsible for the development of thermal allodynia, we focused on a number of cytokines implicated in nociceptive hypersensitivity in mammals (7, 70-73). The first factor we examined was the Tumor

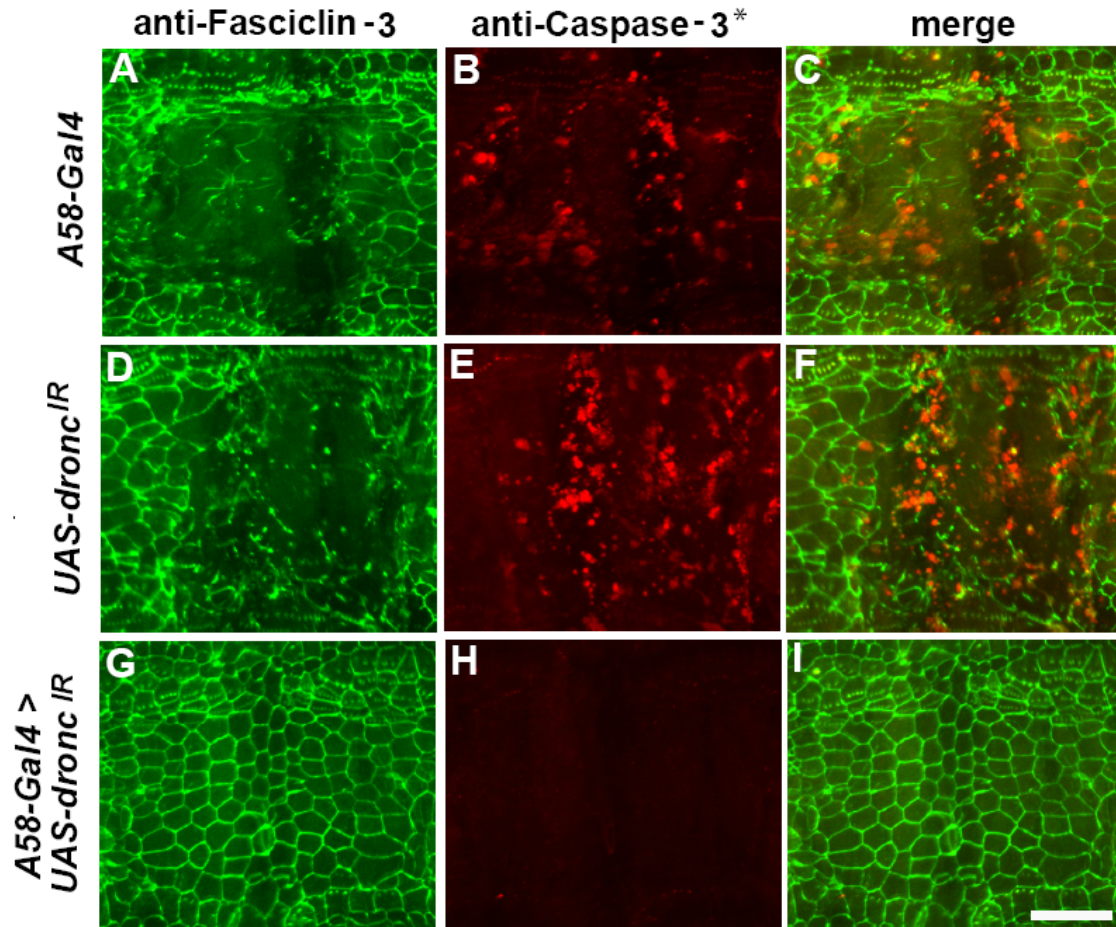


**Figure 3.10 Epidermal knockdown of Dronc blocks UV-induced cell death**

Epidermal whole-mounts with epidermal cell membranes labeled with anti-Fasciclin III (green) and apoptotic cells labeled with anti-cleaved caspase-3 (red). Epidermal cell death was assessed with expression of the *A58-Gal4* driver alone (A-C), *UAS-dronc<sup>IR</sup>* alone (D-F) or both *A58-Gal4* and *UAS-dronc<sup>IR</sup>* in combination (G-I). Scale bar (I) is 100  $\mu$ m. Originally published in (65), and reproduced with permission.

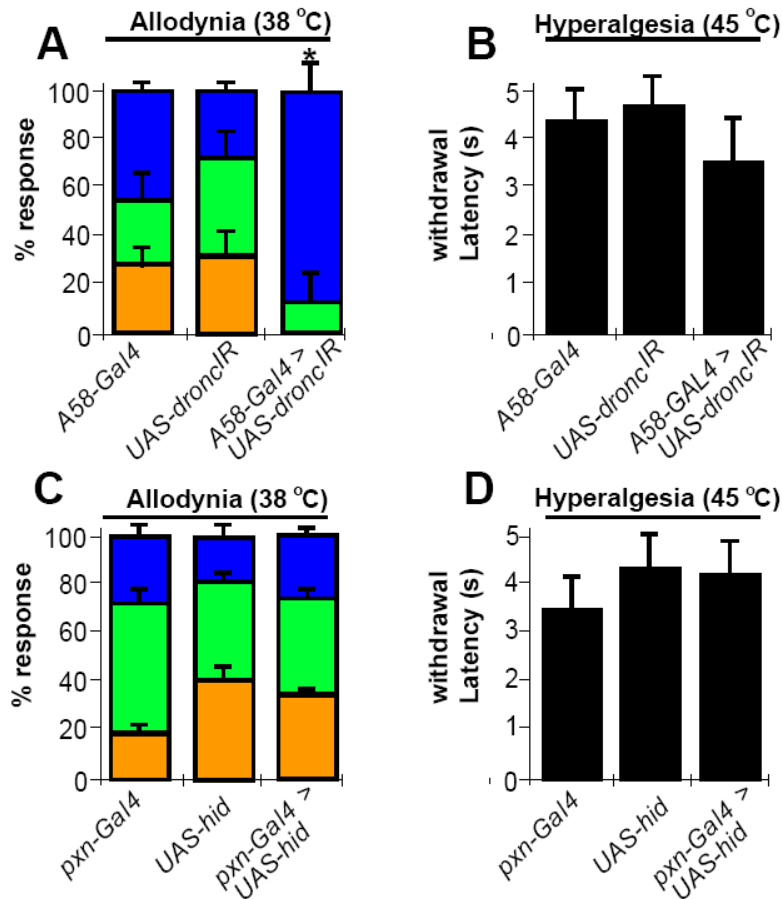


**Figure 3.11 Epidermal cell death is required for development of thermal allodynia**

(A) UV-induced thermal allodynia 24 h post UV when inhibiting epidermal cell death.

Thermal allodynia proceeds in control larvae (A58-Gal4 driver alone or UAS-dronc<sup>IR</sup> alone), but is significantly dampened when the transgenes are expressed together.

P<0.001 by Fisher's Exact test. (B) Assessment of UV-induced thermal hyperalgesia 8 h post UV when inhibiting epidermal cell death. Thermal hyperalgesia occurs in all cases.

(C-D) Assessment of UV-induced thermal allodynia (C) 24 h post UV and hyperalgesia

(D) 8 h post UV when hemocytes are ablated. Thermal allodynia and hyperalgesia occur in all cases. 3 sets of n = 30 (A & C) and n = 50 (B & D). Error bars represent S.E.M.

Originally published in (65), and reproduced with permission.

Necrosis Factor-alpha (TNF $\alpha$ ) homolog, Eiger (74). We found that larvae trans-heterozygous for two *eiger* null mutations (*egr<sup>1</sup>/egr<sup>3</sup>*) (74) failed to develop thermal allodynia following UV exposure (Figure 3.12 A). Because the epidermis appeared to be the only damaged tissue in our sunburn assay, we hypothesized that Eiger may be released from the damaged epidermal cells and act on the TNF Receptor, Wengen (75), in the nociceptors. To test this, we knocked down expression of Eiger via an RNAi transgene (*UAS-eiger<sup>IR</sup>*) in the epidermis. We found that epidermal knockdown of Eiger was sufficient to completely block thermal allodynia, suggesting that the epidermis is the source tissue of Eiger. We observed the same phenotype when knocking down Wengen (*UAS-wengen<sup>IR</sup>*) specifically in nociceptors using *ppk1.9-Gal4* (76), suggesting that the Eiger released from epidermal cells acts directly on nociceptors via Wengen.

To test whether the role of Eiger and Wengen in thermal allodynia is dependent on UV damage, we constitutively activated the TNF signaling pathway in nociceptors by over-expressing Eiger (*UAS-eiger<sup>GS9830</sup>*) (74). While neither the expression of the Gal4 driver nor the UAS construct alone provided a hypersensitive response in the absence of tissue damage, the combination resulted in thermal allodynia (Figure 3.12 B). Thus, activation of the TNF signaling pathway in nociceptors is sufficient to induce thermal allodynia even in the absence of tissue damage.

Although TNF signaling is a known regulator of nociceptive hypersensitivity, it is primarily known for its role in cell death (77). Because of this, we believed that blocking Eiger, like Dronc, prevented the development of thermal allodynia by interfering with epidermal cell death. To test this, we irradiated *eiger* null mutant larvae and examined whether epidermal cell death was blocked. We found that the mutant

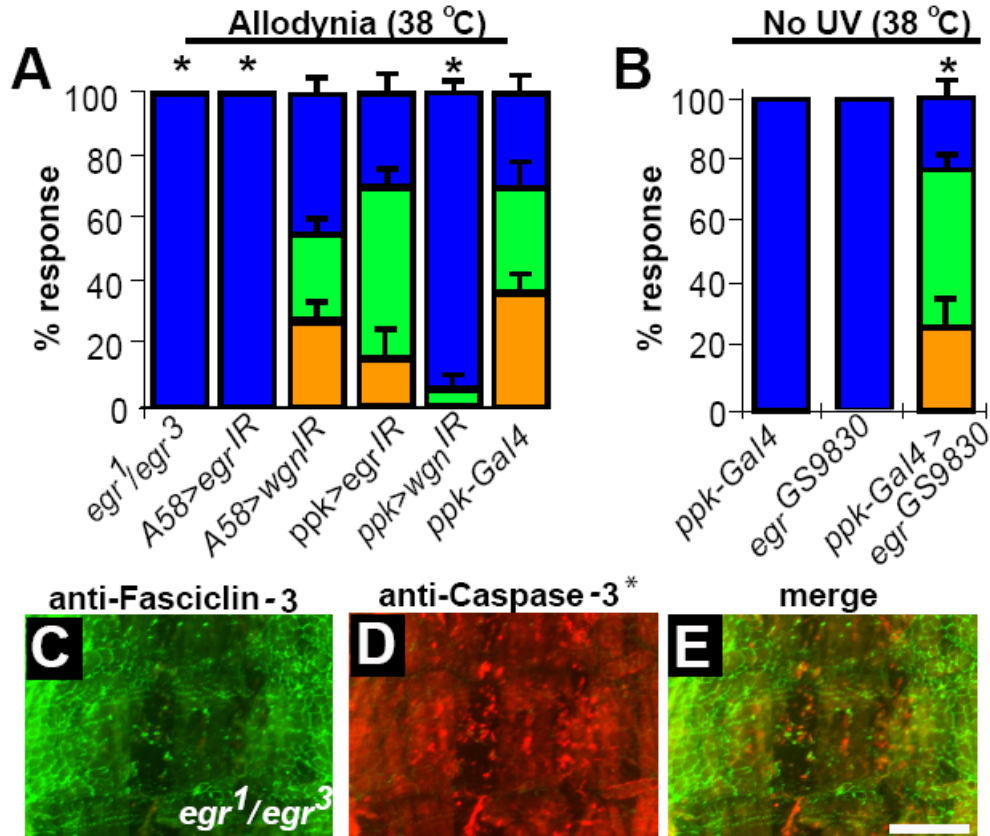


**Figure 3.12 TNF signaling mediates UV-induced thermal allodynia**

(A) Assessment of thermal allodynia 24 h after UV exposure in *eiger* null mutants (*egr<sup>1</sup>/egr<sup>3</sup>*), after knockdown of *eiger* in the epidermis (*A58>egr<sup>IR</sup>*) and nociceptors (*ppk>egr<sup>IR</sup>*), and after knockdown of *wengen* in the epidermis (*A58>wgn<sup>IR</sup>*) and nociceptors (*ppk>wgn<sup>IR</sup>*).  $P < 0.001$  by Fisher's Exact test. 3 sets of  $n = 30$  for each condition. (B) Assessment of thermal allodynia by over-expression of *eiger* (*UAS-egr<sup>GS9830</sup>*) in nociceptors in the absence of UV damage. 3 sets of  $n = 30$  for each condition. (C-E) Whole-mount of *eiger* null mutants 24 h after UV exposure. Epidermal cells are labeled with anti-Fasciclin III (green) and apoptotic cells are labeled with anti-cleaved caspase-3 (red). Scale bar (E) is 100  $\mu\text{m}$ . Error bars represent S.E.M.

Originally published in (65), and reproduced with permission.

larvae still showed epidermal apoptosis 24 hours following UV damage as assessed by morphological damage to epidermal cells and Caspase-3 staining (Figure 3.12 C-E), demonstrating that the role of TNF signaling in thermal allodynia does not involve UV-induced cell death.

To examine if Eiger and Wengen interfere with the development of thermal hyperalgesia, we knocked down expression of Eiger in the epidermis and Wengen in nociceptors using the same methodology used to test for allodynia. We measured the withdrawal latency to a normally noxious stimulus of 45 °C under mock treatment conditions, as well as 8 hours following UV exposure (78). We found that thermal hyperalgesia developed in all cases, illustrated by a significantly lower withdrawal latency following UV damage (Figure 3.13 A). We also found that TNF signaling did not interfere with baseline nociceptive signaling in the absence of tissue damage, as withdrawal responses were identical to those of control larvae at various temperatures (Figure 3.13 B). This demonstrates that TNF signaling is required for the development of thermal allodynia, but not hyperalgesia or baseline nociception.

Combined, these data illustrate a model of damage-induced nociceptive hypersensitivity in *Drosophila* larvae (Figure 3.14), where UV irradiation induces Drone activation in exposed epidermal cells. This damage results in the release of Eiger from damaged epidermal cells, which can directly target nearby nociceptors via Wengen.

## **Discussion**

These results demonstrate that *Drosophila* larvae serve as a useful model for isolating genes required for the development of nociceptive hypersensitivity. Larvae

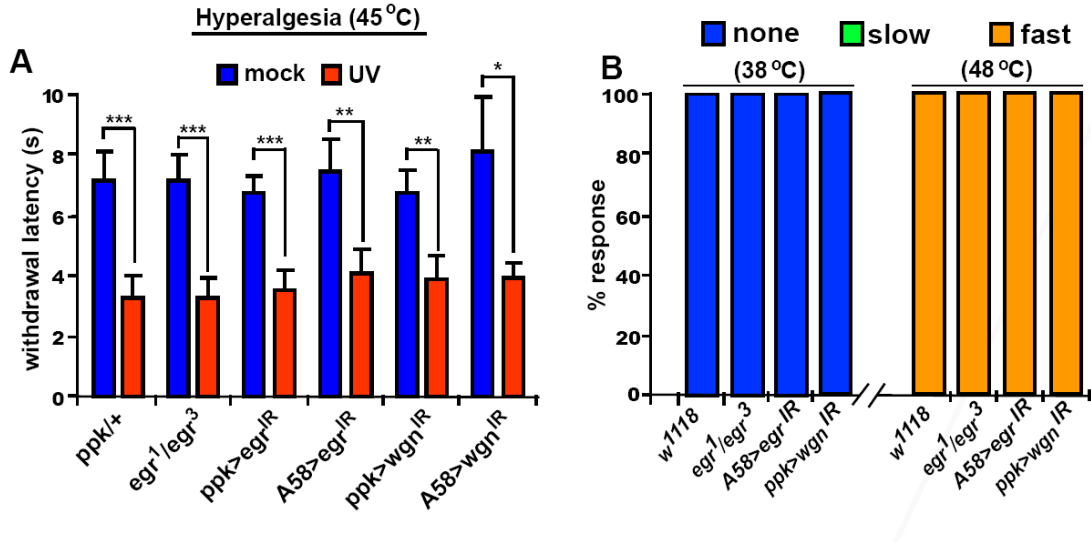


**Figure 3.13** TNF signaling does not affect thermal hyperalgesia or baseline nociception

(A) Assessment of thermal hyperalgesia 8 h after UV exposure in *eiger* null mutants (*egr<sup>1</sup>/egr<sup>3</sup>*), after knockdown of *eiger* in the epidermis (*A58>egr<sup>IR</sup>*) or nociceptors (*ppk>egr<sup>IR</sup>*), and after knockdown of *wengen* in the epidermis (*A58>wgn<sup>IR</sup>*) or nociceptors (*ppk>wgn<sup>IR</sup>*). Thermal hyperalgesia developed in all cases. \*\*\* =  $p < 0.001$ , \*\* =  $p < 0.01$ , and \* =  $p < 0.05$  by Student's t test.  $n = 50$  for each condition. (B)

Assessment of baseline nociception in the absence of tissue damage for the same conditions listed above. Larvae of all genotypes responded the same as control larvae to both 38 °C and 48 °C stimuli. 3 sets of  $n = 30$  for each genotype. Error bars represent S.E.M. Originally published in (78, panel A), and (65, panel B), and reproduced with permission.



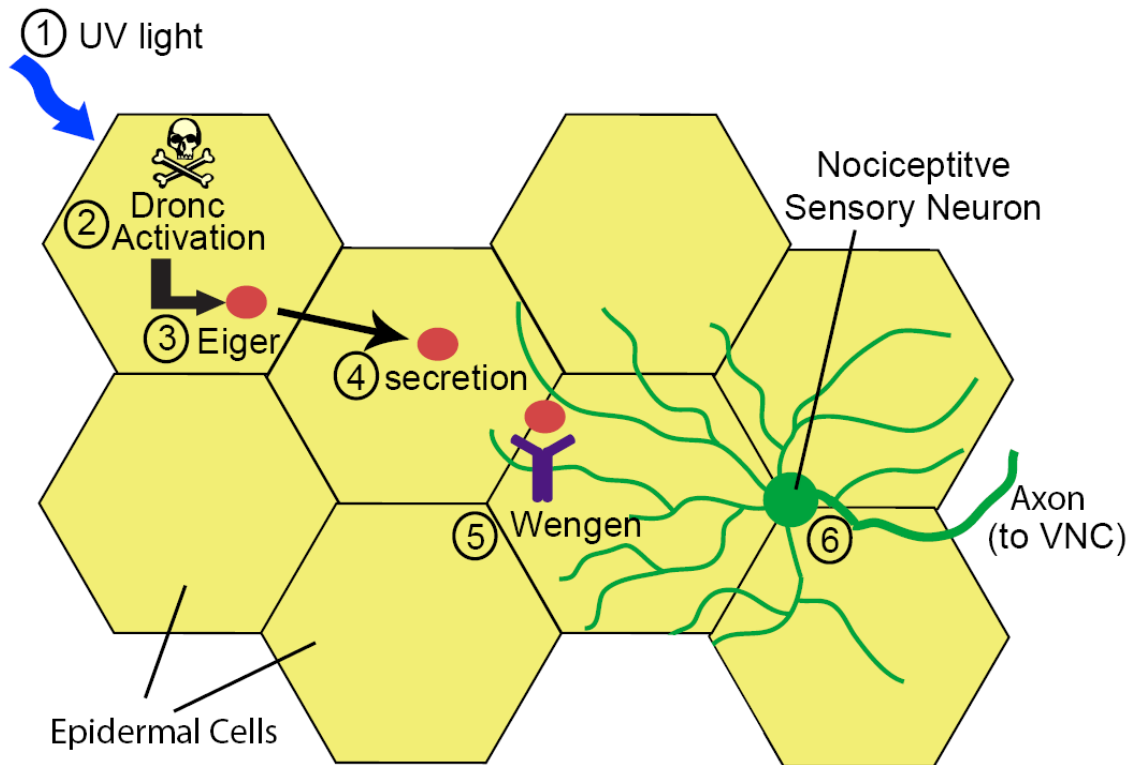


**Figure 3.14 Model for TNF-mediated thermal allodynia**

Overview of events involved in UV-induced thermal allodynia. UV radiation targets epidermal cells (1), which leads to Dronc activation and apoptosis (2). Next, Eiger is either activated or produced (3) and subsequently released or secreted from damaged epidermal cells (4), acting directly on nearby nociceptors via Wengen (5). Activation of Wengen leads to signaling events that allow the nociceptor to become hypersensitive (6).

VNC = Ventral Nerve Cord. Originally published in (65), and reproduced with permission.

develop both thermal allodynia and thermal hyperalgesia following UV irradiation, allowing the possibility of identifying genes mediating distinct forms of hypersensitivity. The requirement of conserved genes in the TNF signaling pathway for the development of thermal allodynia suggests that genes discovered in this system will likely be relevant to mammalian biology as well.

Our data suggest a direct signaling mechanism where damaged epidermal cells release Eiger that acts on nearby nociceptors via Wengen (Figure 3.14). In vertebrates there is large support of an indirect signaling mechanism, whereby circulating macrophages and neutrophils release TNF $\alpha$  and set off an inflammatory cascade (5, 7). In this model, only the downstream mediators, not TNF $\alpha$  itself, physically interact with nearby nociceptors. However, there is growing evidence that a direct signaling mechanism from damaged cells is also involved. TNF $\alpha$  is expressed by human keratinocytes, and this expression increases following UV damage (79, 80). Other studies demonstrated that exposure to TNF $\alpha$  alone is sufficient to modulate the firing properties of neurons (81-85). Perhaps the most useful test would be a tissue-specific knockdown of TNF $\alpha$  in skin cells or the TNF Receptors in nociceptors using mice. Thus, it is possible that the role of TNF signaling works via direct and indirect mechanisms in vertebrates to modulate nociceptive hypersensitivity.

It is unclear how the UV damage causes the release of Eiger from epidermal cells. Over-expression of *eiger* in larval epidermal cells is lethal (data not shown), suggesting that Eiger is either produced after UV damage or kept sequestered from Wengen within the cell. We originally hypothesized that the role of Eiger in development of thermal allodynia was related to the epidermal apoptosis due to the

observation that inhibiting cell death via Dronc knockdown also prevented thermal allodynia. However, our later findings suggested that apoptosis and allodynia are completely separable processes. We found that epidermal knockdown of Eiger prevented the development of thermal allodynia but not apoptosis, while knockdown of Hid, which induces cell death, inhibited epidermal apoptosis but did not affect the development of thermal allodynia (Figure 3.15). Since epidermal apoptosis is not necessary for thermal allodynia, there could be a non-apoptotic function of Dronc in the Eiger-induced hypersensitivity. There are a number of non-apoptotic functions of caspases (86, 87), including processing cytokines into activated forms (88, 89). Interleukin-1 $\beta$ , for example, is cleaved into an activated form by caspases in mammalian cells (90). TNF $\alpha$  also requires processing to be activated (91-94). Although this has not been demonstrated specifically for Eiger, it could be possible that caspase-mediated processing promotes an activated form of Eiger following UV damage.

Our results also reveal a number of differences between the development of UV-induced thermal allodynia and thermal hyperalgesia (Table 3.1). Although the onset of both forms of hypersensitivity can be seen as early as 4 hours post UV, hyperalgesia peaks at 8 hours while allodynia does not peak until much later at 24 hours. This suggests that allodynia and hyperalgesia may be regulated by distinct mechanisms. To further this suggestion, Dronc activity along with TNF signaling are required for the development of thermal allodynia, while neither have an effect on hyperalgesia. Some researchers have suggested that allodynia and hyperalgesia function via one common mechanism, assessed by the observation that both forms of hypersensitivity usually

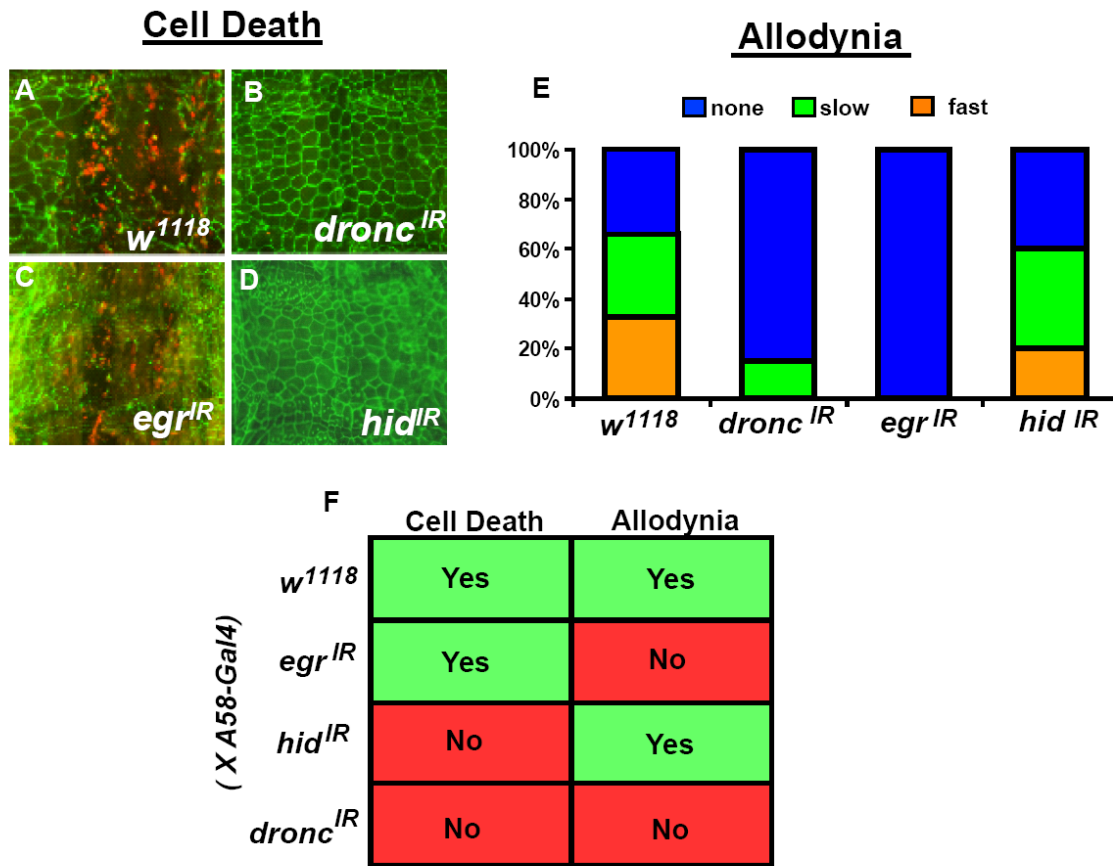


**Figure 3.15 Separation of UV-induced cell death and allodynia**

(A-D) Analysis of UV-induced epidermal cell death using whole-mounts with Fasciclin III (green) and cleaved caspase-3 (red) staining 24 h after UV. *A58-Gal4* larvae were crossed to *w<sup>1118</sup>* (A), *UAS-dronc<sup>IR</sup>* (B), *UAS-eiger<sup>IR</sup>* (C), and *UAS-hid<sup>IR</sup>* (D). (E) Analysis of UV-induced thermal allodynia using a 38 °C 24 h after UV exposure in the same conditions listed above. n = 30 for each condition (F) Comparison of UV-induced cell death and allodynia in control larvae or those with epidermal knockdown of *eiger*, *hid*, or *dronc*.

	Allodynia	Hyperalgesia
onset	4 h	4 h
peak	24 h	8 h
return to baseline	48 h	16 h
role of hemocytes	independent	independent
role of <i>dronc</i>	dependent	independent
role of TNF signaling	dependent	independent

**Table 3.1 Differences between development of thermal allodynia and hyperalgesia**

Comparison between the development of UV-induced thermal allodynia and hyperalgesia, including differences in onset and duration as well as dependence on epidermal cell death, hemocytes, and TNF signaling.

occur together (95). If this were the case, then a genetic distinction between the two processes would not be useful. Our results, however, clearly demonstrate the ability to genetically separate allodynia and hyperalgesia. Further studies should demonstrate whether allodynia and hyperalgesia operate by completely distinct pathways, or if there is a level of convergence at some point (Figure 3.16).

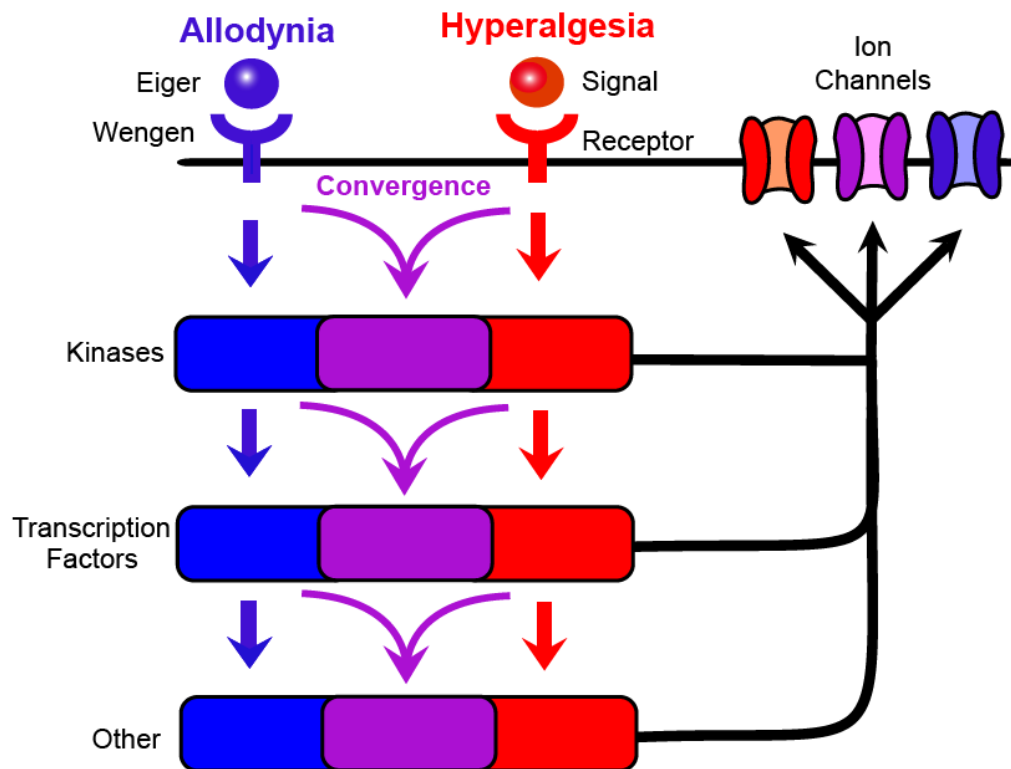


**Figure 3.16 Possible relationships between the regulation of thermal allodynia and hyperalgesia**

The development of thermal allodynia (blue) in *Drosophila* larvae is mediated by TNF signaling. Hyperalgesia is independent of TNF signaling, presumably because it is regulated by separate mechanisms (red). The mechanisms regulating these different forms of hypersensitivity may be completely independent of one another. In contrast, there could be convergence of these mechanisms at various levels of intracellular signaling (purple). These convergence points could be kinases, transcription factors, or other possible downstream targets such as temperature-sensitive ion channels.

Originally published in (78), and reproduced with permission.

## **Chapter 4: Genetic screen for UV-induced thermal allodynia**



## **Introduction**

The results from the previous chapter demonstrate the utility of a genetically tractable model of nociceptive hypersensitivity using *Drosophila* larvae. The identification of Eiger and Wengen as essential for the development of thermal allodynia illustrates how tissue-specific knockdown of target genes can identify conserved regulators of damage-induced hypersensitivity. Moving forward, a major strength of this model is the potential to uncover novel mediators of nociceptive hypersensitivity. To accomplish this, we designed a screen to identify genes that are required within nociceptors for the development of thermal allodynia following UV damage.

We used the Gal4/UAS system (67) to drive gene expression only in nociceptors. To knock down target genes of interest by RNA-interference, we expressed transgenes composed of an inverted-repeat (IR) sequence of a gene that is flanked by an Upstream Activation Sequence (UAS). This type of screening strategy offers several advantages to traditional mutagenesis screens. First, this strategy allows the researcher to target a specific gene of interest. The only limitation to this is the availability of an RNAi transgene for that particular gene. There are a number of stock centers supplying these flies, including the Vienna Drosophila Resource Center (96) as well as the National Institute of Genetics in Japan (<http://www.shigen.nig.ac.jp/fly/nigfly/index.jsp>). With over 85% genome coverage between these sources, there is a large pool of available gene targets. Another key advantage to using a tissue-specific screening strategy is that it does not interfere with the need for a particular gene at an earlier developmental stage or in other tissues. Since a tissue-specific knockdown strategy has been very effective in our laboratory for assessing epidermal wound closure (97), we hypothesized that this

would also serve as a useful strategy to identify novel mediators of nociceptive hypersensitivity.

## **Results**

### Description of Screening strategy

To begin screening for genes required for the development of UV-induced thermal allodynia, we obtained approximately 300 fly stocks bearing UAS-RNAi constructs. This initial list targeted genes coding for known membrane proteins. In particular, we targeted ion channels, G-Protein-Coupled Receptors (GPCRs), and neuropeptide receptors (98-100), along with a small set of kinases. We began with this set of genes due to our previous observation that nociceptor-specific knockdown of Wengen, a membrane receptor for TNF signaling, prevented the development of thermal allodynia. Since signaling from damaged epidermal cells is required for this nociceptive hypersensitivity, we hypothesized that a number of other membrane proteins are involved as well.

Tissue-specific knockdown of the target genes was achieved by mating flies bearing the UAS-RNAi constructs to flies bearing the nociceptor-specific *ppk1.9-Gal4* driver (Figure 4.1). Progeny were raised at 25 °C for 5 days until they reached the third larval instar. Early third-instar larvae were UV irradiated using the standard sunburn assay, and then assessed for the development of thermal allodynia by testing responsiveness to a 38 °C stimulus 24 hours after UV exposure. Positive hits were scored if larvae bearing an RNAi transgene targeting a particular gene displayed a significantly dampened response to the stimulus. To assess whether the gene affected baseline nociception or a specific inability to become hypersensitive, a final test was

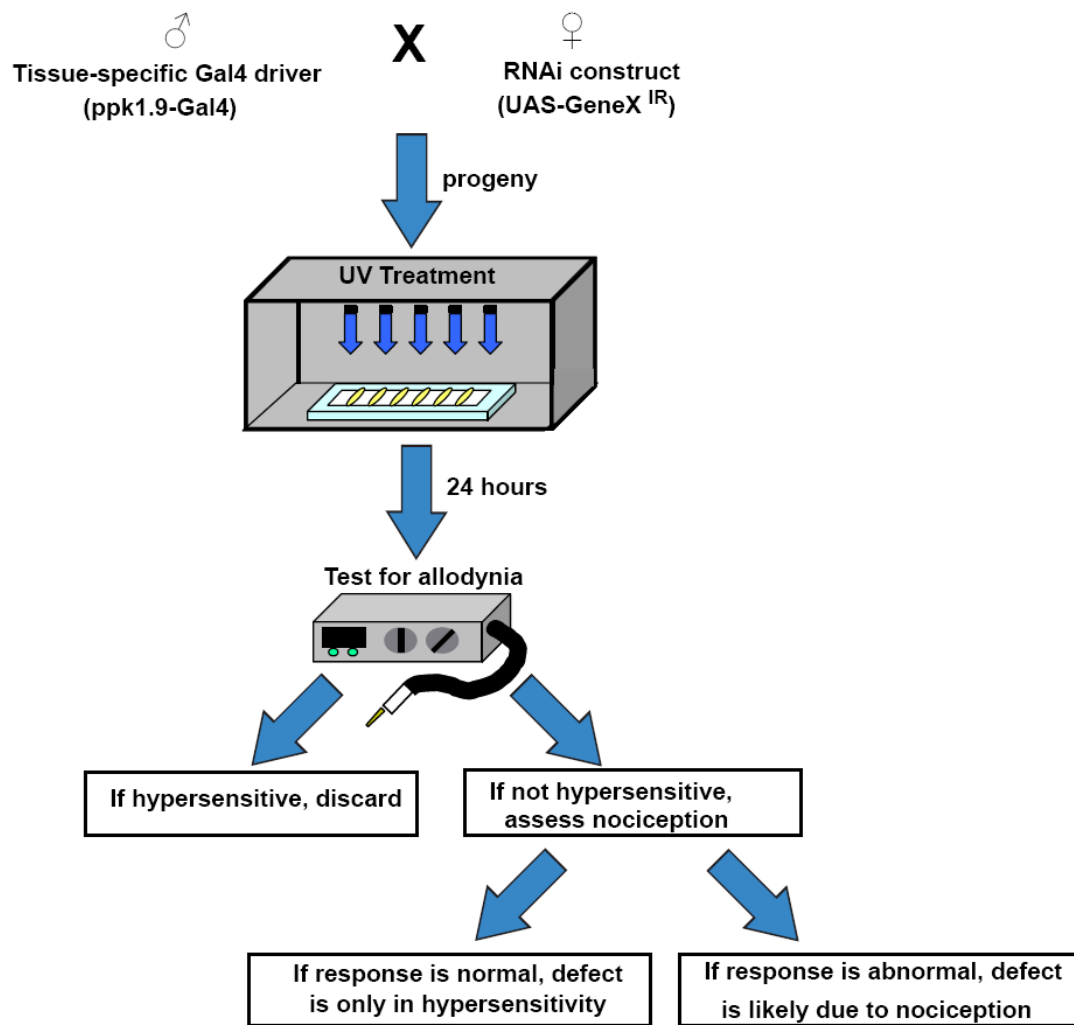


**Figure 4.1 Flowchart for a thermal allodynia screen**

Flies bearing RNAi transgenes were crossed to *ppk1.9-Gal4* flies. Progeny larvae receive UV treatment, and were assessed for thermal allodynia at 38 °C 24 h post UV. If larvae failed to sensitize, baseline nociception was examined at 48 °C to test whether the gene specifically regulates damage-induced hypersensitivity.

conducted where baseline nociception was measured in the absence of UV damage at both 45 °C and 48 °C. We measured the withdrawal latencies to both stimuli, and any lines that had significantly slower response times to these stimuli were categorized as having impaired baseline nociception. If the response to noxious stimuli was normal, then the deficit was categorized as specific to allodynia.

#### Screen reveals a number of novel mediators of thermal allodynia

We obtained 18 positive hits out of our initial pool of 275 target genes (Table 4.1), giving a hit rate of 6.5%. Some of these genes appear to interfere with baseline nociception, but most of them only affect the damage-induced hypersensitivity (Figures 4.2 and 4.3). Among the positive hits are three unnamed “orphan” receptors (CG15327, CG10830, and CG6749). These genes are listed as encoding GPCR’s based on their sequences, but they have not been characterized functionally in any published work. We also identified *Tachykinin-like receptor (Tacr99D)* (101), which is functionally equivalent to the mammalian Substance P Receptor, a key mediator of nociceptive signaling (102). This finding further suggests that there is likely a great deal of conservation in signaling mechanisms in nociceptive hypersensitivity between *Drosophila* and mammals.

Our screen also identified several ion channels. In addition to *painless*, the first identified gene required for nociception in *Drosophila* (19), we also identified *TRPA1* and *inactive (iav)*. TRPA1 is known to mediate thermotaxis (103) while *iav* is required for hearing (104, 105), although neither of these channels had a known role in nociception. The genes in this category all displayed a defect in baseline nociception,

Gene name	CG#	Description
?????	15327	(GPCR) No known function
??????	10830	(GPCR) No known function
CG6749	6749	(GPCR) No known function
dorsal	6667	similar to mammalian Rel/NF- $\kappa$ B. Dorsoventral polarity during embryogenesis
inactive	4536	(Ion Channel) TRP channel necessary for hearing in <i>Drosophila</i>
Or92a	17916	(GPCR) Odorant receptor
p38a	5475	Kinase involved in many processes, including hyperalgesia in mammals
painless	15860	(Ion Channel) TRP channel necessary for thermal pain in <i>Drosophila</i>
pkc53 $\epsilon$	6622	Kinase involved in many processes, including hyperalgesia in mammals
pkd2	6504	cation channel involved in feeding behavior, and smooth muscle contraction
porin2	17137	Ion channel activity
punt	7904	Receptor in TGF-Beta signaling pathway
smoothened	11561	Hedgehog signaling
Takr99D	7887	(GPCR) Tachykinin--like receptor
thickveins	14026	Receptor in TGF-Beta signaling pathway
traf3	4394	Associating factor in TNF signaling pathway
traf6	10961	Associating factor in TNF signaling pathway
TRPA1	5751	(Ion Channel) TRP channel necessary for thermotaxis in <i>Drosophila</i>

**Table 4.1 Genes regulating thermal allodynia in nociceptors**

List of genes that prevent the development of thermal allodynia when knocked down via RNAi in nociceptors. This list includes the name, gene identification number (CG#), and a short description of known functions for each gene.

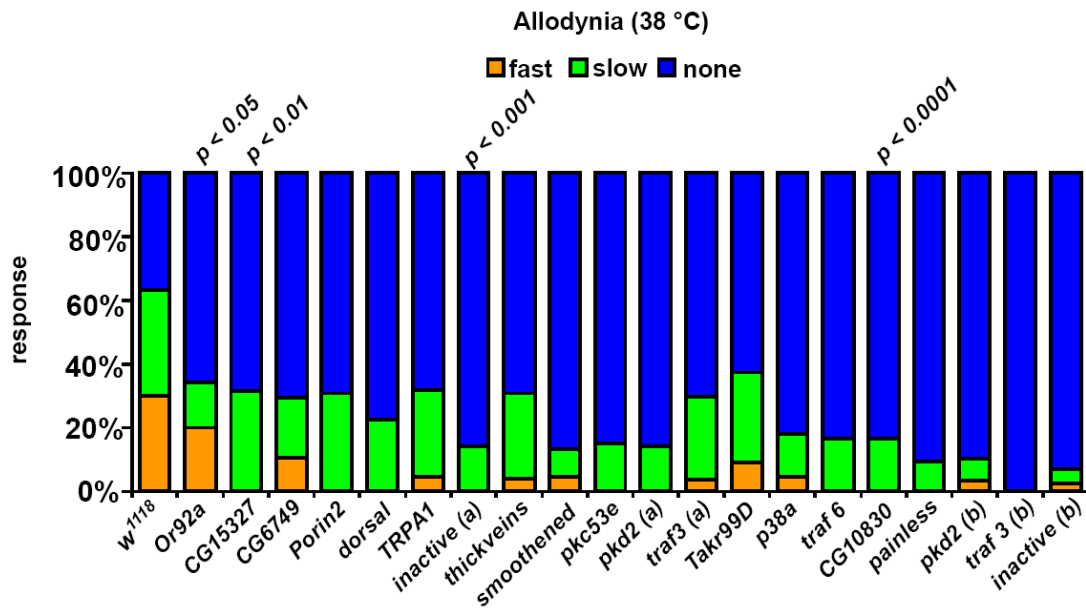


**Figure 4.2 Analysis of genes involved in UV-induced thermal allodynia**

Assessment of thermal allodynia 24 h after UV exposure when genes (listed in Table 3.1) are knocked down in nociceptors. p-value cut-off points are listed using Fisher's Exact test. n = 30 for each genotype.

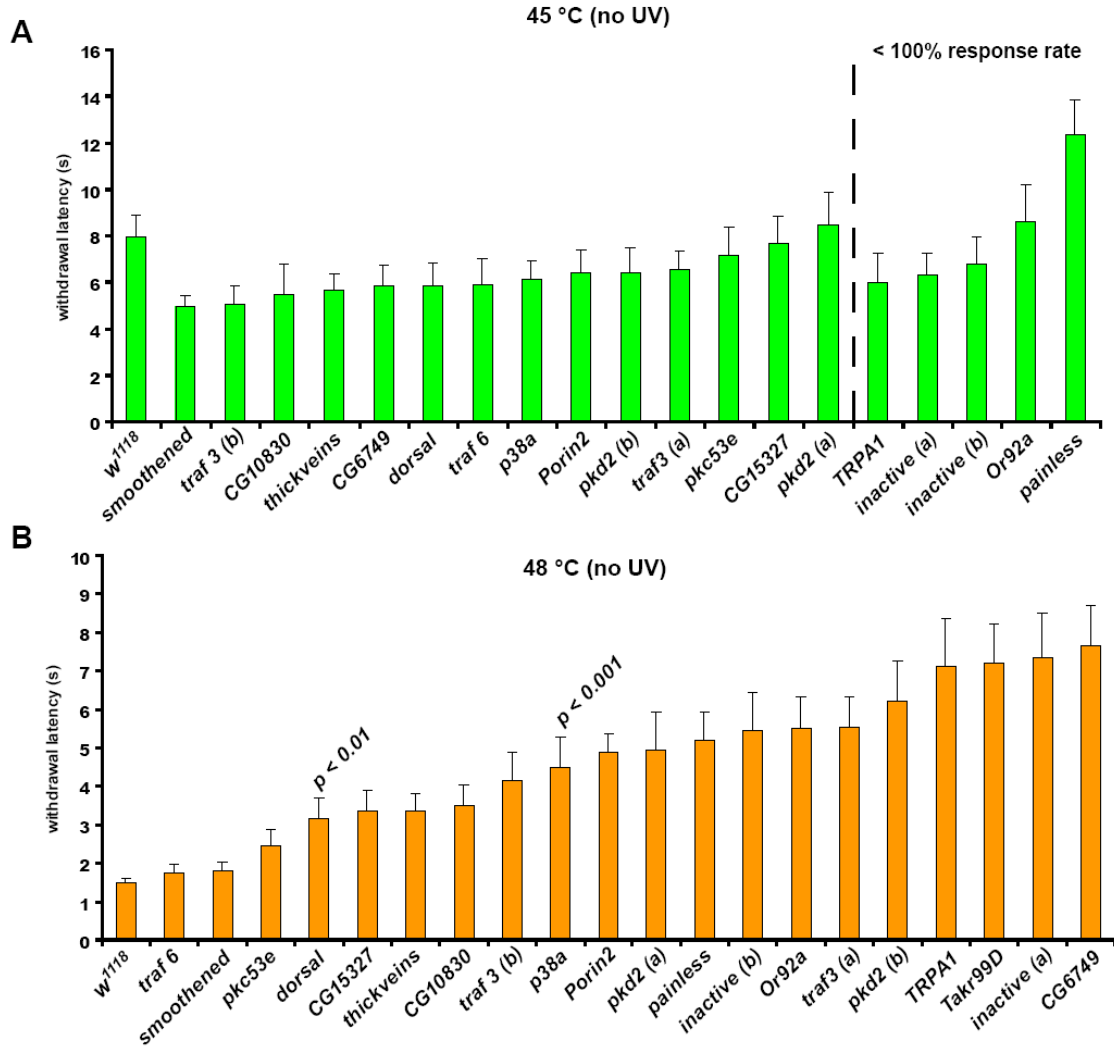


**Figure 4.3 Baseline nociception in positive hits from screen**

Preliminary assessment of baseline nociception at 45 °C (A) and 48 °C (B) when genes (listed in Table 3.1) are knocked down in nociceptors. p-value cut-off points are listed using Student's T test. n = 30 for each genotype. Error bars represent S.E.M.

suggesting that these could be downstream targets of the signaling mechanisms involved in the development of thermal allodynia.

In addition to the membrane proteins, we also targeted genes encoding possible downstream signaling components. The MAP Kinase p38 along with an isoform of Protein Kinase-C (PKC) are both required for thermal allodynia. Since our previous results identified *eiger* and *wengen*, we tested other TNF signaling components, identifying TNF Receptor Associating Factor-3 and -6 (*traf3* and *traf6*). We also found *dorsal* (*dl*), the homolog of the transcription factor Nuclear Factor-kappa B (NF- $\kappa$ B). Although there is only a small link between *dorsal* and *wengen* in *Drosophila* (106), NF- $\kappa$ B is clearly involved in TNF signaling in mammals and plays a prominent role in the maintenance of nociceptive signaling (107, 108).

Finally, we identified components of well-conserved signaling pathways that were never implicated in mediating nociception. These genes include *thickveins* (*tkv*), a receptor in Transforming Growth Factor-Beta (TGF $\beta$ ) signaling (109), along with *smoothened* (*smo*), a central component of Hedgehog (Hh) signaling (110, 111). The identification of these genes illustrates a potential role for morphogen signaling pathways in the regulation of nociceptive signaling. To uncover how these signaling pathways could modulate nociceptive hypersensitivity, we investigated the role of Smo and other Hh signaling components in more detail.

#### Hh signaling mediates thermal allodynia and hyperalgesia

Hh signaling is required for a number of developmental processes, including embryonic patterning (111), cell fate specification (112), axon guidance (113, 114), and proliferation (115). Although Hh and other morphogens are secreted from dying cells to



induce compensatory proliferation in *Drosophila* imaginal discs (116-120), it is unclear whether these signals can also modulate nociceptive signaling. Since knockdown of Smoothed in nociceptors prevents the development of thermal allodynia following UV damage, we investigated the role of other Hh signaling components in this process.

In canonical Hh signaling, Hh binds to and inhibits its receptor, Patched (Ptc). This binding relieves inhibition of the transmembrane protein, Smoothed (Smo), and leads to signal transduction via the kinase Fused (Fu), the end result of which is activation of the transcription factor Cubitus Interruptus (Ci). Activated Ci turns on expression of target genes such as *decapentaplegic* (*dpp*) and *engrailed* (*en*). To examine whether Hh signaling acts within nociceptive sensory neurons and through components of the canonical pathway, we expressed various transgenes that target components of the Hh signaling pathway using the *ppk1.9-Gal4* driver. We found that over-expression of Patched (*UAS-Ptc*) (121) severely limited development of thermal allodynia 24 hours post UV (Figure 4.4 A). In control larvae (*ppk1.9-Gal4* alone) about 70% of larvae exhibited aversive withdrawal, with about half of these responding in less than 5 s. Expression of *UAS-Ptc* and other Hh-interfering transgenes resulted in under 20 % of larvae responding, almost all of which responded slowly (between 5 and 20 s). Interfering with Smoothed activity by expressing a dominant-negative form of the protein (*UAS-smo.5A*) (122) also limited the development of thermal allodynia, complementing the phenotype provided by expression of the Smoothed RNAi transgene. Development of thermal allodynia involves a transcriptional component, as expression of a dominant-negative form of the transcription factor Cubitus Interruptus

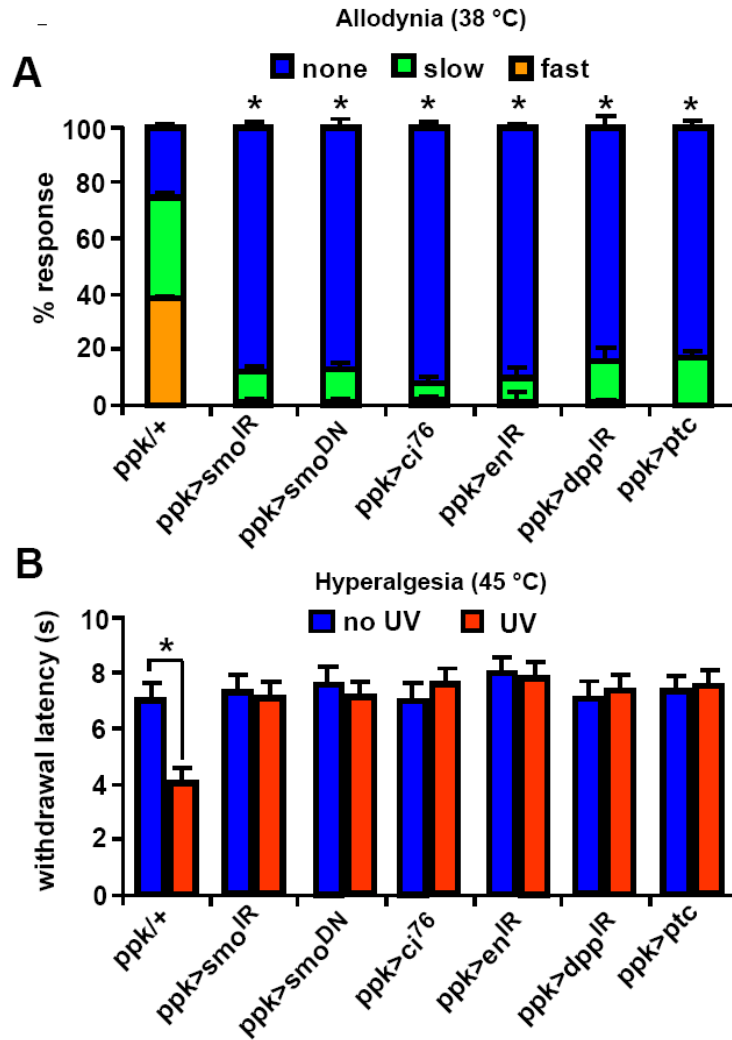


**Figure 4.4 Canonical Hh signaling mediates thermal allodynia and hyperalgesia**

(A-B) *ppk1.9-Gal4* drives (>) expression of the indicated UAS transgenes or no transgene (*ppk1.9-Gal4* x *w<sup>1118</sup>* = *ppk/+*) in nociceptors. (A) Assessment of thermal allodynia for larvae of indicated genotypes using a stimulus of 38 °C 24 h after UV treatment. n = 3 sets of 30 larvae per condition. (B) Assessment of thermal hyperalgesia for larvae of indicated genotypes using a 45 °C stimulus without UV and 8 h after UV treatment. n = 50 larvae per genotype. IR = Inverted Repeat. DN = Dominant Negative. Error bars represent S.E.M.

(*UAS-ci<sup>76</sup>*) (123) prevented the hypersensitivity. Finally, interfering with transcriptional targets of the Hh pathway, including *engrailed* and *dpp*, also prevented thermal allodynia. Together, these results demonstrate that the role of Smoothed in the development of thermal allodynia functions within the canonical Hh signaling pathway.

We also examined whether Hh signaling is required for the development of thermal hyperalgesia following UV damage. We tested larvae of the same genotypes mentioned above for hyperalgesia by stimulating the larvae at 45 °C 8 hours after UV exposure. We found that the average withdrawal latency to this stimulus decreased from 6.9 to 3.9 seconds in control larvae, but there was no decrease in withdrawal latency after interfering with Hh signaling (Figure 4.4 B). Thus, Hh signaling in nociceptors mediates both thermal allodynia and hyperalgesia. This is in contrast to the role of TNF signaling in our model, which only affects thermal allodynia.

While Hh signaling is required for thermal allodynia and hyperalgesia, blocking the pathway had no effect on baseline nociception. In the absence of tissue damage, there were no significant impairments to withdrawal latency measured at 45 °C, with all larvae withdrawing within our 20 s cutoff, and 48 °C, with all larvae withdrawing rapidly (Figure 4.5). Thus, Hh signaling in nociceptors mediates tissue damage-induced changes in the behavioral response threshold without affecting baseline nociception.

To assess whether Hh itself is required for nociceptive hypersensitivity, we tested larvae bearing a temperature-sensitive allele of *hedgehog* (*hh<sup>ts2</sup>*) (124), where Hh signaling is impaired at 29 °C. As with control larvae (*w<sup>1118</sup>*), the *hh<sup>ts2</sup>* mutant larvae did not display an aversive withdrawal behavior in response to a normally subthreshold stimulus of 38 °C when maintained at a permissive temperature of 18 °C. 24 hours after

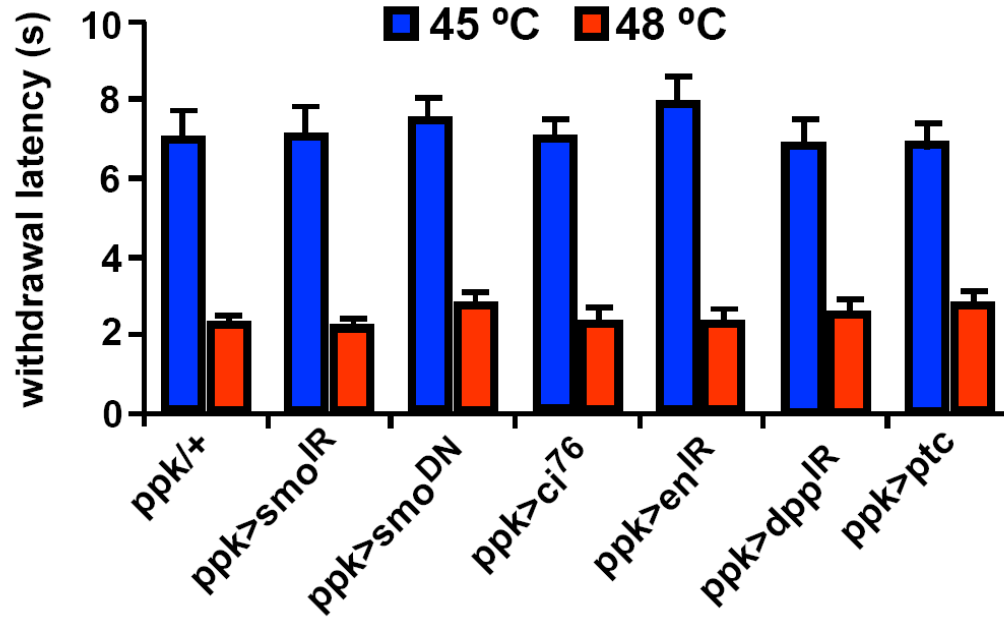


**Figure 4.5 Hh signaling in nociceptors does not affect baseline nociception**

*ppk1.9-Gal4* drives (>) expression of the indicated UAS transgenes or no transgene (*ppk1.9-Gal4* x *w<sup>1118</sup>* = *ppk/+*) in nociceptors. Assessment of baseline nociception for larvae of indicated genotypes using 45 °C and 48 °C stimuli in the absence of tissue damage. n = 50 larvae per condition. Error bars represent S.E.M.

UV exposure, thermal allodynia was observed in both groups when the normally subthreshold stimulus elicited a withdrawal response from the majority of larvae (Figure 4.6 A). However, if the larvae were shifted to a restrictive temperature of 29 °C after UV exposure, the development of thermal allodynia was almost completely blocked in the *hh<sup>ts2</sup>* mutants. We also tested larvae bearing this allele for thermal hyperalgesia. In *w<sup>1118</sup>* or *hh<sup>ts2</sup>* mutant larvae raised at the permissive temperature, a noxious stimulus of 45 °C normally elicited a withdrawal response within 7-8 seconds. 8 hours after exposure to UV, this response was nearly twice as fast, with an average withdrawal latency of 4.2 seconds (Figure 4.6 B). This exaggerated response to noxious stimuli occurred in *hh<sup>ts2</sup>* mutants maintained at the permissive temperature, but was completely absent when the larvae were shifted to the restrictive temperature following UV exposure. Together, these results identify Hh as a critical mediator of thermal allodynia and hyperalgesia.

We also tested whether activation of the Hh pathway in nociceptive sensory neurons results in the development of hypersensitivity in the absence of tissue damage. Constitutive activation of the pathway was achieved by expression of a dominant-negative form of the Hh repressor Patched (*UAS-ptc<sup>1130X</sup>*) (125) or a form of Smoothened that cannot bind to the downstream kinase, Fused (*UAS-Smo<sup>Afu</sup>*) (126). In both cases, we found that non-irradiated larvae exhibited a robust response to a normally subthreshold stimulus of 38 °C (Figure 4.7 A) and displayed an exaggerated response to a normally noxious stimulus of 45 °C (Figure 4.7 B). Together, these results demonstrate that ectopic activation of the Hh signaling pathway can evoke thermal allodynia and hyperalgesia even in the absence of tissue damage.

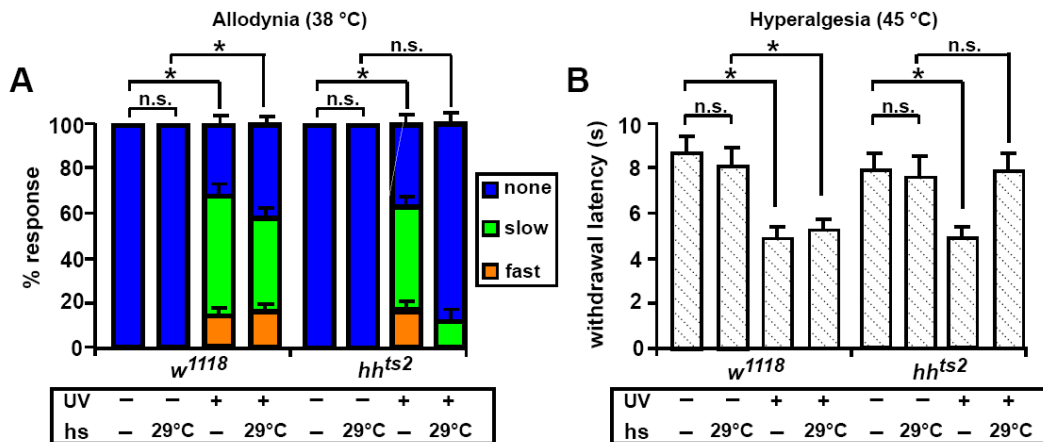


**Figure 4.6 Hh mutants fail to develop thermal allodynia and hyperalgesia**

(A) Assessment of thermal allodynia in both control (*w<sup>1118</sup>*) and *hh* mutant (*hh<sup>ts2</sup>*) larvae. Responses were categorized as “no response” (blue), “slow response” (green), and “fast response” (orange). Development of thermal allodynia was assessed with and without UV damage, and in the presence or absence of a 24 h heat-shock at 29 °C after treatment. n = 3 sets of 30 for each condition. (B) Assessment of thermal hyperalgesia under the same conditions listed above, except measuring withdrawal latency to a 45 °C stimulus 8 h after treatment, and an 8 h heat-shock after treatment, as listed. n = 50 larvae per condition. Error bars represent S.E.M.

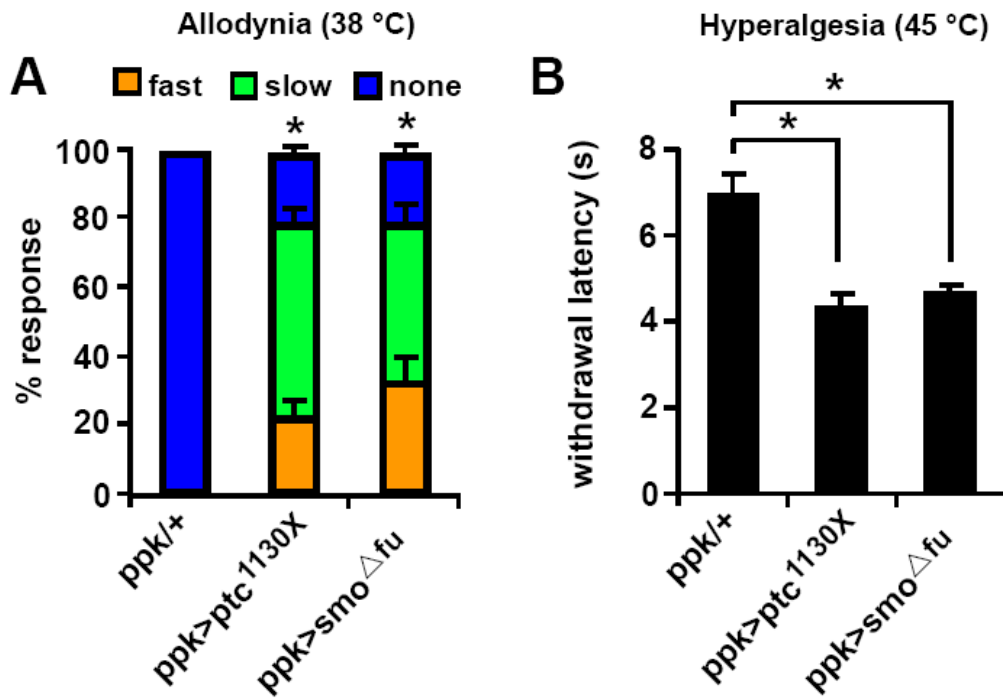


**Figure 4.7 Hh signaling in nociceptors is sufficient for thermal allodynia and hyperalgesia**

Constitutive activation of Hh signaling in the absence of UV irradiation produced thermal allodynia to a 38 °C stimulus (A) and thermal hyperalgesia to a 45 °C stimulus (B). n = 3 sets of 3 larvae for each condition in A, and n = 50 larvae per condition in B. Error bars represent S.E.M.

Since Hh and TNF signaling are both required for the development of thermal allodynia following UV damage, we performed genetic epistasis experiments to test whether Hh-mediated thermal allodynia depends on TNF signaling or vice versa (Figure 4.8 A). To determine whether TNF and Hh signaling depend upon each other in the development of thermal allodynia, we constitutively activated one pathway while simultaneously interfering with the other. As expected, blocking TNF signaling by knocking down nociceptive sensory neuron expression of Wengen dampened ectopic Eiger-induced thermal allodynia (Figure 4.8 B). When Hh signaling was impaired via knockdown of Smoothed, however, the TNF-induced thermal allodynia was not affected, suggesting that Smoothed does not act downstream of TNF in mediating thermal allodynia. Conversely, thermal allodynia caused by constitutive activation of Hh signaling via a dominant-negative form of Patched was dampened by knocking down expression of Smoothed (Figure 4.8 B). When TNF signaling was impaired upon simultaneous Hh activation, however, the Hh-induced thermal allodynia was not blocked, suggesting that TNF signaling is not downstream of Hh in mediating thermal allodynia. Together, these results suggest that TNF- and Hh-induced thermal allodynia operate by distinct and parallel mechanisms.

The Hh signaling pathway is well conserved from flies to mammals, with homologous components present at nearly every level of the pathway (110). It appears that Hh signaling also plays an important role in the development of nociceptive hypersensitivity in mammals, as pharmacological blockade of the pathway via application via cyclopamine (127, 128) prevented analgesic tolerance to morphine analgesia in a rat model of inflammatory pain. Cyclopamine also synergistically augmented morphine



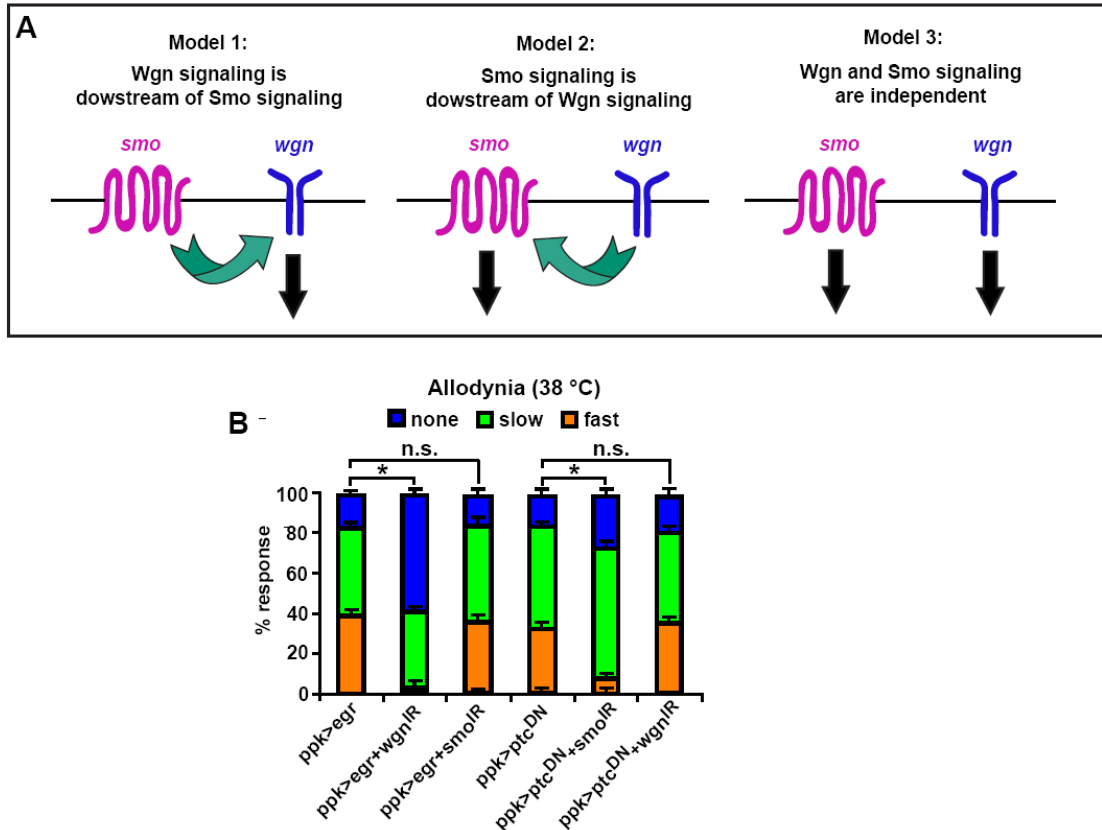


**Figure 4.8 TNF and Hh signaling mediate thermal allodynia independently**

(A) Models illustrating potential relationships between TNF and Hh signaling in the development of thermal allodynia. (B) Behavioral response to a normally non-noxious 38 °C stimulus upon activation of Hh ( $UAS-ptc^{1130X} = ptc^{DN}$ ) or TNF ( $eiger^{GS9830} = egr$ ) signaling in the presence or absence of transgenes blocking each pathway ( $UAS-wengen^{IR}$  to block TNF or  $UAS-smo^{IR}$  to block Hh). \*,  $p < 0.01$  with Fisher's Exact Test. IR = Inverted Repeat. DN = Dominant Negative. N = 3 sets of 30 larvae per condition. Error bars represent S.E.M.

analgesia in a rat model of inflammatory pain (Howard Gutstein, personal communication). Thus, our results demonstrating the requirement of Hh signaling in the development of thermal allodynia are relevant to vertebrate biology, and reveal a novel set of potential therapeutic targets for the alleviation of pain.

### Multiple TRP channels mediate thermal nociception

Further analysis of the TRP channels identified from our screen revealed differences between these channels in their ability to regulate thermal nociception. As previously reported, *painless* mutants show a defect in the detection of noxious stimuli just above the nociceptive threshold. At much higher temperatures such as 55 °C, however, the withdrawal response of *painless* mutants is indistinguishable from controls (19), suggesting that the channel is responsible for detecting only a small range of noxious temperatures. To examine whether one of the other TRP channels identified in our screen mediates noxious temperatures over a different range, we knocked down expression of *painless* or *inactive* in nociceptors and measured withdrawal behavior over a range of noxious temperatures (Figure 4.9). We found that knockdown of *painless* significantly impaired responses at 45 °C compared to controls. At progressively higher temperatures, however, this defect began to diminish, with equivalent responses to control larvae at temperatures above 50 °C. In contrast, we found that knockdown of *inactive* had no effect at 45 °C, but had a defect emerge at higher temperatures of 48 °C and above. This suggests that *inactive* covers a temperature range that is higher than that of *painless*. This is similar to the class of TRPV channels in mammals, where each type of channel responds to a specific range of temperatures (129-131).

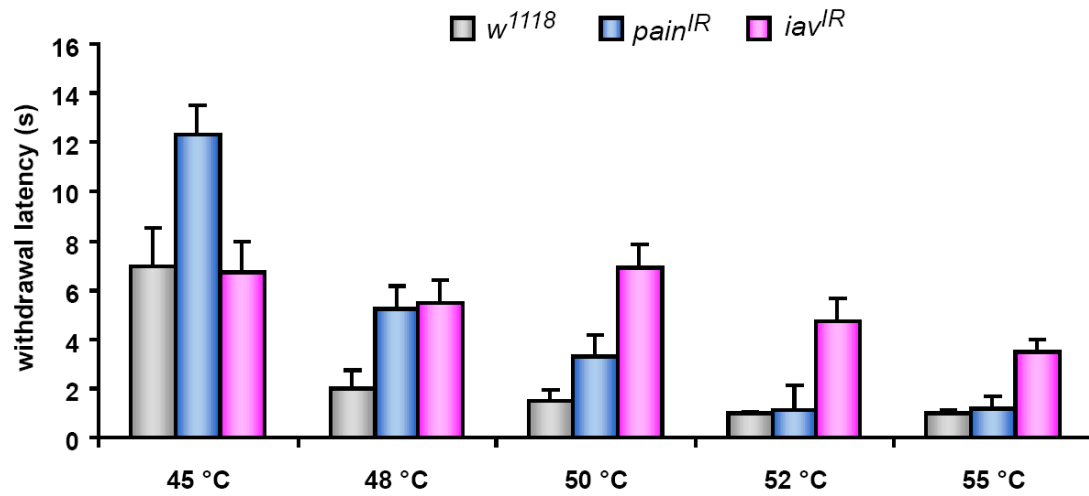


**Figure 4.9 Painless and Inactive respond to a different range of noxious temperatures**

Withdrawal behavior in response to noxious thermal stimuli. *ppk1.9-Gal4* was crossed to *w<sup>1118</sup>* (control) as well as *UAS-iav<sup>IR</sup>* and *UAS-pain<sup>IR</sup>* for nociceptor-specific knockdown of these genes. n = 30 for each condition. Error bars represent S.E.M.

Evidence also suggests that these channels may act together as components of a larger complex. The TRPV channels Inactive and Nanchung, for example, co-localize and depend on each other to function properly to mediate hearing in *Drosophila* chordotonal organs (104). In *c. elegans*, the TRPV Channel proteins OSM-9 and OCR-2 are thought to form a heteromeric channel (132). More recently, TRP channels have been shown to form complexes with each other (133, 134) as well as with other ion channels (135). Knocking these genes down in various combinations in the future should provide further insight as to how these channels regulate nociceptive signaling.

## **Discussion**

The results of our preliminary screen revealed several novel mediators of nociceptive hypersensitivity. We showed the requirement of both TNF and Hh signaling pathways, which appear to act independently in the development of thermal allodynia. It will be important to determine whether the other genes isolated in this screen function within either of these pathways or through additional separate mechanisms. A combination of GPCRs, ion channels, kinases, and transcription factors mediate thermal allodynia, and expansion of the screen will likely identify additional classes of molecules regulating this hypersensitivity.

Another point to consider is how these mediators function within nociceptors to cause thermal allodynia. There are a number of possible mechanisms underlying nociceptive hypersensitivity, including modulation of membrane receptors and ion channels. Sodium channels are well-known targets of modulation, including the mammalian sodium channel Na<sub>v</sub>1.7, which is expressed in dorsal-root ganglia (DRG)

neurons and implicated in several human pain disorders (136). Mutations in the channel (137) or phosphorylation by Extracellular signal-Regulated Kinase (ERK) (138) alter its gating properties, resulting in increased current amplitude and slow deactivation in response to small depolarizations. Application of TNF $\alpha$  to isolated rat DRG neurons also modulates ion channels within nociceptors. TNF $\alpha$  causes hyperexcitability by simultaneously increasing current through sodium channels while limiting current through potassium channels (81), although it is not known if Eiger performs the same functions in *Drosophila* nociceptors. TRP channels, particularly the capsaicin receptor TRPV1, are also phosphorylated by inflammatory mediators (139). Researchers have identified a number of phosphorylation sites on the intracellular portions of the channel (140, 141). Some of these sites are phosphorylated by PKC, which increases the channels probability of opening (11, 12), while other sites are targeted by PKA, which reverses desensitization of the channel (13).

In addition to altering receptors and channels present in the membrane, hypersensitivity could arise due to an increased membrane density of these proteins. At the level of transcription, inflammatory signals increase expression levels of sodium channels, TRPA1, and TRPV1 (142-144). Channels sequestered in intracellular vesicles may also be trafficked to the plasma membrane to increase sensitivity (10, 145, 146).

An increase in synaptic strength could also play a large role in the development of thermal allodynia. In *Drosophila* neuromuscular junctions (NMJs), for example, NF- $\kappa$ B signaling regulates postsynaptic glutamate receptor density (147), while retrograde BMP signaling regulates the number and size of boutons in the presynaptic motor neuron (148-150). While it is unknown whether these same mechanisms are at work in

*Drosophila* nociceptors, the strength of the synapse between nociceptive DRG neurons and cells in the dorsal horn of the spinal cord is a major contributor to nociceptive hypersensitivity in mammals (2). Dissection of the nociceptive circuitry in *Drosophila* would be useful to study this potential mechanism. Although the general projection areas of these neurons were recently discovered (151), their precise targets are currently unknown. Given the positive hits identified in our screen so far, any or all of these mechanisms seem plausible.

Future work will include characterization of the remaining positive hits in a manner similar to that done for *smoothened*. Future screening will encompass any remaining GPCRs and ion channels. A separate screen for the development of thermal hyperalgesia will also be useful. We know that Hh signaling mediates both allodynia and hyperalgesia, while TNF signaling is confined to allodynia. It will be interesting to see if there are any mediators that specifically regulate hyperalgesia. Characterizing these genes should provide greater insight regarding the cellular and molecular mechanisms underlying damage-induced nociceptive hypersensitivity.

## **Chapter 5: Conclusions and future directions**

The results up to this point have answered many questions regarding how the immune system and the nervous system react to local tissue damage. As with most studies, however, they have also introduced a number of interesting questions themselves. Described here are some of the most interesting avenues to pursue in future studies.

#### Future directions for wound-induced inflammation

##### *(1)-screen for genes required for wound attachment*

The finding that wound-induced inflammation in larvae is regulated by adhesive capture of circulating hemocytes advances our understanding of how the immune system recognizes and responds to damaged tissue. An important next step is to identify the molecular mechanisms underlying this recognition and subsequent attachment. A tissue-specific RNAi screen would be useful to isolate genes required either within hemocytes or epidermal cells for adhesive capture of hemocytes to damaged tissues. Using semi-quantitative analysis (see Figure 2.8), larvae could be scored live for the amount of hemocyte accumulation at epidermal wound sites. Genes that are found to be required for attachment to wound sites could also be tested for the ability to detect non-native tissues. This may reveal whether the mechanisms responsible for wound-induced inflammation can distinguish between “damaged” and “non-self” tissues.

##### *(2)-potential differences between sessile and circulating hemocytes*

The results shown here illustrate two apparently separate populations of larval hemocytes: wound-responsive cells in circulation, and sessile cells bound to tissues that are not responsive to epidermal wounds. As previously mentioned, a recent study found



that the population of sessile hemocytes is capable of forming lamellocytes in response to invading pathogens (35) and mechanical disruption of the barrier cuticle (152). Perhaps these cells respond to signals indicative of pathogen invasion as opposed to tissue damage itself. Our results distinguish between these two populations of cells based on motility (circulating or sessile) and their responsiveness to epidermal wounds. It is unclear, however, whether there are any genetic differences between these two groups. Identifying any potential differences in these populations would allow us to fluorescently label or manipulate gene expression in one or both groups. Can the circulating hemocytes form lamellocytes as well? Are these populations completely separate, or can these cells shift between groups? Identifying the functions of these populations of hemocytes should help to address these questions and determine how the larval immune system responds to cellular damage and infection.

#### Future directions for damage-induced nociceptive hypersensitivity

##### *(1)-Different modes of tissue damage*

All of the damage-induced nociceptive hypersensitivity shown thus far is a result of UV damage. It will also be interesting to test whether other forms of tissue damage cause hypersensitivity. Using other modes of tissue damage to induce nociceptive hypersensitivity may reveal shared mechanisms as well as those exclusive to one type of damage. Some of the genes involved in thermal allodynia, for example, may be acting solely in response to UV damage, just as there are several genes involved in cell death that respond specifically to DNA damage associated with UV irradiation (60). Alternative modes of tissue damage would likely include pinch-wound and puncture-

wound assays (16), both of which would be well-suited for this type of analysis. One obvious difference between the UV and wounding assays evident from preliminary data is the onset and duration of hypersensitivity. Whereas the morphological damage to the epidermis took several hours to appear following UV irradiation, the damage is immediate using the wounding assays. This may account for the faster onset of accompanying hypersensitivity as compared to using the UV damage assay (Figure 5.1). The amount of tissue damage is also very different in the wounding assays. While the UV damage spans the entire length of the larvae on the exposed side, both wounding assays cause localized epidermal damage within a single body segment. Thus, it is possible that the nociceptive behavioral response will depend greatly on the proximity of the noxious stimulus to the wound site. Most importantly, these different modes of tissue damage may reveal additional mediators of nociceptive hypersensitivity, revealing potential treatment options for specific forms of damage.

## *(2)-Exploring different types of noxious stimuli*

Up to this point, our studies have focused on nociceptive hypersensitivity elicited by noxious thermal stimuli. However, *Drosophila* larvae may also be a useful model organism in which to study hypersensitivity to other forms of noxious stimuli. In mammals, different classes of nociceptors respond to various types of noxious stimuli. While some respond specifically to exceedingly hot or cold temperatures, others respond to mechanical force or to chemical cues. There are also a number of “polymodal” nociceptors, which respond to a wide variety of noxious stimuli (2).

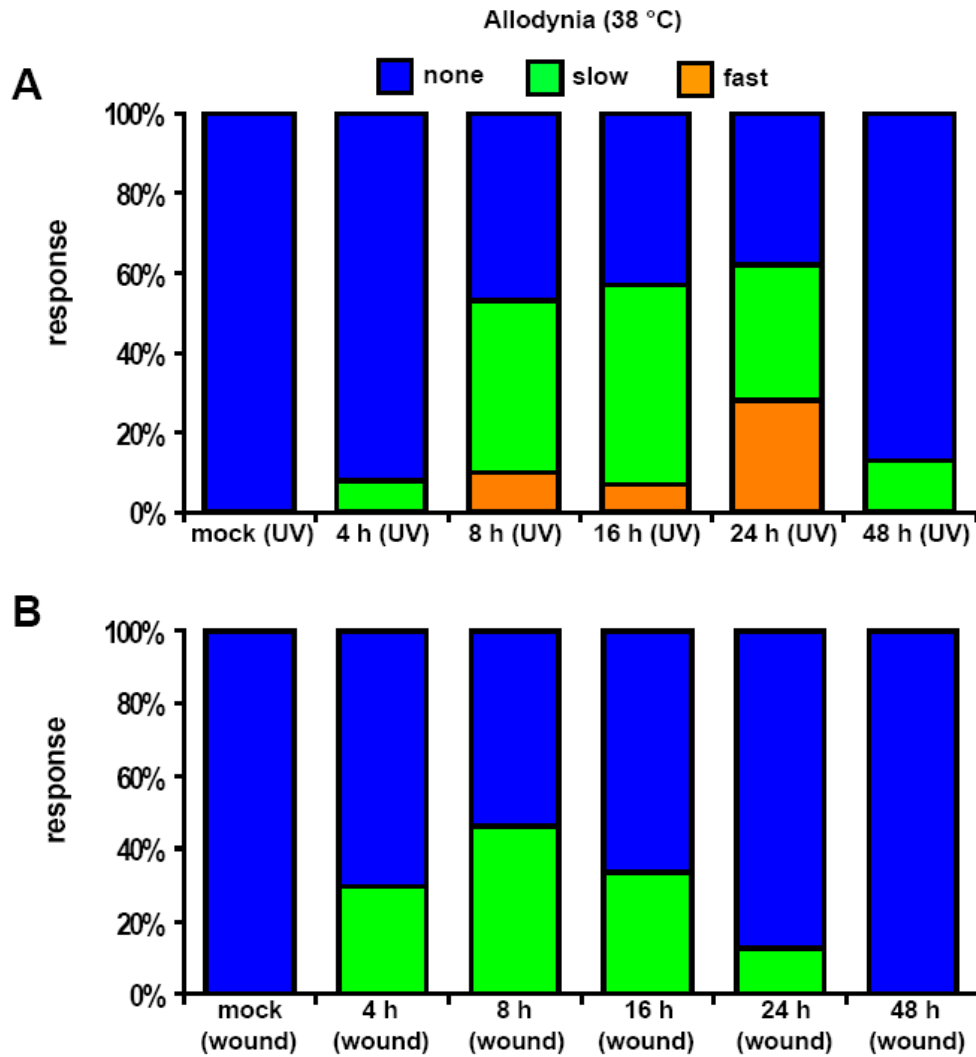


**Figure 5.1 Comparing wound-induced to UV-induced thermal allodynia**

Measurement of withdrawal responses to a normally subthreshold stimulus of 38 °C in mock-treated larvae and at various time-points following UV treatment (A) or wounding (B). Responses were marked as “no response” (blue), “slow response” (green) or “fast response” (orange). n = 30 for each condition.

The Class IV dendritic arborization neurons are the only identified nociceptors in *Drosophila* larvae. Although most of the nociception assays used in the larvae involve thermal nociception, these cells also mediate mechanical nociception, making them polymodal in nature (19, 43). A useful set of experiments could be to determine whether tissue damage affects the mechanical nociceptive threshold in the same way that it influences thermal nociception. These experiments would likely be identical to those described in Chapter 2, but noxious test stimuli would be delivered using von Frey filaments rather than the heat probe. Additionally, nociceptive hypersensitivity could be analyzed in response to noxious cold stimuli. Specific TRP channels in mammals, particularly TRPM8, detect cold environmental stimuli (153, 154). *Drosophila* larvae can distinguish between warm and cool temperatures in thermotaxis (103, 155), and this distinction is made through activation of specific TRP channels (156). Whether *Drosophila* larvae respond to noxious cold stimuli, however, is unknown. These experiments will likely help to identify the differences in modality-specific nociception, as well as the mechanisms underlying damage-induced hypersensitivity in each case.

### *(3)- Identifying the circuitry for nociception in Drosophila larvae*

A major strength of using *Drosophila* as a model organism to study nociception is the ability to manipulate gene expression in specific tissues. The goal of our studies to this point was to identify mediators of nociceptive hypersensitivity that act specifically within primary nociceptors. However, there are also likely to be changes further downstream in nociceptive signaling that have an impact on damage-induced hypersensitivity. To this end, it will be helpful to identify the neurons downstream of

the primary nociceptors. The terminals of nociceptors are located in the dorsal neuropil in the head region (151), but the specific cellular targets are unclear. There are a number of available Gal4 lines that drive expression in distinct subsets of *Drosophila* neurons (157). We can assess whether any of these lines target expression in the nociceptive pathway by blocking synaptic transmission via expression of a tetanus toxin (*UAS-TeTxLC*) (158) and testing the resulting nociceptive threshold. Of particular interest are the cellular targets immediately downstream of the primary nociceptors. Alterations in synaptic strength between these neurons may parallel “central sensitization” in mammals, characterized by a strengthened connection between primary nociceptors and downstream Dorsal Horn neurons (2).

#### *(4)- Drosophila larvae as a model for chronic hypersensitivity*

Identifying the molecular mediators of damage-induced nociceptive hypersensitivity is certainly relevant for the treatment of chronic pain disorders in humans. It is unclear if *Drosophila* will be able to serve as a model for this directly, although there are a number of worthwhile possibilities. The most straightforward way of testing this is to use a time-point where the UV-induced allodynia and/or hyperalgesia is diminished. For allodynia, this would be approximately 48 hours after UV irradiation (Figure 3.7). It may be possible to search for a condition where the peak response at 24 hours persists throughout the entirety of larval development. While this type of hypersensitivity would be considered chronic since it would be measured after the damaged tissue is healed (see Figure 3.4), it would not provide much time past the 48-hour time-point to assess any further changes due to the onset of metamorphosis. One

possible method for eliminating this issue is to use mutants that remain in larval development for exceedingly long periods. For example, some *ecdysoneless* (*ecd*) mutants remain larvae for up to 21 days under certain conditions (159). This would allow changes to be assessed following UV damage for much longer, although one would have to take into account any possible effects that the initial mutation may have on nociceptive hypersensitivity itself. One final possibility is to use adult *Drosophila* to model damage-induced hypersensitivity. There is a model of nociception in adult *Drosophila* as assessed by a “jumping assay” (160), and this could also be used to test for hypersensitivity after tissue damage. Although the assay is very labor-intensive, this method would allow chronic changes to be studied for a longer duration than with the larval assays.

Even if *Drosophila* cannot be used to directly model chronic pain disorders, the results from our system at the very least provide other model systems with a list of potential molecular targets to treat these disorders. If the chronic pain is simply the result of components of the “hypersensitivity machinery” that fail to turn off after the damaged tissue is healed, then the genes identified in our system would be likely candidates for those components.

Interfering with the mediators responsible for nociceptive hypersensitivity is a major strategy for the treatment of inflammatory pain syndromes. Blocking TNF $\alpha$  with a neutralizing antibody, for example, has been used with some success in treating the accompanying pain in rheumatoid arthritis (161). A similar approach is also being carried out for antagonists of NGF (162). Thus, the mediators of nociceptive

hypersensitivity uncovered in *Drosophila* could serve as potential therapeutic targets for the treatment of pain disorders.

Investigating these areas of interest should help to shed light on how the immune and nervous systems detect and respond to tissue damage.

## **Chapter 6: Materials and Methods**



## Fly stocks and Genetics

All fly stocks were maintained at 25 °C with the exception of temperature-sensitive mutants described below. The GAL4/UAS system (67) was used to drive targeted gene expression in the larval epidermis (*A58-Gal4*) (16), hemocytes (*Pxn-Gal4*) (17), and nociceptors (*ppk1.9-Gal4*) (76).

*Wound-Induced Inflammation:* *Nrg-GFP<sup>00305</sup>;Pxn-Gal4,UAS-2xEYFP* larvae were used for live imaging, carrying a *UAS-2xEYFP* transgene (34) to fluorescently label hemocytes and a protein-trap GFP insertion in *neuroglian* (*Nrg-GFP<sup>00305</sup>*) (33) to visualize epidermal cell membranes. A *UAS-lacZ.NZ* transgene (Bloomington stock center) was driven via *Pxn-Gal4* to visualize wound-adherent hemocytes using TEM. *Pxn-Gal4,UAS-GFP* was used to fluorescently label hemocytes and block GTPase activity by expression of *UAS-rac1.N17<sup>DN</sup>*, *UAS-rhoL.N25<sup>DN</sup>*, and *UAS-cdc42.N17<sup>DN</sup>* (163). *UAS-bsk<sup>DN</sup>* (164) was used to disrupt JNK signaling in the larval epidermis and block wound closure.

*Nociceptive Hypersensitivity:* *w<sup>1118</sup>* larvae were used as controls for all hypersensitivity experiments unless otherwise noted. *UAS-eGFP* (34) was used to fluorescently label nociceptors when driven with *ppk1.9-Gal4*. *UAS-droncIR* (National Institute of Genetics, Japan) was used to block apoptosis in larval epidermal cells, and *UAS-hid* (69) was used to eliminate larval hemocytes. *msn-lacZ* (165) served as a transcriptional reporter for JNK signaling and an indication of cellular stress (16). *eiger<sup>1</sup>* and *eiger<sup>3</sup>* (74) were used to test for the development of thermal allodynia in the absence of Eiger. *UAS-eiger<sup>IR</sup>* (74) and *UAS-wengen<sup>IR</sup>* (75) were used to knock down TNF signaling in the

larval epidermis and nociceptors. *eiger*<sup>GS9830</sup> (*UAS-eiger*) (74) was used to over-express *eiger* in nociceptors.

*Tissue-Specific screen for thermal allodynia:* The following *UAS-RNAi* lines were obtained from the Vienna Drosophila Resource Center (VDRC) (96): 6749 (44856) targeting CG6749; 6667 (45998) targeting Dorsal; 11561 (9542) targeting Smoothened; 4536 (7126) and (7128) targeting Inactive; 5475 (52277) targeting p38 MAPK; 15860 (39477) targeting Painless; 6622 (27699) targeting Protein Kinase C; 6504 (6941) targeting Polycystic Kidney Disease-2; 7904 (848) targeting Punt; 7887 (1372) targeting Takykinin-like Receptor 99D; 14026 (862) targeting Thickveins; 4394 (34836) targeting TNF Receptor Associating Factor-3; 10961 (16125) targeting TNF Receptor Associating Factor-6; and 5751 (37249) targeting TRPA1. We also tested the following *UAS-RNAi* lines from the National Institute of Genetics in Japan

(<http://www.shigen.nig.ac.jp/fly/nigfly/index.jsp>): 10830 (*R-1*) targeting CG10830; 17916 (*R-3*) targeting Odorant Receptor 92a; 15327 (*R-2*) targeting CG15327; 17137 (*R-1*) targeting Porin-2;

*The role of Hh signaling in nociceptive hypersensitivity:* For heat-shock experiments, UV- or mock-treated *hh*<sup>ts2</sup> (124) and paired *w*<sup>1118</sup> control larvae were raised at 18 °C until they reached the third larval instar to insure normal embryonic patterning. After treatment, larvae were either returned to the permissive temperature of 18 °C or placed at the restrictive temperature of 29 °C until assessment of thermal hyperalgesia (8 h, 45 °C) or thermal allodynia (24 h, 38 °C). We drove expression of UAS transgenes in larval nociceptive sensory neurons using *ppk1.9-Gal4* (76). *UAS-smo.5A* (122), *UAS-ptc* (121), *UAS-ci*<sup>76</sup> (123), and *UAS-dpp*<sup>IR</sup> (166) were used to inhibit Hh signaling, along

with the following *UAS-RNAi* lines from the VDRC: *11561 (9542)* targeting *Smoothed*; and *9015 (105678)* targeting *Engrailed*. *UAS-ptc<sup>1130X</sup>* (125) and *UAS-Smo<sup>Δfu</sup>* (126) were used to constitutively activate Hh signaling in nociceptors. The UAS-bearing EP allele *eiger<sup>GS9830</sup>* (74) was used to overexpress *eiger*. *UAS-wengen<sup>IR</sup>* (75) was used to inhibit TNF signaling.

### Pinch Wound Assay

Early third-instar larvae were lightly anesthetized with ethyl ether. Larvae were “pinched”, as originally described (16), by grabbing the dorsal side of the larvae with blunted #5 dissection forceps (Fine Science Tools) and squeezing for approximately 10 seconds. For consistency, all wounds were made in a single abdominal segment (A4, A5, or A6), centered between segment boundaries and between the dorsal trunks, two major branches of the tracheal system that run along the anterior-posterior axis. Larvae were returned to food at 25 °C immediately after wounding.

### Whole-mount preparation

Epidermal whole-mounts were prepared by dissection in Phosphate Buffered Saline (PBS) using fine dissection scissors (Fine Science Tools), #5 dissection forceps, and 0.1 mm pins. Larvae were pinned ventral-side-up at the anterior and posterior end on a Sylgard surface (Dow Corning Corporation). An incision was made along the entire ventral side of the larvae, and both sides along the incision were spread and pinned. For visual clarity, we removed many of the internal tissues with forceps. The remaining epidermal whole-mounts were fixed in 4% formaldehyde for 1 hour at room

temperature. Fixed samples were washed in PBS, and either stored briefly at 4 °C or immediately prepared for immunohistochemistry.

#### Whole-mount Immunofluorescence

Whole-mount samples were “blocked” by incubation for 1 hour at room temperature in PHT, a solution of PBS, Heat-inactivated normal goat serum (1%), Triton X-100 (0.3%), and Sodium azide (0.02%). After blocking, primary antibodies were added and incubated for 3 hours at room temperature or overnight at 4 °C. A list of primary antibodies and their concentrations (in PHT) is below. Samples were then washed 6 times in PHT. Next secondary antibodies were added and incubated in the dark for 3 hours at room temperature or overnight at 4 °C. A list of secondary antibodies and their concentrations (in PHT) is below. Secondary antibodies were removed, followed by an additional 6 washes in PHT. Samples were then mounted cuticle side up on glass slides using Vectashield mounting media (Vector Laboratories) and covered with a glass coverslip. Samples were viewed with a Leica MZ16FA stereomicroscope using a Planapo 1.0x or 1.6x objective, and images were acquired using a Leica DFC350FX digital camera. Primary antibodies were mouse anti-fasciclin-III (167) (Developmental Studies Hybridoma Bank, 1:50), rabbit anti-Peroxidasin (168) (1:300), rabbit anti-GFP (Molecular Probes, 1:500), and rabbit anti-activated-Caspase-3 (Cell Signaling, 1:150). Secondary Antibodies were goat-anti-mouse Cy3 (1:1000), goat-anti-mouse FITC (1:300), goat-anti-rabbit-Cy3 (1:1000) and goat-anti-rabbit-FITC (1:300) (Jackson ImmunoResearch).

### Live Imaging and Video Microscopy

For live imaging of wound-induced inflammation, *Nrg-GFP;Pxn-Gal4,UAS-2xEYFP* larvae were mounted on a glass slide. The anterior and posterior ends of the larvae were taped down using double-sided scotch tape to limit mobility but allow peristaltic body motions. Images were acquired using a Leica MZ16FA stereomicroscope with a Planapo 1.0X objective and a Leica DRC350FZ monochrome digital camera. To analyze the circulatory dynamics of hemocytes in both wounded and unwounded larvae, real-time movies were captured with images taken once every 400 ms for durations of up to 40 s. To analyze the accumulation of hemocytes at wound sites over longer periods of time, we made time-lapse movies. In these movies, frames were taken every 2 minutes or every 5 minutes over a period of 2-4 hours. We used Image-Pro AMS Software (Media Cybernetics) with the Scope-Pro Advanced Acquisition plug-in for image analysis. To measure the speed and motion paths of circulating hemocytes, we used the Image Pro Object Tracking Tool.

### Electron Microscopy

Transmission Electron Microscopy (TEM) analysis: As originally described (16, 32), larvae were dissected and fixed in 2% paraformaldehyde, 3% glutaraldehyde, and 2.5% dimethylsulfoxide (DMSO) in a sodium phosphate buffer. Fixed samples were trimmed near the wound and incubated at 4 °C for 1 hour in 1% osmium tetroxide. Samples were then incubated and stained at 4 °C overnight in 0.5% uranyl acetate and dehydrated with ethanol solutions. Dehydrated samples were embedded in SPURR resin (Electron Microscopy Sciences). A JEOL JEM 1010 transmission electron microscope was used

to view sections (90 nM) of tissue samples. Images were acquired on an AMT (Advanced Microscopy Techniques) digital photo system. Scanning Electron Microscopy (SEM) analysis: As originally described (16, 32), larvae were dissected and fixed in the same manner as listed above for TEM analysis. Tissue samples were dehydrated using ethanol, placed in hexamethyldisilazane, and then dried in a vacuum. Dried samples were mounted on carbon tabs (Electron Microscopy Sciences) and sputter-coating with gold to 0.1 kÅ. Images were acquired using a Philips 525 scanning electron microscope and a Semicaps digital camera.

#### X-gal staining

Larvae bearing a *msn-lacZ* transgene were stained with X-gal (5-bromo-4-chloro-3-indolyl-D-galactopyranoside) to detect  $\beta$ -galactosidase activity, as originally described (16), in epidermal cells at various time-points following UV irradiation. Larvae were dissected in PBS and fixed in 2% glutaraldehyde for 15 minutes at room temperature. Fixed samples were stained at 37 °C for 1.5 hours with an X-Gal solution composed of 150 mM NaCl, 10 mM Na<sub>2</sub>HPO<sub>4</sub>, 3 mM K<sub>4</sub>[FeII(CN)<sub>6</sub>], 3 mM K<sub>3</sub>[FeIII(CN)<sub>6</sub>], 1 mM MgCl<sub>2</sub>, 0.1% Triton X-100, and 2% X-gal.

#### Inhibition of larval mobility and peristalsis

*Nrg-GFP;Pxn-Gal4,UAS-2xEYFP* larvae were anesthetized using ethyl ether or 250  $\mu$ l of Flynap (Carolina Biological Supply), a mixture of ethanol and triethylamine, as originally described (32). Larvae were then wounded and immobilized by mounting them on a glass slide (Corning) via double-sided tape for 2 hours at room temperature.

Afterwards, samples were scored live using a semi-quantitative analysis to measure the accumulation of hemocytes at wound areas when larvae were immobilized (group anesthetized with ethyl ether) or immobilized with additional inhibition of peristalsis (group anesthetized with Flynap).

### Sunburn Assay

As originally described (65), early third instar larvae were lightly anesthetized using ethyl ether and mounted dorsal-side-up on a glass slide with a thin strip of double-sided-tape. Mounted larvae were placed in a Spectrolinker XL-1000 UV crosslinker (Spectronics Corporation). For survival experiments, larvae were exposed to doses ranging from 0 mJ/cm<sup>2</sup> (“mock treatment”) to 50 mJ/cm<sup>2</sup> at a 254 nm wavelength over a duration of approximately 5 seconds. For all subsequent hypersensitization experiments, the standard UV dose was 20 mJ/cm<sup>2</sup>. After UV treatment larvae were placed back on food.

### Analysis of nociceptive behavior

Noxious thermal stimuli were delivered using a custom-designed thermal probe, as originally described (65). The temperature was set on a thermal control unit (Thermal Solutions, Inc) which was capable of maintaining a constant set-point temperature within  $\pm 0.1$  °C across the range of 23 °C to 70 °C. The probe itself consisted of an insulated acrylic handle, a cartridge heater (Watlow Electric Manufacturing Company, FIREROD<sup>®</sup> Cartridge Heater), a thermocouple to provide constant feedback to the thermal control unit, and a 300  $\mu$ m micro-fabricated brass tip. The tip was small enough

in diameter to stimulate the larvae within an individual body segment. Thermal stimuli were presented along the dorsal midline of the larvae, within abdominal segments A4-A6 and viewed under a Leica MZ6 light microscope. Withdrawal latency was measured as the time of the initiation of the withdrawal response to the stimulus up to a 20 s cutoff. The behavioral response is defined as at least one complete 360° roll in response to the stimulus. To avoid any possible affects of habituation to repeated stimuli, each individual received only one stimulus. To assess baseline nociception, larvae were stimulated at either 45 °C or 48 °C in absence of UV, with the average withdrawal latency plotted for each condition. To test for the development of thermal allodynia, larvae were stimulated at 38 °C (the highest subthreshold temperature in the absence of tissue damage) 24 h after UV exposure. Larvae were stimulated up to 20 s, and the behavior was placed into one of three categories: No Response (no response within 20 s), Slow Response (5 s < response < 20 s), or Fast Response (response  $\geq$  5 s). To test for the development of thermal hyperalgesia, larvae were stimulated at 45 °C (the lowest temperature at which all larvae respond in the absence of tissue damage) 8 h after UV exposure, with the average withdrawal latency plotted for each condition.

### Statistical analysis

For wound-induced inflammation, Student's t test was used to analyze the accumulation of hemocytes at wound sites and the rate of wound closure. To assess the effect of mobility and peristalsis on hemocytes accumulation categorically, we used Fisher's exact test. For UV-induced nociceptive hypersensitivity, Fisher's exact test was used to assess differences in categorical data, including the development of thermal allodynia.



Bonferroni corrections were added to test for multiple comparisons as listed. Student's t test or one-way analysis of variance (ANOVA) was used in all other cases. Error bars in all figures represent the Standard Error of the Mean (S.E.M).

## **Bibliography**

1. Martin, P., and S. J. Leibovich. 2005. Inflammatory cells during wound repair: the good, the bad and the ugly. *Trends Cell Biol* 15:599-607.
2. Basbaum, A. I., D. M. Bautista, G. Scherrer, and D. Julius. 2009. Cellular and molecular mechanisms of pain. *Cell* 139:267-284.
3. Hucho, T., and J. D. Levine. 2007. Signaling pathways in sensitization: toward a nociceptor cell biology. *Neuron* 55:365-376.
4. Dray, A. 1995. Inflammatory mediators of pain. *Br J Anaesth* 75:125-131.
5. Marchand, F., M. Perretti, and S. B. McMahon. 2005. Role of the immune system in chronic pain. *Nat Rev Neurosci* 6:521-532.
6. Moalem, G., and D. J. Tracey. 2006. Immune and inflammatory mechanisms in neuropathic pain. *Brain Res Rev* 51:240-264.
7. Cunha, T. M., W. A. Verri, Jr., J. S. Silva, S. Poole, F. Q. Cunha, and S. H. Ferreira. 2005. A cascade of cytokines mediates mechanical inflammatory hypernociception in mice. *Proc Natl Acad Sci U S A* 102:1755-1760.
8. Cheng, J. K., and R. R. Ji. 2008. Intracellular signaling in primary sensory neurons and persistent pain. *Neurochem Res* 33:1970-1978.
9. Caterina, M. J., M. A. Schumacher, M. Tominaga, T. A. Rosen, J. D. Levine, and D. Julius. 1997. The capsaicin receptor: a heat-activated ion channel in the pain pathway. *Nature* 389:816-824.
10. Ji, R. R., T. A. Samad, S. X. Jin, R. Schmoll, and C. J. Woolf. 2002. p38 MAPK activation by NGF in primary sensory neurons after inflammation increases TRPV1 levels and maintains heat hyperalgesia. *Neuron* 36:57-68.

11. Bhawe, G., H. J. Hu, K. S. Glauner, W. Zhu, H. Wang, D. J. Brasier, G. S. Oxford, and R. W. t. Gereau. 2003. Protein kinase C phosphorylation sensitizes but does not activate the capsaicin receptor transient receptor potential vanilloid 1 (TRPV1). *Proc Natl Acad Sci U S A* 100:12480-12485.
12. Vellani, V., S. Mapplebeck, A. Moriondo, J. B. Davis, and P. A. McNaughton. 2001. Protein kinase C activation potentiates gating of the vanilloid receptor VR1 by capsaicin, protons, heat and anandamide. *J Physiol* 534:813-825.
13. Bhawe, G., W. Zhu, H. Wang, D. J. Brasier, G. S. Oxford, and R. W. t. Gereau. 2002. cAMP-dependent protein kinase regulates desensitization of the capsaicin receptor (VR1) by direct phosphorylation. *Neuron* 35:721-731.
14. Bosch, M., F. Serras, E. Martin-Blanco, and J. Baguna. 2005. JNK signaling pathway required for wound healing in regenerating *Drosophila* wing imaginal discs. *Dev Biol* 280:73-86.
15. Ferrandon, D., J. L. Imler, C. Hetru, and J. A. Hoffmann. 2007. The *Drosophila* systemic immune response: sensing and signalling during bacterial and fungal infections. *Nat Rev Immunol* 7:862-874.
16. Galko, M. J., and M. A. Krasnow. 2004. Cellular and genetic analysis of wound healing in *Drosophila* larvae. *PLoS Biol* 2:E239.
17. Stramer, B., W. Wood, M. J. Galko, M. J. Redd, A. Jacinto, S. M. Parkhurst, and P. Martin. 2005. Live imaging of wound inflammation in *Drosophila* embryos reveals key roles for small GTPases during in vivo cell migration. *J Cell Biol* 168:567-573.

18. Wood, W., and A. Jacinto. 2007. *Drosophila melanogaster* embryonic haemocytes: masters of multitasking. *Nat Rev Mol Cell Biol* 8:542-551.
19. Tracey, W. D., Jr., R. I. Wilson, G. Laurent, and S. Benzer. 2003. *painless*, a *Drosophila* gene essential for nociception. *Cell* 113:261-273.
20. Seong, S. Y., and P. Matzinger. 2004. Hydrophobicity: an ancient damage-associated molecular pattern that initiates innate immune responses. *Nat Rev Immunol* 4:469-478.
21. Petri, B., and M. G. Bixel. 2006. Molecular events during leukocyte diapedesis. *FEBS J* 273:4399-4407.
22. Niethammer, P., C. Grabher, A. T. Look, and T. J. Mitchison. 2009. A tissue-scale gradient of hydrogen peroxide mediates rapid wound detection in zebrafish. *Nature* 459:996-999.
23. Wood, W., C. Faria, and A. Jacinto. 2006. Distinct mechanisms regulate hemocyte chemotaxis during development and wound healing in *Drosophila melanogaster*. *J Cell Biol* 173:405-416.
24. Pastor-Pareja, J. C., M. Wu, and T. Xu. 2008. An innate immune response of blood cells to tumors and tissue damage in *Drosophila*. *Dis Model Mech* 1:144-154; discussion 153.
25. Elrod-Erickson, M., S. Mishra, and D. Schneider. 2000. Interactions between the cellular and humoral immune responses in *Drosophila*. *Curr Biol* 10:781-784.
26. Lanot, R., D. Zachary, F. Holder, and M. Meister. 2001. Postembryonic hematopoiesis in *Drosophila*. *Dev Biol* 230:243-257.

27. Franc, N. C., P. Heitzler, R. A. Ezekowitz, and K. White. 1999. Requirement for croquemort in phagocytosis of apoptotic cells in *Drosophila*. *Science* 284:1991-1994.
28. Zettervall, C. J., I. Anderl, M. J. Williams, R. Palmer, E. Kurucz, I. Ando, and D. Hultmark. 2004. A directed screen for genes involved in *Drosophila* blood cell activation. *Proc Natl Acad Sci U S A* 101:14192-14197.
29. Evans, C. J., and U. Banerjee. 2003. Transcriptional regulation of hematopoiesis in *Drosophila*. *Blood Cells Mol Dis* 30:223-228.
30. Paladi, M., and U. Tepass. 2004. Function of Rho GTPases in embryonic blood cell migration in *Drosophila*. *J Cell Sci* 117:6313-6326.
31. Rizki, T. 1978. The circulatory system and associated cells and tissues. In *The genetics and biology of Drosophila*. W. T. Ashburner M, editor. Academic Press, London. 397-452.
32. Babcock, D. T., A. R. Brock, G. S. Fish, Y. Wang, L. Perrin, M. A. Krasnow, and M. J. Galko. 2008. Circulating blood cells function as a surveillance system for damaged tissue in *Drosophila* larvae. *Proc Natl Acad Sci U S A*.
33. Morin, X., R. Daneman, M. Zavortink, and W. Chia. 2001. A protein trap strategy to detect GFP-tagged proteins expressed from their endogenous loci in *Drosophila*. *Proc Natl Acad Sci U S A* 98:15050-15055.
34. Halfon, M. S., S. Gisselbrecht, J. Lu, B. Estrada, H. Keshishian, and A. M. Michelson. 2002. New fluorescent protein reporters for use with the *Drosophila* Gal4 expression system and for vital detection of balancer chromosomes. *Genesis* 34:135-138.

35. Markus, R., B. Laurinyecz, E. Kurucz, V. Honti, I. Bajusz, B. Sipos, K. Somogyi, J. Kronhamn, D. Hultmark, and I. Ando. 2009. Sessile hemocytes as a hematopoietic compartment in *Drosophila melanogaster*. *Proc Natl Acad Sci U S A* 106:4805-4809.
36. Moreira, S., B. Stramer, I. Evans, W. Wood, and P. Martin. Prioritization of competing damage and developmental signals by migrating macrophages in the *Drosophila* embryo. *Curr Biol* 20:464-470.
37. Brock, A. R., D. T. Babcock, and M. J. Galko. 2008. Active cop, passive cop: developmental stage-specific modes of wound-induced blood cell recruitment in *Drosophila*. *Fly (Austin)* 2:303-305.
38. Fadeel, B., P. Quinn, D. Xue, and V. Kagan. 2007. Fat(al) attraction: oxidized lipids act as "eat-me" signals. *HFSP J* 1:225-229.
39. Platt, N., R. P. da Silva, and S. Gordon. 1998. Recognizing death: the phagocytosis of apoptotic cells. *Trends Cell Biol* 8:365-372.
40. Pech, L. L., and M. R. Strand. 1996. Granular cells are required for encapsulation of foreign targets by insect haemocytes. *J Cell Sci* 109 ( Pt 8):2053-2060.
41. Clark, K. D., L. L. Pech, and M. R. Strand. 1997. Isolation and identification of a plasmatocyte-spreading peptide from the hemolymph of the lepidopteran insect *Pseudaletia includens*. *J Biol Chem* 272:23440-23447.
42. Woolf, C. J., and Q. Ma. 2007. Nociceptors--noxious stimulus detectors. *Neuron* 55:353-364.

43. Hwang, R. Y., L. Zhong, Y. Xu, T. Johnson, F. Zhang, K. Deisseroth, and W. D. Tracey. 2007. Nociceptive neurons protect *Drosophila* larvae from parasitoid wasps. *Curr Biol* 17:2105-2116.
44. Leyshon, R. T. 2009. Coping with chronic pain: current advances and practical information for clinicians. *Work* 33:369-372.
45. Rauck, R. L. 2009. What is the case for prescribing long-acting opioids over short-acting opioids for patients with chronic pain? A critical review. *Pain Pract* 9:468-479.
46. Clatworthy, A. L., and E. Grose. 1999. Immune-mediated alterations in nociceptive sensory function in *Aplysia californica*. *J Exp Biol* 202:623-630.
47. Farr, M., J. Mathews, D. F. Zhu, and R. T. Ambron. 1999. Inflammation causes a long-term hyperexcitability in the nociceptive sensory neurons of *Aplysia*. *Learn Mem* 6:331-340.
48. Illich, P. A., and E. T. Walters. 1997. Mechanosensory neurons innervating *Aplysia* siphon encode noxious stimuli and display nociceptive sensitization. *J Neurosci* 17:459-469.
49. Wittenburg, N., and R. Baumeister. 1999. Thermal avoidance in *Caenorhabditis elegans*: an approach to the study of nociception. *Proc Natl Acad Sci U S A* 96:10477-10482.
50. Walters, E. T., P. A. Illich, J. C. Weeks, and M. R. Lewin. 2001. Defensive responses of larval *Manduca sexta* and their sensitization by noxious stimuli in the laboratory and field. *J Exp Biol* 204:457-469.

51. Burrell, B. D., and C. L. Sahley. 1998. Generalization of habituation and intrinsic sensitization in the leech. *Learn Mem* 5:405-419.
52. Kavaliers, M. 1988. Evolutionary and comparative aspects of nociception. *Brain Res Bull* 21:923-931.
53. Walters, E. T. 2008. Evolutionary Aspects of Pain. In *Pain*. A. I. B. Basbaum, M.C., editor. Academic Press/Elsevier, Burlington, MA. 175-184.
54. Smith, E. S., and G. R. Lewin. 2009. Nociceptors: a phylogenetic view. *J Comp Physiol A Neuroethol Sens Neural Behav Physiol*.
55. Benzer, S. 1967. BEHAVIORAL MUTANTS OF *Drosophila* ISOLATED BY COUNTERCURRENT DISTRIBUTION. *Proc Natl Acad Sci U S A* 58:1112-1119.
56. Caterina, M. J., A. Leffler, A. B. Malmberg, W. J. Martin, J. Trafton, K. R. Petersen-Zeitz, M. Koltzenburg, A. I. Basbaum, and D. Julius. 2000. Impaired nociception and pain sensation in mice lacking the capsaicin receptor. *Science* 288:306-313.
57. Davis, J. B., J. Gray, M. J. Gunthorpe, J. P. Hatcher, P. T. Davey, P. Overend, M. H. Harries, J. Latcham, C. Clapham, K. Atkinson, S. A. Hughes, K. Rance, E. Grau, A. J. Harper, P. L. Pugh, D. C. Rogers, S. Bingham, A. Randall, and S. A. Sheardown. 2000. Vanilloid receptor-1 is essential for inflammatory thermal hyperalgesia. *Nature* 405:183-187.
58. Grueber, W. B., L. Y. Jan, and Y. N. Jan. 2002. Tiling of the *Drosophila* epidermis by multidendritic sensory neurons. *Development* 129:2867-2878.



59. Matsumura, Y., and H. N. Ananthaswamy. 2004. Toxic effects of ultraviolet radiation on the skin. *Toxicol Appl Pharmacol* 195:298-308.
60. Kulms, D., and T. Schwarz. 2000. Molecular mechanisms of UV-induced apoptosis. *Photodermatol Photoimmunol Photomed* 16:195-201.
61. Bishop, T., D. W. Hewson, P. K. Yip, M. S. Fahey, D. Dawbarn, A. R. Young, and S. B. McMahon. 2007. Characterisation of ultraviolet-B-induced inflammation as a model of hyperalgesia in the rat. *Pain* 131:70-82.
62. Davies, S. L., C. Siau, and G. J. Bennett. 2005. Characterization of a model of cutaneous inflammatory pain produced by an ultraviolet irradiation-evoked sterile injury in the rat. *J Neurosci Methods* 148:161-166.
63. Luo, X., O. Puig, J. Hyun, D. Bohmann, and H. Jasper. 2007. Foxo and Fos regulate the decision between cell death and survival in response to UV irradiation. *Embo J* 26:380-390.
64. Rebollar, E., V. Valadez-Graham, M. Vazquez, E. Reynaud, and M. Zurita. 2006. Role of the p53 homologue from *Drosophila melanogaster* in the maintenance of histone H3 acetylation and response to UV-light irradiation. *FEBS Lett* 580:642-648.
65. Babcock, D. T., C. Landry, and M. J. Galko. 2009. Cytokine signaling mediates UV-induced nociceptive sensitization in *Drosophila* larvae. *Curr Biol* 19:799-806.
66. Julius, D., and A. I. Basbaum. 2001. Molecular mechanisms of nociception. *Nature* 413:203-210.

67. Brand, A. H., and N. Perrimon. 1993. Targeted gene expression as a means of altering cell fates and generating dominant phenotypes. *Development* 118:401-415.
68. Dorstyn, L., P. A. Colussi, L. M. Quinn, H. Richardson, and S. Kumar. 1999. DRONC, an ecdysone-inducible *Drosophila* caspase. *Proc Natl Acad Sci U S A* 96:4307-4312.
69. Igaki, T., H. Kanuka, N. Inohara, K. Sawamoto, G. Nunez, H. Okano, and M. Miura. 2000. Drob-1, a *Drosophila* member of the Bcl-2/CED-9 family that promotes cell death. *Proc Natl Acad Sci U S A* 97:662-667.
70. Cunha, F. Q., S. Poole, B. B. Lorenzetti, and S. H. Ferreira. 1992. The pivotal role of tumour necrosis factor alpha in the development of inflammatory hyperalgesia. *Br J Pharmacol* 107:660-664.
71. Scholz, J., and C. J. Woolf. 2007. The neuropathic pain triad: neurons, immune cells and glia. *Nat Neurosci* 10:1361-1368.
72. Vogel, C., S. Stallforth, and C. Sommer. 2006. Altered pain behavior and regeneration after nerve injury in TNF receptor deficient mice. *J Peripher Nerv Syst* 11:294-303.
73. Woolf, C. J., A. Allchorne, B. Safieh-Garabedian, and S. Poole. 1997. Cytokines, nerve growth factor and inflammatory hyperalgesia: the contribution of tumour necrosis factor alpha. *Br J Pharmacol* 121:417-424.
74. Igaki, T., H. Kanda, Y. Yamamoto-Goto, H. Kanuka, E. Kuranaga, T. Aigaki, and M. Miura. 2002. Eiger, a TNF superfamily ligand that triggers the *Drosophila* JNK pathway. *Embo J* 21:3009-3018.

75. Kanda, H., T. Igaki, H. Kanuka, T. Yagi, and M. Miura. 2002. Wengen, a member of the Drosophila tumor necrosis factor receptor superfamily, is required for Eiger signaling. *J Biol Chem* 277:28372-28375.
76. Ainsley, J. A., J. M. Pettus, D. Bosenko, C. E. Gerstein, N. Zinkevich, M. G. Anderson, C. M. Adams, M. J. Welsh, and W. A. Johnson. 2003. Enhanced locomotion caused by loss of the Drosophila DEG/ENaC protein Pickpocket1. *Curr Biol* 13:1557-1563.
77. Bazzoni, F., and B. Beutler. 1996. The tumor necrosis factor ligand and receptor families. *N Engl J Med* 334:1717-1725.
78. Babcock, D. T., and M. J. Galko. 2009. Two sides of the same coin no longer: Genetic separation of nociceptive sensitization responses. *Communicative & Integrative Biology* 2:58-60.
79. Dy, L. C., Y. Pei, and J. B. Travers. 1999. Augmentation of ultraviolet B radiation-induced tumor necrosis factor production by the epidermal platelet-activating factor receptor. *J Biol Chem* 274:26917-26921.
80. Kock, A., T. Schwarz, R. Kirnbauer, A. Urbanski, P. Perry, J. C. Ansel, and T. A. Luger. 1990. Human keratinocytes are a source for tumor necrosis factor alpha: evidence for synthesis and release upon stimulation with endotoxin or ultraviolet light. *J Exp Med* 172:1609-1614.
81. Czeschik, J. C., T. Hagenacker, M. Schafers, and D. Busselberg. 2008. TNF-alpha differentially modulates ion channels of nociceptive neurons. *Neurosci Lett* 434:293-298.

82. Jin, X., and R. W. t. Gereau. 2006. Acute p38-mediated modulation of tetrodotoxin-resistant sodium channels in mouse sensory neurons by tumor necrosis factor- $\alpha$ . *J Neurosci* 26:246-255.
83. Sorkin, L. S., W. H. Xiao, R. Wagner, and R. R. Myers. 1997. Tumour necrosis factor- $\alpha$  induces ectopic activity in nociceptive primary afferent fibres. *Neuroscience* 81:255-262.
84. Zelenka, M., M. Schafers, and C. Sommer. 2005. Intraneural injection of interleukin-1 $\beta$  and tumor necrosis factor- $\alpha$  into rat sciatic nerve at physiological doses induces signs of neuropathic pain. *Pain* 116:257-263.
85. Parada, C. A., J. J. Yeh, E. K. Joseph, and J. D. Levine. 2003. Tumor necrosis factor receptor type-1 in sensory neurons contributes to induction of chronic enhancement of inflammatory hyperalgesia in rat. *Eur J Neurosci* 17:1847-1852.
86. Feinstein-Rotkopf, Y., and E. Arama. 2009. Can't live without them, can live with them: roles of caspases during vital cellular processes. *Apoptosis* 14:980-995.
87. Yi, C. H., and J. Yuan. 2009. The Jekyll and Hyde functions of caspases. *Dev Cell* 16:21-34.
88. Iversen, L., and C. Johansen. 2008. Inflammasomes and inflammatory caspases in skin inflammation. *Expert Rev Mol Diagn* 8:697-705.
89. Kuranaga, E., and M. Miura. 2007. Nonapoptotic functions of caspases: caspases as regulatory molecules for immunity and cell-fate determination. *Trends Cell Biol* 17:135-144.

90. Thornberry, N. A., H. G. Bull, J. R. Calaycay, K. T. Chapman, A. D. Howard, M. J. Kostura, D. K. Miller, S. M. Molineaux, J. R. Weidner, J. Aunins, and et al. 1992. A novel heterodimeric cysteine protease is required for interleukin-1 beta processing in monocytes. *Nature* 356:768-774.
91. Black, R. A., C. T. Rauch, C. J. Kozlosky, J. J. Peschon, J. L. Slack, M. F. Wolfson, B. J. Castner, K. L. Stocking, P. Reddy, S. Srinivasan, N. Nelson, N. Boiani, K. A. Schooley, M. Gerhart, R. Davis, J. N. Fitzner, R. S. Johnson, R. J. Paxton, C. J. March, and D. P. Cerretti. 1997. A metalloproteinase disintegrin that releases tumour-necrosis factor-alpha from cells. *Nature* 385:729-733.
92. Moss, M. L., S. L. Jin, J. D. Becherer, D. M. Bickett, W. Burkhart, W. J. Chen, D. Hassler, M. T. Leesnitzer, G. McGeehan, M. Milla, M. Moyer, W. Rocque, T. Seaton, F. Schoenen, J. Warner, and D. Willard. 1997. Structural features and biochemical properties of TNF-alpha converting enzyme (TACE). *J Neuroimmunol* 72:127-129.
93. Moss, M. L., S. L. Jin, M. E. Milla, D. M. Bickett, W. Burkhart, H. L. Carter, W. J. Chen, W. C. Clay, J. R. Didsbury, D. Hassler, C. R. Hoffman, T. A. Kost, M. H. Lambert, M. A. Leesnitzer, P. McCauley, G. McGeehan, J. Mitchell, M. Moyer, G. Pahel, W. Rocque, L. K. Overton, F. Schoenen, T. Seaton, J. L. Su, J. D. Becherer, and et al. 1997. Cloning of a disintegrin metalloproteinase that processes precursor tumour-necrosis factor-alpha. *Nature* 385:733-736.
94. Arduise, C., T. Abache, L. Li, M. Billard, A. Chabanon, A. Ludwig, P. Mauduit, C. Boucheix, E. Rubinstein, and F. Le Naour. 2008. Tetraspanins regulate

- ADAM10-mediated cleavage of TNF- $\alpha$  and epidermal growth factor. *J Immunol* 181:7002-7013.
95. Sandkuhler, J. 2009. Models and mechanisms of hyperalgesia and allodynia. *Physiol Rev* 89:707-758.
  96. Dietzl, G., D. Chen, F. Schnorrer, K. C. Su, Y. Barinova, M. Fellner, B. Gasser, K. Kinsey, S. Oppel, S. Scheiblaue, A. Couto, V. Marra, K. Keleman, and B. J. Dickson. 2007. A genome-wide transgenic RNAi library for conditional gene inactivation in *Drosophila*. *Nature* 448:151-156.
  97. Wu, Y., A. R. Brock, Y. Wang, K. Fujitani, R. Ueda, and M. J. Galko. 2009. A blood-borne PDGF/VEGF-like ligand initiates wound-induced epidermal cell migration in *Drosophila* larvae. *Curr Biol* 19:1473-1477.
  98. Brody, T., and A. Cravchik. 2000. *Drosophila melanogaster* G protein-coupled receptors. *J Cell Biol* 150:F83-88.
  99. Hewes, R. S., and P. H. Taghert. 2001. Neuropeptides and neuropeptide receptors in the *Drosophila melanogaster* genome. *Genome Res* 11:1126-1142.
  100. Littleton, J. T., and B. Ganetzky. 2000. Ion channels and synaptic organization: analysis of the *Drosophila* genome. *Neuron* 26:35-43.
  101. Birse, R. T., E. C. Johnson, P. H. Taghert, and D. R. Nassel. 2006. Widely distributed *Drosophila* G-protein-coupled receptor (CG7887) is activated by endogenous tachykinin-related peptides. *J Neurobiol* 66:33-46.
  102. Honor, P., P. M. Menning, S. D. Rogers, M. L. Nichols, A. I. Basbaum, J. M. Besson, and P. W. Mantyh. 1999. Spinal substance P receptor expression and

- internalization in acute, short-term, and long-term inflammatory pain states. *J Neurosci* 19:7670-7678.
103. Rosenzweig, M., K. M. Brennan, T. D. Tayler, P. O. Phelps, A. Patapoutian, and P. A. Garrity. 2005. The *Drosophila* ortholog of vertebrate TRPA1 regulates thermotaxis. *Genes Dev* 19:419-424.
  104. Gong, Z., W. Son, Y. D. Chung, J. Kim, D. W. Shin, C. A. McClung, Y. Lee, H. W. Lee, D. J. Chang, B. K. Kaang, H. Cho, U. Oh, J. Hirsh, M. J. Kernan, and C. Kim. 2004. Two interdependent TRPV channel subunits, inactive and Nanchung, mediate hearing in *Drosophila*. *J Neurosci* 24:9059-9066.
  105. Kim, J., Y. D. Chung, D. Y. Park, S. Choi, D. W. Shin, H. Soh, H. W. Lee, W. Son, J. Yim, C. S. Park, M. J. Kernan, and C. Kim. 2003. A TRPV family ion channel required for hearing in *Drosophila*. *Nature* 424:81-84.
  106. Shen, B., H. Liu, E. Y. Skolnik, and J. L. Manley. 2001. Physical and functional interactions between *Drosophila* TRAF2 and Pelle kinase contribute to Dorsal activation. *Proc Natl Acad Sci U S A* 98:8596-8601.
  107. Boersma, M. C., and M. K. Meffert. 2008. Novel roles for the NF-kappaB signaling pathway in regulating neuronal function. *Sci Signal* 1:pe7.
  108. Niederberger, E., and G. Geisslinger. 2008. The IKK-NF-kappaB pathway: a source for novel molecular drug targets in pain therapy? *FASEB J* 22:3432-3442.
  109. Raftery, L. A., and D. J. Sutherland. 1999. TGF-beta family signal transduction in *Drosophila* development: from Mad to Smads. *Dev Biol* 210:251-268.
  110. Hooper, J. E., and M. P. Scott. 2005. Communicating with Hedgehogs. *Nat Rev Mol Cell Biol* 6:306-317.

111. Nusslein-Volhard, C., and E. Wieschaus. 1980. Mutations affecting segment number and polarity in *Drosophila*. *Nature* 287:795-801.
112. Briscoe, J. 2009. Making a grade: Sonic Hedgehog signalling and the control of neural cell fate. *EMBO J* 28:457-465.
113. Charron, F., E. Stein, J. Jeong, A. P. McMahon, and M. Tessier-Lavigne. 2003. The morphogen sonic hedgehog is an axonal chemoattractant that collaborates with netrin-1 in midline axon guidance. *Cell* 113:11-23.
114. Yam, P. T., S. D. Langlois, S. Morin, and F. Charron. 2009. Sonic hedgehog guides axons through a noncanonical, Src-family-kinase-dependent signaling pathway. *Neuron* 62:349-362.
115. Amankulor, N. M., D. Hambardzumyan, S. M. Pyonteck, O. J. Becher, J. A. Joyce, and E. C. Holland. 2009. Sonic hedgehog pathway activation is induced by acute brain injury and regulated by injury-related inflammation. *J Neurosci* 29:10299-10308.
116. Fan, Y., and A. Bergmann. 2008. Distinct mechanisms of apoptosis-induced compensatory proliferation in proliferating and differentiating tissues in the *Drosophila* eye. *Dev Cell* 14:399-410.
117. Huh, J. R., M. Guo, and B. A. Hay. 2004. Compensatory proliferation induced by cell death in the *Drosophila* wing disc requires activity of the apical cell death caspase Dronc in a nonapoptotic role. *Curr Biol* 14:1262-1266.
118. Perez-Garijo, A., F. A. Martin, and G. Morata. 2004. Caspase inhibition during apoptosis causes abnormal signalling and developmental aberrations in *Drosophila*. *Development* 131:5591-5598.



119. Perez-Garijo, A., E. Shlevkov, and G. Morata. 2009. The role of Dpp and Wg in compensatory proliferation and in the formation of hyperplastic overgrowths caused by apoptotic cells in the *Drosophila* wing disc. *Development* 136:1169-1177.
120. Ryoo, H. D., T. Gorenc, and H. Steller. 2004. Apoptotic cells can induce compensatory cell proliferation through the JNK and the Wingless signaling pathways. *Dev Cell* 7:491-501.
121. Johnson, R. L., J. K. Grenier, and M. P. Scott. 1995. patched overexpression alters wing disc size and pattern: transcriptional and post-transcriptional effects on hedgehog targets. *Development* 121:4161-4170.
122. Collins, R. T., and S. M. Cohen. 2005. A genetic screen in *Drosophila* for identifying novel components of the hedgehog signaling pathway. *Genetics* 170:173-184.
123. Aza-Blanc, P., F. A. Ramirez-Weber, M. P. Laget, C. Schwartz, and T. B. Kornberg. 1997. Proteolysis that is inhibited by hedgehog targets Cubitus interruptus protein to the nucleus and converts it to a repressor. *Cell* 89:1043-1053.
124. Ma, C., Y. Zhou, P. A. Beachy, and K. Moses. 1993. The segment polarity gene hedgehog is required for progression of the morphogenetic furrow in the developing *Drosophila* eye. *Cell* 75:927-938.
125. Johnson, R. L., L. Milenkovic, and M. P. Scott. 2000. In vivo functions of the patched protein: requirement of the C terminus for target gene inactivation but not Hedgehog sequestration. *Mol Cell* 6:467-478.

126. Malpel, S., S. Claret, M. Sanial, A. Brigui, T. Piolot, L. Daviet, S. Martin-Lannere, and A. Plessis. 2007. The last 59 amino acids of Smoothed cytoplasmic tail directly bind the protein kinase Fused and negatively regulate the Hedgehog pathway. *Dev Biol* 303:121-133.
127. Cooper, M. K., J. A. Porter, K. E. Young, and P. A. Beachy. 1998. Teratogen-mediated inhibition of target tissue response to Shh signaling. *Science* 280:1603-1607.
128. Incardona, J. P., W. Gaffield, R. P. Kapur, and H. Roelink. 1998. The teratogenic Veratrum alkaloid cyclopamine inhibits sonic hedgehog signal transduction. *Development* 125:3553-3562.
129. Dhaka, A., V. Viswanath, and A. Patapoutian. 2006. Trp ion channels and temperature sensation. *Annu Rev Neurosci* 29:135-161.
130. Patapoutian, A., A. M. Peier, G. M. Story, and V. Viswanath. 2003. ThermoTRP channels and beyond: mechanisms of temperature sensation. *Nat Rev Neurosci* 4:529-539.
131. Tominaga, M., and M. J. Caterina. 2004. Thermosensation and pain. *J Neurobiol* 61:3-12.
132. Tobin, D., D. Madsen, A. Kahn-Kirby, E. Peckol, G. Moulder, R. Barstead, A. Maricq, and C. Bargmann. 2002. Combinatorial expression of TRPV channel proteins defines their sensory functions and subcellular localization in *C. elegans* neurons. *Neuron* 35:307-318.

133. Alessandri-Haber, N., O. A. Dina, X. Chen, and J. D. Levine. 2009. TRPC1 and TRPC6 channels cooperate with TRPV4 to mediate mechanical hyperalgesia and nociceptor sensitization. *J Neurosci* 29:6217-6228.
134. Ambudkar, I. S., and H. L. Ong. 2007. Organization and function of TRPC channelosomes. *Pflugers Arch* 455:187-200.
135. Kottgen, M., B. Buchholz, M. A. Garcia-Gonzalez, F. Kotsis, X. Fu, M. Doerken, C. Boehlke, D. Steffl, R. Tauber, T. Wegierski, R. Nitschke, M. Suzuki, A. Kramer-Zucker, G. G. Germino, T. Watnick, J. Prenen, B. Nilius, E. W. Kuehn, and G. Walz. 2008. TRPP2 and TRPV4 form a polymodal sensory channel complex. *J Cell Biol* 182:437-447.
136. Dib-Hajj, S. D., T. R. Cummins, J. A. Black, and S. G. Waxman. 2007. From genes to pain: Na v 1.7 and human pain disorders. *Trends Neurosci* 30:555-563.
137. Cummins, T. R., S. D. Dib-Hajj, and S. G. Waxman. 2004. Electrophysiological properties of mutant Nav1.7 sodium channels in a painful inherited neuropathy. *J Neurosci* 24:8232-8236.
138. Stambouliau, S., J. S. Choi, H. S. Ahn, Y. W. Chang, L. Tyrrell, J. A. Black, S. G. Waxman, and S. D. Dib-Hajj. ERK1/2 Mitogen-Activated Protein Kinase Phosphorylates Sodium Channel Nav1.7 and Alters Its Gating Properties. *J Neurosci* 30:1637-1647.
139. Szallasi, A., F. Cruz, and P. Geppetti. 2006. TRPV1: a therapeutic target for novel analgesic drugs? *Trends Mol Med* 12:545-554.

140. Lishko, P. V., E. Procko, X. Jin, C. B. Phelps, and R. Gaudet. 2007. The ankyrin repeats of TRPV1 bind multiple ligands and modulate channel sensitivity. *Neuron* 54:905-918.
141. Zhang, X., L. Li, and P. A. McNaughton. 2008. Proinflammatory mediators modulate the heat-activated ion channel TRPV1 via the scaffolding protein AKAP79/150. *Neuron* 59:450-461.
142. Black, J. A., S. Liu, M. Tanaka, T. R. Cummins, and S. G. Waxman. 2004. Changes in the expression of tetrodotoxin-sensitive sodium channels within dorsal root ganglia neurons in inflammatory pain. *Pain* 108:237-247.
143. Obata, K., H. Katsura, T. Mizushima, H. Yamanaka, K. Kobayashi, Y. Dai, T. Fukuoka, A. Tokunaga, M. Tominaga, and K. Noguchi. 2005. TRPA1 induced in sensory neurons contributes to cold hyperalgesia after inflammation and nerve injury. *J Clin Invest* 115:2393-2401.
144. Zhang, X., J. Huang, and P. A. McNaughton. 2005. NGF rapidly increases membrane expression of TRPV1 heat-gated ion channels. *EMBO J* 24:4211-4223.
145. Schmidt, M., A. E. Dubin, M. J. Petrus, T. J. Earley, and A. Patapoutian. 2009. Nociceptive signals induce trafficking of TRPA1 to the plasma membrane. *Neuron* 64:498-509.
146. Van Buren, J. J., S. Bhat, R. Rotello, M. E. Pauza, and L. S. Premkumar. 2005. Sensitization and translocation of TRPV1 by insulin and IGF-I. *Mol Pain* 1:17.

147. Heckscher, E. S., R. D. Fetter, K. W. Marek, S. D. Albin, and G. W. Davis. 2007. NF-kappaB, IkappaB, and IRAK control glutamate receptor density at the *Drosophila* NMJ. *Neuron* 55:859-873.
148. Keshishian, H., and Y. S. Kim. 2004. Orchestrating development and function: retrograde BMP signaling in the *Drosophila* nervous system. *Trends Neurosci* 27:143-147.
149. McCabe, B. D., S. Hom, H. Aberle, R. D. Fetter, G. Marques, T. E. Haerry, H. Wan, M. B. O'Connor, C. S. Goodman, and A. P. Haghghi. 2004. Highwire regulates presynaptic BMP signaling essential for synaptic growth. *Neuron* 41:891-905.
150. O'Connor-Giles, K. M., L. L. Ho, and B. Ganetzky. 2008. Nervous wreck interacts with thickveins and the endocytic machinery to attenuate retrograde BMP signaling during synaptic growth. *Neuron* 58:507-518.
151. Grueber, W. B., B. Ye, C. H. Yang, S. Younger, K. Borden, L. Y. Jan, and Y. N. Jan. 2007. Projections of *Drosophila* multidendritic neurons in the central nervous system: links with peripheral dendrite morphology. *Development* 134:55-64.
152. Markus, R., E. Kurucz, F. Rus, and I. Ando. 2005. Sterile wounding is a minimal and sufficient trigger for a cellular immune response in *Drosophila melanogaster*. *Immunol Lett* 101:108-111.
153. Bautista, D. M., J. Siemens, J. M. Glazer, P. R. Tsuruda, A. I. Basbaum, C. L. Stucky, S. E. Jordt, and D. Julius. 2007. The menthol receptor TRPM8 is the principal detector of environmental cold. *Nature* 448:204-208.

154. Peier, A. M., A. Moqrich, A. C. Hergarden, A. J. Reeve, D. A. Andersson, G. M. Story, T. J. Earley, I. Dragoni, P. McIntyre, S. Bevan, and A. Patapoutian. 2002. A TRP channel that senses cold stimuli and menthol. *Cell* 108:705-715.
155. Hamada, F. N., M. Rosenzweig, K. Kang, S. R. Pulver, A. Ghezzi, T. J. Jegla, and P. A. Garrity. 2008. An internal thermal sensor controlling temperature preference in *Drosophila*. *Nature* 454:217-220.
156. Rosenzweig, M., K. Kang, and P. A. Garrity. 2008. Distinct TRP channels are required for warm and cool avoidance in *Drosophila melanogaster*. *Proc Natl Acad Sci U S A* 105:14668-14673.
157. Pfeiffer, B. D., A. Jenett, A. S. Hammonds, T. T. Ngo, S. Misra, C. Murphy, A. Scully, J. W. Carlson, K. H. Wan, T. R. Lavery, C. Mungall, R. Svirskas, J. T. Kadonaga, C. Q. Doe, M. B. Eisen, S. E. Celniker, and G. M. Rubin. 2008. Tools for neuroanatomy and neurogenetics in *Drosophila*. *Proc Natl Acad Sci U S A* 105:9715-9720.
158. Sweeney, S. T., K. Broadie, J. Keane, H. Niemann, and C. J. O'Kane. 1995. Targeted expression of tetanus toxin light chain in *Drosophila* specifically eliminates synaptic transmission and causes behavioral defects. *Neuron* 14:341-351.
159. Garen, A., L. Kauvar, and J. A. Lepesant. 1977. Roles of ecdysone in *Drosophila* development. *Proc Natl Acad Sci U S A* 74:5099-5103.
160. Xu, S. Y., C. L. Cang, X. F. Liu, Y. Q. Peng, Y. Z. Ye, Z. Q. Zhao, and A. K. Guo. 2006. Thermal nociception in adult *Drosophila*: behavioral characterization and the role of the painless gene. *Genes Brain Behav* 5:602-613.

161. Atzeni, F., M. Turiel, F. Capsoni, A. Doria, P. Meroni, and P. Sarzi-Puttini. 2005. Autoimmunity and anti-TNF-alpha agents. *Ann N Y Acad Sci* 1051:559-569.
162. Hefti, F. F., A. Rosenthal, P. A. Walicke, S. Wyatt, G. Vergara, D. L. Shelton, and A. M. Davies. 2006. Novel class of pain drugs based on antagonism of NGF. *Trends Pharmacol Sci* 27:85-91.
163. Luo, L., Y. J. Liao, L. Y. Jan, and Y. N. Jan. 1994. Distinct morphogenetic functions of similar small GTPases: *Drosophila* Drac1 is involved in axonal outgrowth and myoblast fusion. *Genes Dev* 8:1787-1802.
164. Adachi-Yamada, T., M. Nakamura, K. Irie, Y. Tomoyasu, Y. Sano, E. Mori, S. Goto, N. Ueno, Y. Nishida, and K. Matsumoto. 1999. p38 mitogen-activated protein kinase can be involved in transforming growth factor beta superfamily signal transduction in *Drosophila* wing morphogenesis. *Mol Cell Biol* 19:2322-2329.
165. Braun, A., B. Lemaitre, R. Lanot, D. Zachary, and M. Meister. 1997. *Drosophila* immunity: analysis of larval hemocytes by P-element-mediated enhancer trap. *Genetics* 147:623-634.
166. Ni, J. Q., M. Markstein, R. Binari, B. Pfeiffer, L. P. Liu, C. Villalta, M. Booker, L. Perkins, and N. Perrimon. 2008. Vector and parameters for targeted transgenic RNA interference in *Drosophila melanogaster*. *Nat Methods* 5:49-51.
167. Patel, N. H., P. M. Snow, and C. S. Goodman. 1987. Characterization and cloning of fasciclin III: a glycoprotein expressed on a subset of neurons and axon pathways in *Drosophila*. *Cell* 48:975-988.

168. Nelson, R. E., L. I. Fessler, Y. Takagi, B. Blumberg, D. R. Keene, P. F. Olson, C. G. Parker, and J. H. Fessler. 1994. Peroxidasin: a novel enzyme-matrix protein of *Drosophila* development. *EMBO J* 13:3438-3447.



## **Vita**

Daniel Talbot Babcock was born on October 7, 1982 in Philadelphia, Pennsylvania. He graduated from Glasgow High School, Newark, Delaware in 2001. After graduation, he attended the University of Delaware and received his Bachelor degree with a major in neuroscience in 2005. In the Fall of 2005, he entered the University of Texas Health Science Center at Houston Graduate School of Biomedical Sciences.

### Permanent address:

8380 El Mundo st #609

Houston, TX 77054